

Electrocatalytic reactions of inorganic nitrogen-containing compounds

Citation for published version (APA):

Vooy's, de, A. C. A. (2001). *Electrocatalytic reactions of inorganic nitrogen-containing compounds*. [Phd Thesis 1 (Research TU/e / Graduation TU/e), Chemical Engineering and Chemistry]. Technische Universiteit Eindhoven. <https://doi.org/10.6100/IR545208>

DOI:

[10.6100/IR545208](https://doi.org/10.6100/IR545208)

Document status and date:

Published: 01/01/2001

Document Version:

Publisher's PDF, also known as Version of Record (includes final page, issue and volume numbers)

Please check the document version of this publication:

- A submitted manuscript is the version of the article upon submission and before peer-review. There can be important differences between the submitted version and the official published version of record. People interested in the research are advised to contact the author for the final version of the publication, or visit the DOI to the publisher's website.
- The final author version and the galley proof are versions of the publication after peer review.
- The final published version features the final layout of the paper including the volume, issue and page numbers.

[Link to publication](#)

General rights

Copyright and moral rights for the publications made accessible in the public portal are retained by the authors and/or other copyright owners and it is a condition of accessing publications that users recognise and abide by the legal requirements associated with these rights.

- Users may download and print one copy of any publication from the public portal for the purpose of private study or research.
- You may not further distribute the material or use it for any profit-making activity or commercial gain
- You may freely distribute the URL identifying the publication in the public portal.

If the publication is distributed under the terms of Article 25fa of the Dutch Copyright Act, indicated by the "Taverne" license above, please follow below link for the End User Agreement:

www.tue.nl/taverne

Take down policy

If you believe that this document breaches copyright please contact us at:

openaccess@tue.nl

providing details and we will investigate your claim.

Electrocatalytic Reactions of Inorganic Nitrogen-containing Compounds

Proefschrift

ter verkrijging van de graad van doctor aan de Technische
Universiteit Eindhoven, op gezag van de Rector Magnificus,
prof.dr. M. Rem, voor een commissie aangewezen door het
College voor Promoties in het openbaar te verdedigen op
woensdag 13 juni 2001 om 16.00 uur

door

Arnoud Cornelis Adriaan de Vooy

geboren te Bunnik

Dit proefschrift is goedgekeurd door de promotoren:

prof.dr. J.A.R. van Veen

en

prof.dr. R.A. van Santen

Copromotor:

dr. M.T.M. Koper

The work described in this thesis has been carried out at the Schuit Institute of Catalysis within the Laboratory of Inorganic Chemistry and Catalysis, Eindhoven University of Technology. Financial support has been supplied by the Netherlands Organization for Scientific Research (NWO)

Printed at the University Press Facilities, Eindhoven University of Technology

CIP-DATA LIBRARY TECHNISCHE UNIVERSITEIT EINDHOVEN

Vooy, A.C.A. de

Electrocatalytic reactions of inorganic nitrogen-containing compounds / by A.C.A. de Vooy. - Eindhoven : Technische Univeristeit Eindhoven, 2001.

Proefschrift. - ISBN 90-386-2832-3

NUGI 813

Trefwoorden: elektrochemie ; cyclische voltammetrie / heterogene katalyse / nitraten / stikstofoxiden / ammoniak

Subject headings: electrochemistry ; cyclic voltammetry / hereogeneous catalysis / nitrates / nitrogen oxides / ammonia

Contents:

1.	Introduction	1
2.	Electrocatalytic reduction of nitrate on palladium/copper electrodes	9
3.	Mechanistic study of the nitric oxide reduction on a polycrystalline platinum electrode	33
4.	Mechanistic study on the electrocatalytic reduction of nitric oxide on transition-metal electrodes	53
5.	Mechanistic features of the nitric oxide oxidation on transition metal Electrodes	71
6.	The role of adsorbates in the electrochemical oxidation of ammonia on noble and transition metal electrodes	85
7.	The nature of chemisorbates formed from ammonia on gold and palladium electrodes as discerned from surface-enhanced raman spectroscopy	113
	Summary	123
	Samenvatting	126
	Appendix 1	129
	List of publications	137
	Dankwoord	138
	Curriculum Vitae	139

Chapter 1: Introduction

The present Ph.D. thesis is devoted to the electrochemical reactions of small nitrogen-containing inorganic molecules and ions at transition-metal (platinum, palladium, rhodium, iridium and ruthenium) and coinage metal (gold, silver and copper) electrodes. The main motivation for this research is the environmental problems caused by these molecules and ions (most notably ammonia and nitrate) in waste and drinking water. This has led to lower tolerated levels in water, which have to be met with new and improved processes.

Reactions of inorganic nitrogen-containing molecules have been investigated for a long time, motivated by both economical and environmental interests. Economically motivated processes include the oxidation of ammonia to nitric oxide (the Ostwald process [1]), the oxidation of nitric oxide to nitrates (in the production of fertilizer and explosives [1]) and the production of hydroxylamine [2], which all have been studied to a considerable extent. Most recent research, however, is environmentally motivated, concentrating on, e.g., the exhaust gas catalyst, the De-NO_x process and waste water treatment. The reason behind these environmental concerns is that most small N-containing molecules are toxic, as is shown in table 1.

Table 1, toxicity of small N-containing molecules and ions

	NH ₃	N ₂ H ₄	H ₂ NOH	N ₂	N ₂ O	NO	NO ₂ ⁻	NO ₂	NO ₃ ⁻
Maximum acceptable concentration (m.a.c.) [3]	25 ppm	0.1 ppm		-	25 ppm	25 ppm		2 ppm	2 ppm (HNO ₃)
Tolerated level in water	0.5 mg/l			-			0.1 mg/l		50 mg/l

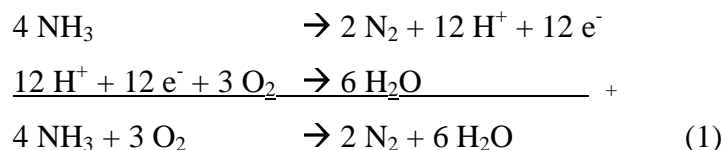
Table 1 makes it clear that the selectivity of any reaction designed to eliminate one of these toxic species must be tightly controlled. If the aim is to reduce NO₃⁻, for instance, no NO₂⁻ or NH₃ should be produced (whose tolerated levels in water are lower than of NO₃⁻). The only acceptable product is N₂.

Most research to date has focussed on gas phase reactions, and little attention has been given to reactions in the aqueous phase. However, interest in the latter is increasing, with the higher demands on clean waste and drinking water, as mentioned above.

To effectively eliminate N-bearing toxic species from water, catalysts are used. In most cases they are based on relatively noble metals, for two reasons. The first reason is that noble metals are the best dehydrogenation (and hydrogenation) catalysts, i.e. the best oxidation (and reduction) catalysts, as has already been shown for the reduction of nitric acid [4]. The second reason is that noble metals, by definition, show the greatest resistance to corrosion in aqueous media: other metals tend to be oxidized in water, or, even worse, will dissolve.

Most catalysts work on the principle that the reactants are adsorbed at the surface, intermediates and products are formed, and the products desorb from the surface. The surface therefore plays a crucial role in catalysis. This is reflected in the techniques used in analyzing catalysts, as most of them are surface sensitive. The way the metallic catalysts operate and the role of adsorbates in the mechanism of oxidations/reductions of nitrogen-containing compounds will be the main theme of this thesis.

The reactions studied in the present Ph.D. thesis are all redox reactions, i.e., the reactant is either oxidized or reduced. The overall non-electrochemical reaction is a combination of two redox reactions, an oxidation reaction and a reduction reaction. In the electrochemical setup the oxidation and the reduction reaction can be separated at the two electrodes, which allows for the redox reactions to be studied individually. An example is the ammonia oxidation with oxygen, which is a combination of the ammonia oxidation and the oxygen reduction:



The relationship between the two redox reactions is given by the electrical potential, which is dependent on the concentration (or partial pressure) of the reactants, and the electrical current, which equals the rate of the reaction times the

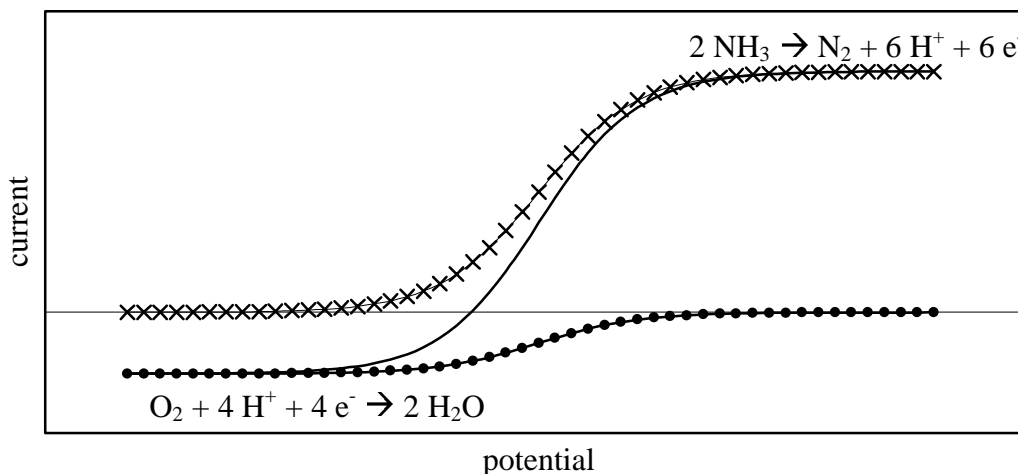


Figure 1.1: example of current-potential plots, crosses the oxidation reaction, filled dots the reduction reaction, solid line the total current

number of electrons per reacted molecule. An example is given in figure 1, in which the ammonia oxidation, the oxygen reduction and the superposition of the two are given. At the point where the total current is equal to zero (the open circuit potential, OCP), the situation is the same as the non-electrochemical situation. The rate of the reaction is equal to the current of one of the components at OCP. Note that both the OCP and the rate of the reaction will change when the current-potential plot of one of the reactions changes. At high, respectively low, potentials the current of the ammonia oxidation, respectively oxygen reduction, becomes constant with potential, because the reaction rate becomes limited by the transport of the reactant to the surface.

It is possible to record the current-potential plots individually, and in a later stage calculate the OCP and determine the rate of the reaction under non-electrochemical conditions. When this is done it is assumed that the oxidation and reduction are independent of each other, i.e., when the oxidation reaction is replaced by another oxidation, or a potentiostat, the effect on the reduction reaction is negligible, and vice versa. A case where this assumption is shown to be valid is encountered in chapter 2, where it is shown that the reduction of NO_3^- does not depend on the choice of H_2 , HCOOH or a potentiostat as a reductor.

An indication a reaction can be seen as two independent redox reactions is when the electrochemical model gives a better fit to the data than classical catalytic models, based on gas phase experiments. An example is seen during the partial oxidation of sugar [5], where the electrochemical model gives a good description of the formation and removal of surface oxides, and their relation to the rate of the reaction. Another example is given in chapter 6, in which it is shown that the oxidation of NH_3 with oxygen in water is described more accurately with an electrochemical model than by a model based on analogies with the gas phase reaction.

The replacement of one of the redox reactions, for instance the oxygen reduction, with a potentiostat is very convenient, since specific theories and methods have been developed in electrochemistry, which can be used to clarify the mechanism of the reaction. Examples are the current-potential analysis (Tafel slope analysis) [6], stripping voltammetry and the Rotating Disk Electrode; the latter two are introduced in appendix 1.

In addition of the availability of the theories and methods mentioned, it eliminates a number of fundamental and practical problems. One such problem is that the overall reaction might not be limited by the redox reaction under investigation, but by the other redox reaction. If one wants to study the oxidation of ammonia, for example, the reaction might be limited by the transport of oxygen to the surface, not by the oxidation of ammonia itself. Figure 1 shows an example of this situation, the rate of the reaction is determined by the rate of oxygen diffusion to the surface. If the oxygen reduction is replaced by a potentiostat, the transport of oxygen can of course not be rate limiting, and the reaction rate observed can be assigned to the ammonia oxidation. A second possible problem is that the potential at the surface can be inhomogeneous, because the concentration of one of the reactants (which determines the potential) can vary at the surface. In the case of the ammonia oxidation, there can be parts of the surface where the concentration of oxygen is higher (for instance due to bubbles of oxygen or air), which leads to a higher degree of oxidation of the surface and/or the products. This can have a great effect on the performance and the stability of the catalyst. In electrochemistry the catalyst is placed under potential control, which leads to a better defined state of the surface and of the adsorbates.

Additional information on the catalytic reaction can be obtained by using a combination of electrochemical methods with other techniques. In Differential Electrochemical Mass Spectroscopy (DEMS, [7-9]) the inlet of a mass spectrometer is placed near the electrode, so the amount and type of gaseous products formed at the electrode can be determined. It is especially useful in determining the selectivity of a reaction, and in fact the selectivity to NO_2 , NO , N_2O and/or N_2 was determined in this fashion. With an Electrochemical Quartz Crystal Microbalance (EQCM [10,11]) the electrode is placed on a quartz crystal and during the processes the mass changes of the electrode are determined. It is used when heavy molecules or ions adsorb/desorb, or to determine if, and by how much, the electrode material dissolves in the electrolyte. Surface Enhanced Raman Spectroscopy (SERS [12-15]) can be used to determine the nature of the adsorbate at the surface by its vibrational frequencies. InfraRed Absorption-reflection Spectroscopy (IRAS) should also be mentioned, although it is not used in this thesis, since it can also be used to determine the nature of the adsorbates at the surface. Note that all techniques are *in situ*, as information is obtained under reaction conditions.

Outline of this thesis

The objective throughout this thesis is to understand reactions of small, inorganic nitrogen-containing molecules and ions at the surface on a molecular level. Especially the nature of the molecules or fragments bonded at the surface, and their relationship to the activity and selectivity is investigated.

The research carried out can be roughly divided into three areas: the reduction of NO_3^- (chapter 2), the reduction and oxidation of NO (chapters 3, 4 and 5), and the oxidation of NH_3 (chapters 6 and 7). These reactions occur sometimes simultaneously or in sequence, for instance the reduction of NO is a key reaction in the reduction of NO_3^- . The chapters should therefore not be viewed upon as being separate, but as links in a chain of reactions.

In chapter 2 the reduction of NO_3^- on noble metal/copper electrodes is discussed, with a focus on palladium/copper. It is shown that the activity is determined by the amount of copper at the surface, the selectivity towards N_2 by the amount of palladium at the surface. Both the activity and selectivity to N_2 decrease

when the concentration of NO_3^- at the surface is decreased, either by decreasing the bulk concentration of NO_3^- or by competitive adsorption with other ions.

Chapter 3 deals with the reduction of NO at platinum. The focus is on the mechanism of the reaction, which in fact turns out to be two mechanisms, depending on potential. At high potentials N_2O is formed, by a reaction pathway that includes an NO dimer species. At lower potentials the selectivity changes to NH_3 , by a pathway similar to that of the reduction of adsorbed NO.

The study of the reduction of NO is extended to the other noble metals in chapter 4. The reaction pathways found for platinum turn out to be valid for the other noble metals as well; N_2O is formed by an NO surface dimer intermediate, and NH_3 is formed similarly to the reduction of adsorbed NO. It is argued that the reaction to N_2 , formed at potentials between the formation of N_2O and NH_3 , occurs through the reduction of previously formed N_2O .

Chapter 5 focuses on the oxidation of NO. Both the oxidation of adsorbed NO and of solution NO turn out to be almost independent of the choice of the metal. Although a complete view of the oxidation mechanism has not been obtained, the importance of the presence of surface metal oxides is shown.

In chapter 6 the oxidation of NH_3 on transition and coinage metals is described. In all cases the deactivation of the catalyst is related on the formation of N_{ads} ; only metals which form $\text{NH}_{x,\text{ads}}$ intermediates (platinum and iridium) show continuous selective oxidation of NH_3 . The coinage metals show no activity, and no $\text{NH}_{x,\text{ads}}$ or N_{ads} at the surface. The ease of formation of N_{ads} is linked to its heat of adsorption.

The proof that N_{ads} is indeed the species responsible for the deactivation of the transition metal catalysts during the ammonia oxidation is given in chapter 7, using in situ SERS measurements. The palladium- N_{ads} vibration is detected in the potential window where the electrode is deactivated. Gold only shows reversible adsorption of NH_3 , with no N_{ads} formed.

References:

- [1] D.A. King, in *Studies in Surface Science and Catalysis*, G.F. Froment and K.C. Waugh (Ed.) (1997) 79
- [2] C.G.M. van de Moesdijk, in *Catalysis of Organic Reactions in Chemical Industries*, J.R. Kosak (Ed.), vol. 18, Marcel Dekker, New York (1984) 379

- [3] Chemiekaarten, 5th ed., Samsom publishers, Alphen aan de Rijn
- [4] A.K. Vijh, *J. Catal.* 32 (1974) 230
- [5] A.P. Markusse, B.F.M. Kuster and J.C. Schouten, *J. Mol. Catal. A* 158 (2000) 215
- [6] *Techniques and Mechanisms in Electrochemistry*, P.A. Christensen and A. Hamnett, Blackie Academic & Professional 1994
- [7] J.F.E. Gootzen, Ph.-D thesis, Eindhoven University of Technology, 1997
- [8] J. Willsau and J. Heitbaum, *J. Electroanal. Chem.* 194 (1985) 27
- [9] T. Frelink, Ph.-D thesis Eindhoven University of Technology, 1995
- [10] W. Visscher, J.F.E. Gootzen, A.P. Cox and J.A.R. van Veen, *Electrochim. Acta* 43 (1998) 533
- [11] *Electrochemical Methods*, A.J. Bard and L.R. Faulkner, J. Wiley & Sons, New York 1980
- [12] M.J.Weaver, S.Zou, H.Y.H.Chan, *Anal.Chem.* 72 (2000) A38
- [13] H.Y.H.Chan, S.Zou, M.J.Weaver, *J.Phys.Chem.B* 103 (1999) 11141
- [14] S.Zou, H.Y.H.Chan, C.T.Williams, M.J.Weaver, *Langmuir* 16 (2000) 754
- [15] X.Gao, Y.Zhang, M.J.Weaver, *Langmuir* 8 (1992) 668

Chapter 2: Electrocatalytic Reduction of Nitrate on Palladium/Copper Electrodes.

Abstract

The reduction of NO_3^- on palladium/copper electrodes has been studied using differential electrochemical mass spectroscopy (DEMS), rotating ring-disk electrodes (RRDE) and quartz microbalance electrodes (EQM). In acidic electrolytes the activity increases linearly with Cu coverage, in alkaline electrolytes a different dependence on coverage is observed. One monolayer of Cu gives a different selectivity from bulk copper. The adsorption of NO_3^- is competitive with SO_4^{2-} , whereas Cl^- adsorption blocks the reduction. Competitive adsorption lowers both the activity and the selectivity to N_2 .

Copper activates the first electron transfer, the role of palladium is to steer the selectivity towards N_2 . The trends in activity and selectivity are explained in terms of coverage of N-species.

1. Introduction.

The reduction of nitrate has gained renewed attention due to environmental problems like overfertilisation and the increasing costs of the purification of drinking water. The usual techniques (ion-exchange and biofiltration) have major disadvantages [1], and for this reason the direct reduction with H_2 using a catalyst is being investigated. Noble metals are the best hydrogenation catalysts and therefore the first choice for reducing nitrate. As the noble metals have very low activity a promoter is necessary. Known promoters are germanium (for the production of hydroxylamine) [2], copper [1], tin [3] and indium [3] (for the production of N_2).

A number of articles have been published on the catalytic reduction of nitrate with H_2 [1,3-8] or formic acid [3] as a reductor, using palladium/copper on silica. It was observed that with increasing copper percentage the activity increases but the selectivity towards N_2 decreases. NH_3 and NO_2^- are formed as side products, whereas only traces of N_2O could be detected [4]. The reduction is strongly dependent on pH: in alkaline solvents NH_3 is formed, in acidic solvents NO_2^- [5]. The selectivity to NH_3 increases with higher hydrogen flow rates [1].

To explain the increase in NO_2^- and NH_3 the reduction of NO_2^- has also been investigated (the first step in the reduction of nitrate is the formation of NO_2^- [1,2]). Both activity and selectivity towards N_2 are decreased by copper [6].

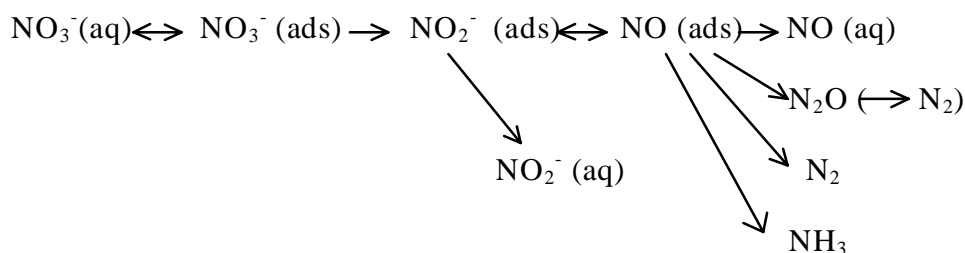
The activity and selectivity of the palladium/copper catalyst is very dependent on the preparation method [7,9]. CO-FTIR experiments on palladium-copper alloy catalysts [10] show that different preparation methods can give differences in surface composition: bulk segregation, surface segregation and alloying have all been observed. For a better understanding it would be useful to be able to control the surface composition of the catalyst. This can be achieved electrochemically by underpotential deposition of copper (copper is able to form a reversible UPD-layer [e.g. 11]). The amount of copper at the surface can be tuned by varying the deposition potential.

The mechanism of the reduction of nitrate is independent of the reductor, e.g. hydrogen or formic acid. This fact leads to two possible mechanisms. 1: NO_3^- reacts

with adsorbed H on the surface. 2: NO_3^- reacts by a local cell mechanism, i.e. by reduction of NO_3^- on one part of the surface and oxidation of the reductor at another part of the surface; electrons go through the metal and protons go through the solution to make the stoichiometry complete. In both cases electrochemical methods should be useful for clarifying the mechanism and the role of copper in the elementary steps. In the second case this is obvious, in the first case there is no difference between H(ads) formed by the dissociation of H_2 or by the reduction of a proton, $\text{H}^+ + \text{e}^- \rightarrow \text{H(ads)}$.

The conventional Langmuir-Hinselwood kinetic approach [8] shows that hydrogen and NO_3^- adsorb on different sites, which would be an indication for the second mechanism. To translate the electrochemical to the catalytic experiments the hydrogen partial pressure would relate to the potential and the activity to the electrical current.

The reaction scheme that is proposed from the kinetic approach [8,12] is the following:



Reaction scheme 1:

The first step (adsorption of NO_3^-) is a fast and reversible process. This was derived from the observation that the kinetic order to NO_3^- is 0.7 [8]. This value is typical for a reaction with a relatively low coverage of reacting species at the surface (if the coverage were high the order would be zero). Since the reaction is kinetically controlled, not diffusion controlled, this suggests that NO_3^- is bonded weakly to the surface. This could make the reaction liable to competitive adsorption effects. Our first objective is to determine the effects of competitive adsorption on the reaction.

The second step (reduction of NO_3^- to NO_2^-) is known to be the rate determining step. This is verified by electrochemical experiments which showed the first electron transfer to be rate determining [13], both on palladium and copper

electrodes and in acidic electrolytes. NO_2^- has been observed as an intermediate during the reaction [e.g.8]. Our second objective is to determine the role of copper in the rate determining step (palladium has no activity for NO_3^- reduction). The pH of the solution has also an effect on the activity [5], so the measurements will be performed in both acidic and alkaline electrolytes. We decided not to measure in pH-neutral electrolytes because the solution would have to be buffered. As will be shown in our results the buffering ions will probably have an effect on the reaction, and the result would differ from NO_3^- being reduced in drinking water.

The third step is the selectivity controlling reaction step. NO_2^- , NO, N_2O , N_2 , and NH_3 are the possible products; N_2 is the desired product. The selectivity towards N_2 decreases with the copper content, but pure palladium gives a high selectivity towards N_2 [e.g. 1,14]. The selectivity is also dependent on pH [14]. Sometimes [14,15] the direct pathway for producing N_2 from NO is omitted, N_2O is written as a necessary intermediate in the formation of N_2 . In another case [12] N_2O is not mentioned as a possible product. Our third objective is to identify the roles of copper and palladium on the selectivity, both in the NO_3^- reduction as in the reduction of the intermediates. If possible the path by which N_2 is formed will be identified.

Overall we will determine the dependence of the reaction on the copper coverage, on different anions in the solution and on the pH. From these measurements we will formulate a model involving all three described steps.

2. Experimental

Cyclic voltammetry, amperometry rotating disk (RDE), and rotating ring-disk electrode (RRDE) measurements were carried out with an Autolab Pgstat 20 with bipotentiostat module. Detection of non-gaseous oxidisable products was performed in the RRDE setup by applying a constant potential to the palladium/copper disk and scanning the platinum ring.

The selectivity to gaseous products was defined as the amount of gaseous products divided by the Faradaic current and determined using differential electrochemical mass spectroscopy (DEMS). DEMS measurements were performed with a Leybold Quadruvac PGA 100 Mass Spectrometer. Details of the experimental setup are given elsewhere [16]. The products were examined for N_2 ($m/z = 28$) and N_2O ($m/z = 44$). The signal was calibrated by oxidation of a monolayer CO to CO_2

and corrected for sensitivity and fragmentation probability [17]. Activities and selectivities were determined potentiostatically using steady state currents.

The quartz microbalans system consists of palladium deposited on a gold covered quartz crystal (5 MHz, Phelps electronics) in a teflon encasing [18]. The frequency was measured with a Philips PM 6680/016 frequency counter.

We have tried to establish the NO-coverage during the reduction of NO_3^- using IR-spectroscopy (Biorad FTS 45A spectrometer, equipped with a liquid nitrogen cooled MCT detector). The setup is described in detail in ref. [19]. Useful IR-spectra can only be obtained in a potential window of at least 0.1 V in which Faradaic current is virtually absent. No such region is available for the Pd/Cu system, and no conclusive results could be obtained.

Submonolayers of copper were obtained by underpotential deposition between 0.25 and 0.6 V from a solution of 20 mM Cu^{2+} in either 0.1 M HClO_4 or H_2SO_4 depending on the electrolyte during nitrate reduction. The coverage of copper was determined after each measurement from the oxidation charge of $\text{Cu} \rightarrow \text{Cu}^{2+}$ compared to the oxidation charge of a monolayer CO:

$$\Theta_{\text{Cu}} = \frac{Q_{\text{Cu} - \text{ox}}}{Q_{\text{CO} - \text{ox}}} \quad (1)$$

Palladium electrodes were prepared by electrodeposition from a $5 \cdot 10^{-2}$ M PdCl_2 in 0.2 M HCl + 0.3 M HClO_4 solution on a palladium foil. A deposition current of 10 mA/cm² was used.

A Hg/HgSO₄ electrode in saturated K₂SO₄ was used as a reference electrode in acidic electrolytes, a Hg/HgO electrode in 0.1 M KOH was used in alkaline electrolytes. All potentials in the text will be referred to the reversible hydrogen electrode (RHE).

All chemicals were obtained from Merck (p.a. grade). NaNO₃ was used as the source of NO₃⁻, unless otherwise specified. NO (purity 2.0, washed in a solution of 2 M KOH) and N₂O (purity 2.5) were provided by Hoekloos. Great care was taken to avoid contact between oxygen and NO. Ultrapure water (18.2 MΩ), obtained with an Elga purifying system, was used for all electrolytes.

3. Results

3.1. Reduction of nitrate

3.1.1 DEMS- measurements

The activity of the electrode at 0.02 V versus copper coverage at pH = 0.3 and $[\text{NO}_3^-] = 0.1 \text{ M}$ is plotted in figure 1a. The reduction current increases linearly with the copper coverage. Electrolytes containing HClO_4 show a higher activity than those containing H_2SO_4 . Electrolytes containing only HNO_3 give the same results as NaNO_3 in HClO_4 . Both trends have been observed at any potential between 0 and 0.3 V. A bulk copper electrode has the same activity as an UPD-copper electrode at high coverages. The actual activity however does change with the applied potential with a Tafel slope of 111 mV/dec.

The selectivity to N_2 versus copper coverage is plotted in figures 1b, to N_2O in figure 1c. The selectivity to NO could not be determined accurately because N_2O fragmentates to NO inside the mass spectrometer and this interferes with the determination of the selectivity. The amount of NO produced however is small.

In both HClO_4 and H_2SO_4 the selectivity towards N_2 decreases with θ_{Cu} , while the selectivity towards N_2O increases linearly. In an electrolyte containing HClO_4 far more N_2O is produced than if H_2SO_4 is used as an electrolyte. Like the trends in the activity both trends are seen at different potentials. The selectivity changes only slightly with potential. For instance at a copper coverage of 1 the selectivity to N_2O increases from 80 % at 0.02 V to 95 % at 0.22 V. The same trend holds for low copper coverages. For instance at a copper coverage of 0.28 the selectivity to N_2 increases from 40 % at 0.02 V to 50 % at 0.22 V. This can be attributed to increased NH_4^+ formation at more negative potentials. Besides NH_4^+ NO_2^- is formed during the reduction (as will be discussed in the next section) and for this reason the combined selectivity to N_2 and N_2O is always less than 100 % at any given copper coverage. If bulk copper is deposited (the copper coverage will be above 1) the selectivity to N_2O decreases and NO is formed in large quantities.

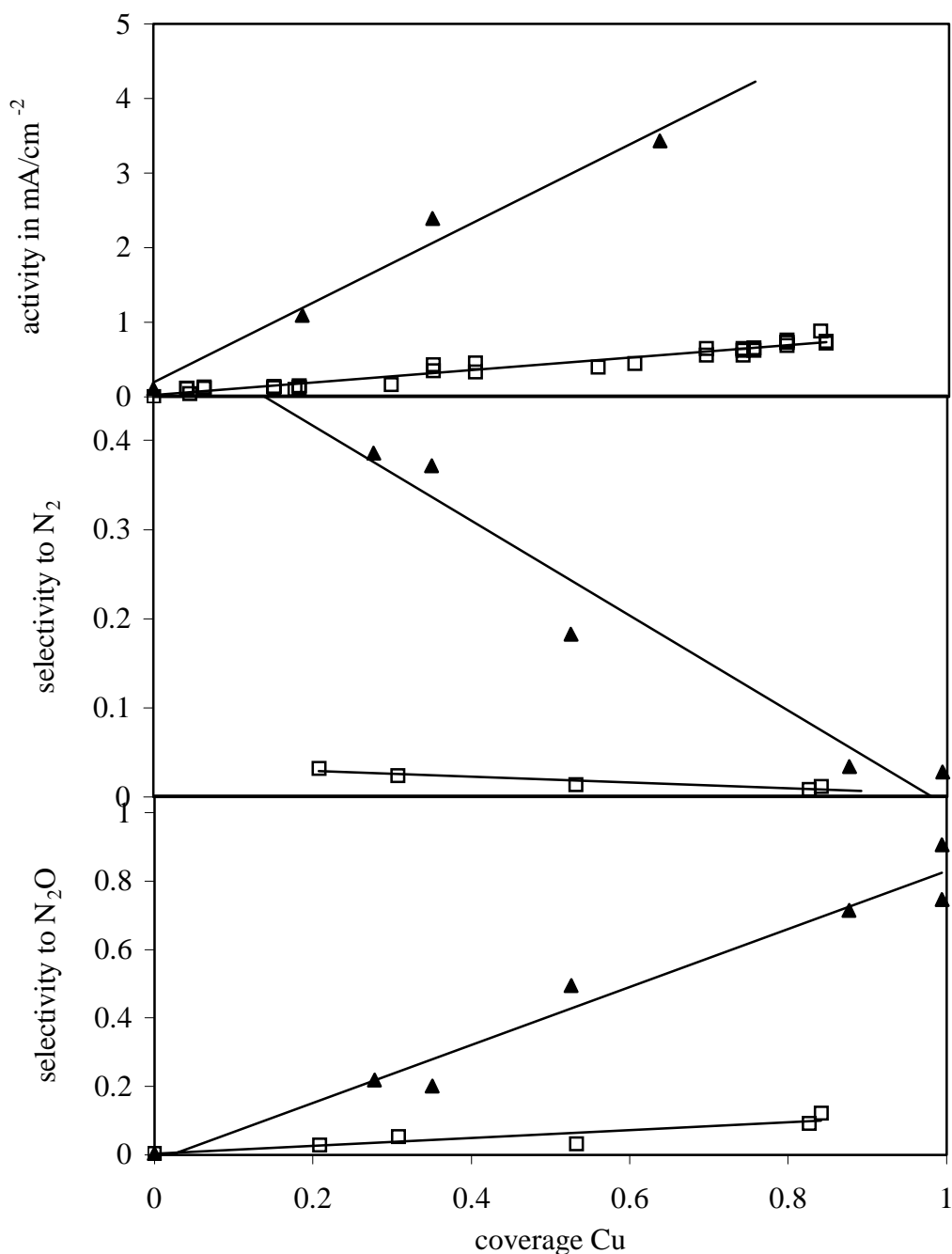


Figure 2.1: activity and selectivity versus Cu coverage in HClO₄ (filled triangles) and H₂SO₄ (open squares), $V = 0.02$ V, $pH = 0.3$, $[NO_3^-] = 0.1$ M

The kinetic order of the NO₃⁻ concentration with respect to the activity is 0.7, which has also been reported in literature for the drinking water catalyst [5].

The selectivity versus the nitrate concentration at 0.02 V at a copper coverage of 0.9 is plotted in figure 2. The selectivity to N₂O increases with concentration. The other products are NH₄⁺ and NO₂⁻.

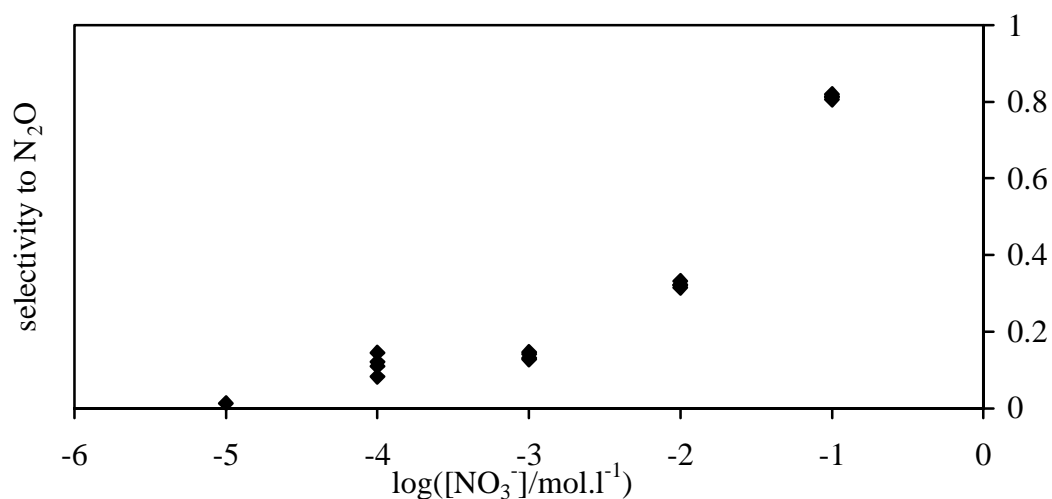


Figure 2.2: selectivity of the reduction of NO_3^- versus the concentration, $V = 0.02$ V, $\text{pH} = 0.3$, Cu coverage is 0.9

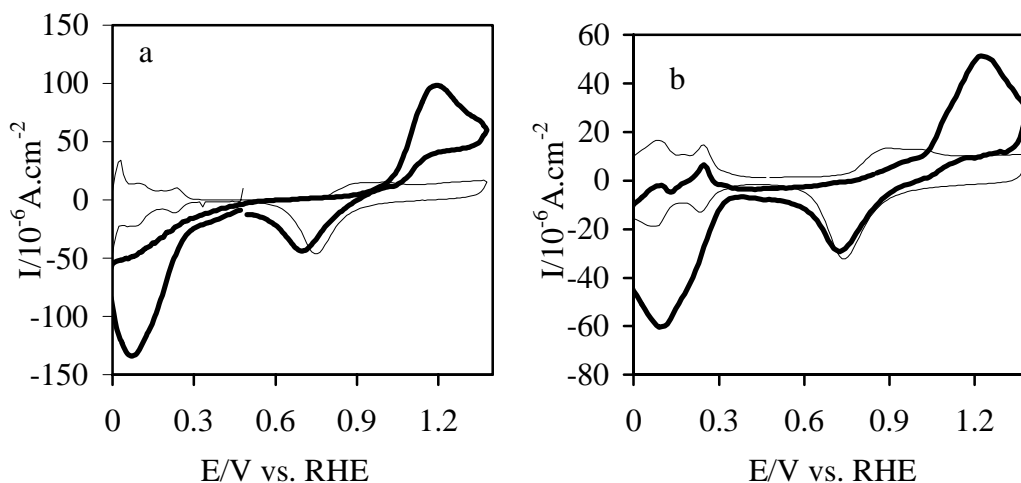


Figure 2.3; a: cyclic voltammogram of platinum ring during reduction of NO_3^- in H_2SO_4 , $\text{pH} = 0.3$, $[\text{NO}_3^-] = 0.1$ M, $E_{\text{disk}} = 0.02$ V, Cu coverage disk is 0.9; b: cyclic voltammogram of NO in H_2SO_4 on platinum, $\text{pH} = 0.3$, $[\text{NO}_2^-] = 10^{-3}$ M, thick lines are the measurement, thin lines are the blank.

3.1.2 RRDE-measurements

The species detected at the ring are incompletely reduced products of the nitrate reduction. The most likely products are HNO_2 or NO as the cyclic voltammograms (figure 3a) show reduction and oxidation currents at approximately the same potentials as in a solution containing HNO_2 or NO (figure 3b). The reduction

of HNO_2 to NO is very fast and reversible [20], and therefore no difference can be observed between the two species. The other products (NO_3^- , N_2O , N_2 and NH_4^+) can not be oxidized in water. No potential range in the cyclic voltammograms is available at which the current is proportional to the NO concentration, so it is difficult to quantify the NO concentration.

3.1.3. Quartz Microbalance experiments

To follow the adsorption of anions and its effect on the current the mass of the electrode was monitored during NO_3^- reduction. The mass should increase when SO_4^{2-} is adsorbed to the surface, and simultaneously the current should decrease. The results of this experiment, however, do not show a clear increase in mass when SO_4^{2-} is adsorbed. We have not been able to determine the reason.

In a subsequent experiment, we added Cl^- to the solution. Cl^- was chosen since Cl^- binds strongly to metal electrodes and therefore the anion effect should be more pronounced. When we adsorbed Cl^- the mass of the electrode decreased regardless of the presence of NO_3^- in the solution. Presumably the decrease in mass is due to the chloride ions displacing either nitrate or perchlorate ions from the double layer or change the adsorption of the water molecules to the surface.

In figure 4, the results are plotted of the Cl^- adsorption during the NO_3^- reduction. At $t = 0$ s a small amount of Cl^- was added (the total concentration Cl^- in the cell was 10^{-3} M). The change in mass at $t = 0$ s can be attributed to the change in water level above the electrode. At $t = 92$ s the solution was stirred to transport the Cl^- towards the electrode. At $t = 142$ s the Cl^- reached the electrode and adsorbed to the surface, resulting in a decrease in mass. Simultaneously the reduction current decreases due to competitive adsorption of the Cl^- ions. Note the decrease in mass and current run parallel. No attempts were made to interpret the change in mass in figure 4 in terms of the number of adsorbed ions and molecules.

When Cl^- was replaced by I^- a similar decrease in current is observed parallel to a large increase in mass. The same mass decrease respectively increase has been observed in experiments without NO_3^- .

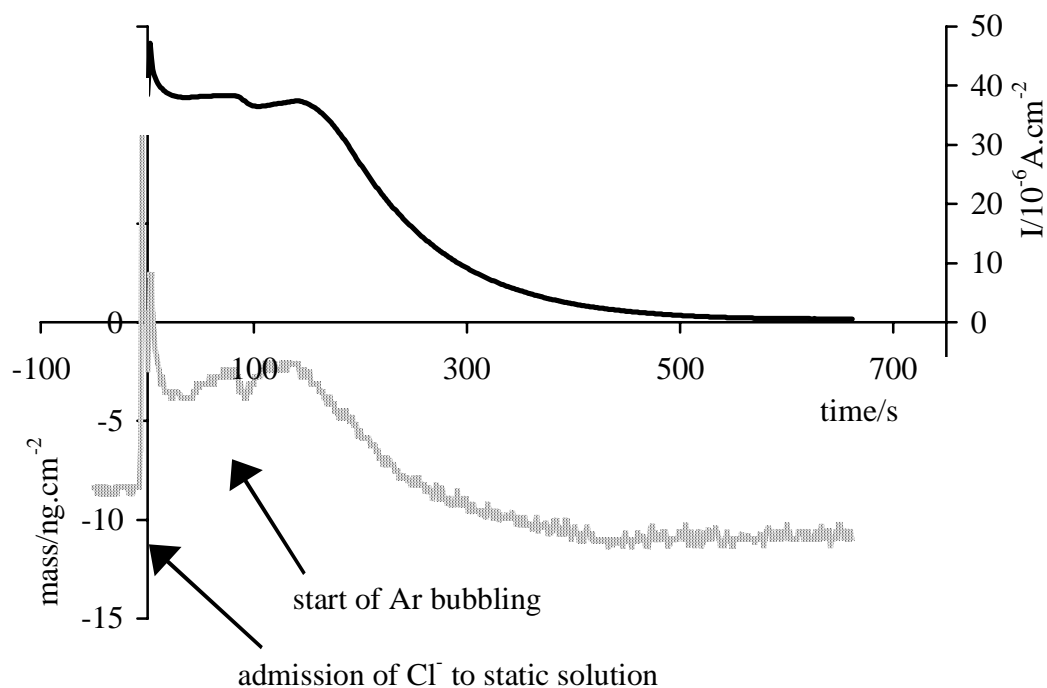


Figure 2.4: activity and mass of a PdCu electrode upon adsorption of Cl^- , solid line is current, dotted line is frequency, $V = 0.07 \text{ V}$, $[\text{NO}_3^-] = 0.1 \text{ M}$, supporting electrolyte is 0.5 M HClO_4 , Cu coverage is 1

3.2. Reduction of intermediates

To study the reactions following the first step ($\text{NO}_3^- + 2 \text{H}^+ + 2 \text{e}^- \rightarrow \text{NO}_2^- + \text{H}_2\text{O}$) the reduction of the intermediates, NO_2^- , NO and N_2O , was studied. Pure palladium and palladium with a copper coverage of 1 were taken as electrodes.

3.2.1. Nitrite reduction

Rotating disk experiments (RDE) show a difference in activity between palladium and copper in H_2SO_4 of about 10:1.

A large difference in selectivity, using DEMS, is observed between palladium and copper on palladium electrodes. The main product on a palladium electrode is N_2 , copper deposited on palladium produces N_2O with only traces N_2 . At more negative potentials the selectivity to gaseous products decreases for both electrodes, so the

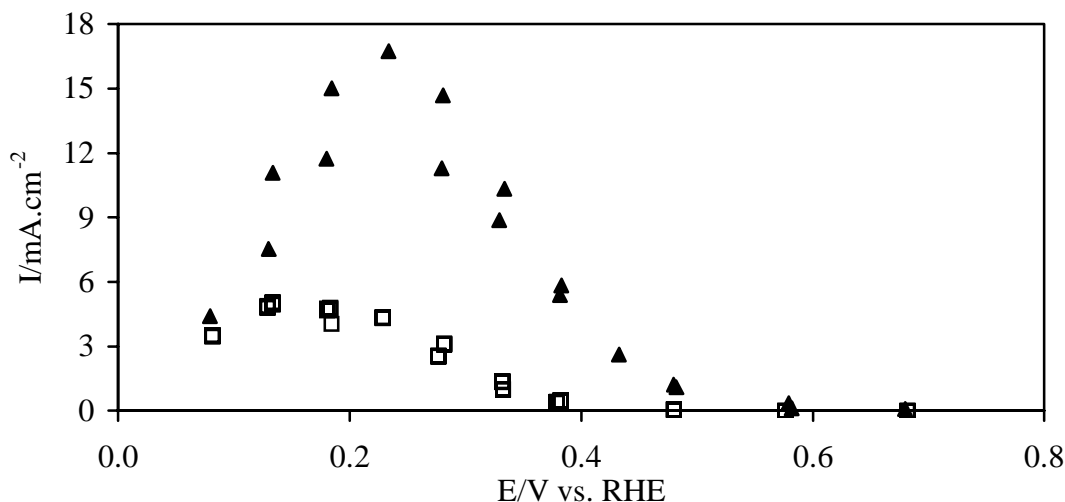


Figure 2.5: N_2O reduction on Pd in $HClO_4$ (closed triangles) and H_2SO_4 (open squares), $pH = 0.3$, solution saturated with N_2O

major product becomes NH_4^+ . A change from $HClO_4$ to H_2SO_4 has little effect on the selectivity.

3.2.2. NO reduction

The reduction of NO shows the same selectivity as the reduction of NO_2^- . Copper on palladium shows a large production of N_2O , palladium of N_2 . The reduction becomes diffusion limited due to the low solubility of NO, so a RDE setup was used.

The reduction of NO on palladium does not depend on the use of H_2SO_4 or $HClO_4$. The rate on copper electrodes however does depend on the anion used, the activity electrode in $HClO_4$ was higher than in H_2SO_4 . The activity of the palladium electrode was about 7 times higher than that of a monolayer copper on palladium electrode in H_2SO_4 , in $HClO_4$ the ratio is about 4:1 (Pd vs. Cu on Pd). These results were obtained in a copper containing solution (10 mM Cu^{2+}) at 0.24 V vs. RHE, i.e. at the potential between the UPD layer deposition and the bulk deposition. This was done to prevent changes in the copper coverage due to simultaneous oxidation of copper and reduction of NO, which leads to poor reproducibility.

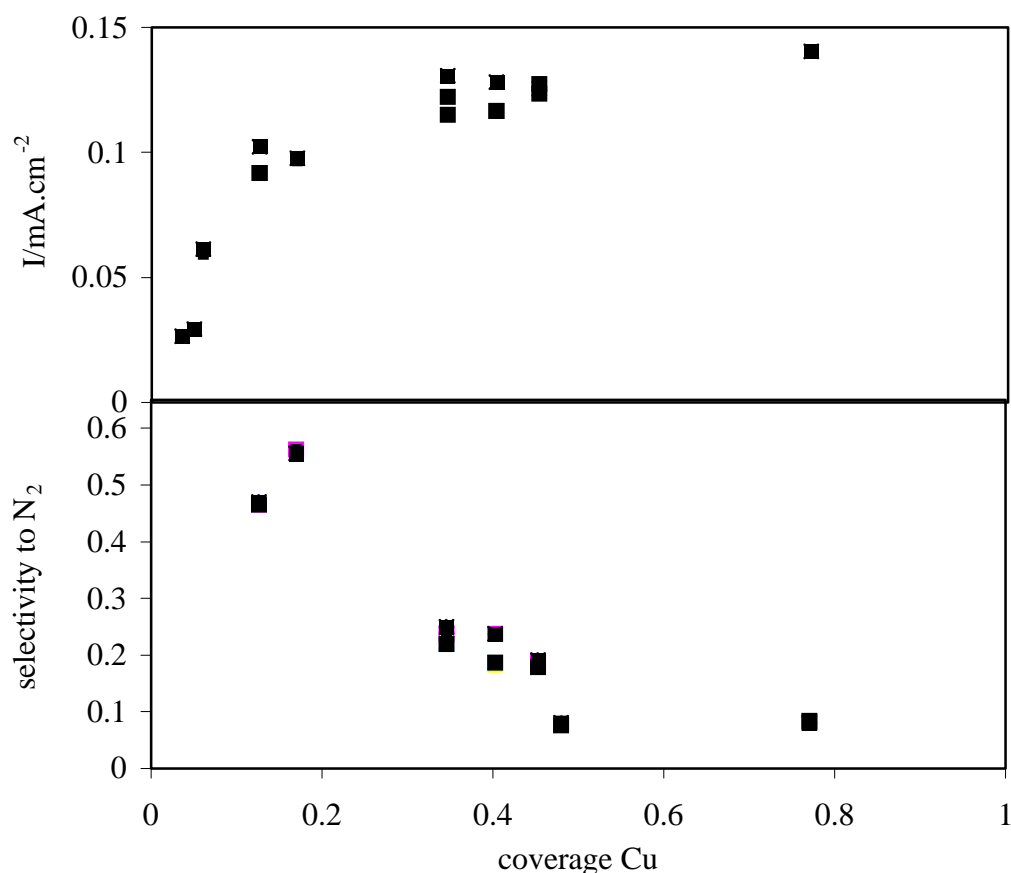


Figure 2.6: activity and selectivity of NO_3^- reduction versus copper coverage in 0.5 M NaOH, $V = 0.02$ V, $[NO_3^-] = 0.1$ M

3.2.3. N_2O reduction

The reduction of N_2O on palladium (figure 5) shows an anion effect, just as NO_3^- did, and the reduction is inhibited by H-adsorption. The selectivity to N_2 is always 100 %. Copper on palladium shows little activity for N_2O reduction.

3.3. Alkaline electrolytes

3.3.1. NO_3^- reduction

In alkaline electrolytes the activity is increased by copper, but the activity reaches a plateau value (figure 6a). Bulk copper electrodes have the same activity as copper at high coverage on palladium. This trend is independent of the potential (the

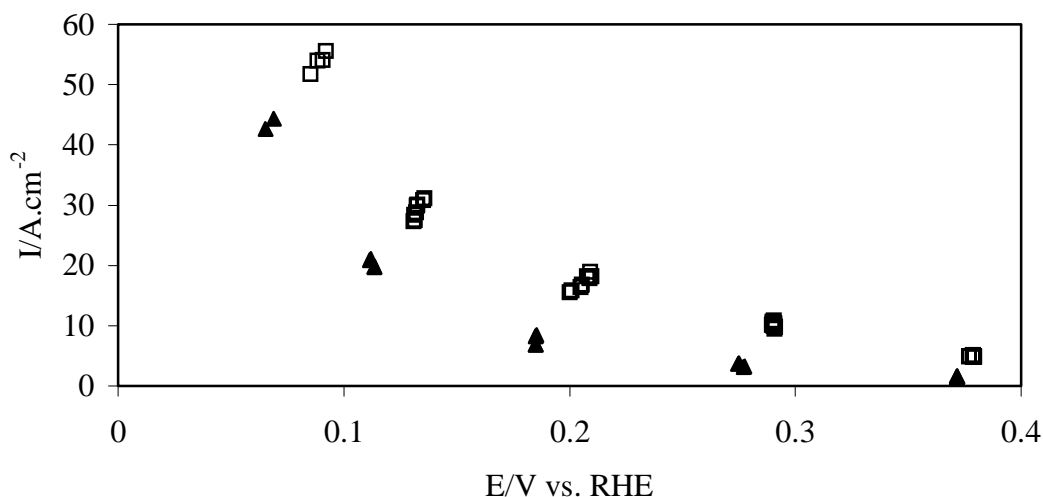


Figure 2.7: activity of palladium and copper for the reduction of NO_2^- in 0.5 M KOH, $[\text{NO}_2^-] = 0.1 \text{ M}$, open squares palladium, closed triangles copper

activity itself shows a Tafel slope of 106 mV/dec). The kinetic order of the concentration at high copper coverages is 0.7.

The selectivity to N_2 decreases with increasing copper coverage (figure 6b). The anions used in the deposition of the copper could have an effect on the selectivity, but the reproducibility of the experiments was too poor to state this with certainty. Only traces of N_2O are formed.

During RRDE-experiments on the reduction of NO_3^- NO_2^- is formed, since the cyclic voltamogram of the ring shows the same features as the cyclic voltamogram of NO_2^- , similar to the situation in acidic electrolytes. The cyclic voltamogram of NO_2^- shows little concentration dependence, so that the amount of NO_2^- produced could not be determined.

The addition of ClO_4^- or SO_4^{2-} to the solution has no effect on activity or selectivity. This is also the case during the reduction of NO_2^- and N_2O . The addition of Cl^- only deactivates the electrode slightly, unlike in the case of acidic electrolytes. I^- , however, does deactivate the electrode.

3.3.2. NO_2^- reduction

In figure 7 the reduction of NO_2^- on a palladium and a palladium/copper electrode with high copper coverage are compared. Copper is less active than palladium. Copper is also less active for the reduction of NO_2^- than for the reduction of NO_3^- .

The selectivity changes from N_2 on palladium to a combination of N_2 and N_2O on copper. This is similar to acidic electrolytes, the change is however less. The rate of reduction of NO_2^- on a palladium electrode shows a kinetic order of virtually zero, indicating a strong adsorption of NO_2^- and a relatively slow reduction. On a copper electrode the kinetic order of the concentration is about 0.5, indicating weaker adsorption.

3.3.3. N_2O reduction

The reduction of N_2O at palladium in alkaline electrolytes starts at more positive potentials than in acidic electrolytes. Copper shows little activity compared to palladium. The selectivity to N_2 is 100 % under all conditions.

4. Discussion

4.1. Activity

The first step in mechanism 1 is the adsorption of NO_3^- to the surface. The importance of this step is shown by the difference in activity between NO_3^- in HClO_4 or H_2SO_4 . This can only be explained by the difference in adsorption between the ClO_4^- and SO_4^{2-} ions. The adsorption of NO_3^- can be hindered by adsorption of SO_4^{2-} , as has been shown on platinum [21].

We tried to confirm this by EQMB experiments. The mass difference upon SO_4^{2-} adsorption was however too small to observe the expected results. When an ion is used that adsorbs even stronger the expected result was observed: upon adsorption of Cl^- , as seen by a mass decrease, the activity decreases, as seen by a decrease in Faradaic current. The mass decrease due to Cl^- adsorption runs parallel to the current

decrease of the NO_3^- reduction. This implies that Cl^- blocks the NO_3^- reduction sites in a one to one fashion. The anion effect can be seen during the reduction of N_2O as well, as has been reported in the literature [22].

The anion effects, together with the kinetic order of approximately 1, show that the activity is determined by the number of NO_3^- ions at the surface. This is depicted in figure 8 as step 1.

The second step in mechanism 1 is the reduction of NO_3^- . In acidic electrolytes the activity of the electrode is linear with copper coverage at coverages below 1 and constant above 1. This shows the role of copper as a promoter very clearly; the initial step of the reduction only takes place at the copper sites. The activity as a function of the copper coverage gives a straight line through the origin. This step is depicted in figure 8 as step 2. The electrical current does not only depend on activity, but also on the number of electrons consumed per reduced NO_3^- ion, i.e. on the selectivity. In this case however the effect would be small: the number of electrons “consumed” per NO_3^- would change from 5 (N_2) at low copper coverages to 4 (N_2O) at high copper coverages. This change is too small to be detected, given the statistical uncertainty of the measurements.

The third step in mechanism 1 is desorption or reduction of NO_2^- . The activity for this step will depend on the rate of desorption versus the rate of reduction. This will be discussed for palladium and for copper. It should be noted that the reduction from NO_2^- to NO is very fast, and NO is probably the adsorbate (as for platinum and rhodium [23]). This explains the similarity of the cyclic voltamograms of NO_2^- and NO .

NO adsorbs strongly on palladium. The first argument is the absence of an anion effect of the reduction of NO . A second argument comes from adsorbate studies, where NO will not desorb upon changing of the electrolyte with a blank solution. A third argument comes from gas phase experiments: NO adsorbed on palladium desorbs at a much higher temperature (400-500 K e.g. [24]) than NO adsorbed on copper (150-200K at low coverage NO [25]).

NO adsorbs weakly on copper. This can be seen during RRDE-experiments on palladium/copper electrodes: NO_2^- or NO can be detected at the ring, proving that

NO_2^- , or NO, desorbs from the copper surface. The RRDE-experiments could not be performed on pure palladium electrodes since these have little activity towards NO_3^- reduction. Secondly NO adsorbs competitively with SO_4^{2-} . In alkaline electrolytes the kinetic order is not zero, also indicating weak adsorption on copper.

This step is depicted in figure 8 as step 3. It is assumed that NO will either diffuse in the bulk solution and readsorb or that it will diffuse over the surface to palladium sites. The reason for this assumption will be discussed in the next section.

There is still one paradox. NO is expected to be reduced fast compared to NO_3^- , because the rate determining step of the latter is the first step. The fact that NO can be detected during RRDE-experiments would suggest that the reduction of NO is relatively slow compared to the reduction of NO_3^- . In acidic solutions this paradox can be solved. The absolute values of the current of NO_3^- reduction on Cu on Pd and NO_2^- on Pd are comparable. If a low kinetic order for NO_2^- in acidic electrolytes is assumed, as is the case in alkaline solutions, then the reduction current at the same concentration are comparable. This would explain why it can be detected at the ring, but will not be the rate determining step. In alkaline solutions however the reduction of NO_2^- is approximately 100 times faster than the reduction of NO_3^- at the same concentration, potential and electrode (figure 6 and 7).

4.2. Selectivity

The selectivity determining step in mechanism 1 is the third step, after the rate determining step has been performed. The selectivity towards N_2O is increasing with increasing copper coverage. In the case of HClO_4 as an electrolyte the selectivity is even linear with the coverage. The difference can also be seen during the reduction of NO_2^- : palladium electrodes produce mainly N_2 , copper deposited on palladium produces mainly N_2O .

Bulk copper electrodes give a different selectivity from UPD-copper electrodes, NO instead of N_2O . This shows that palladium plays a role in the catalysis by influencing the copper at the surface. A comparison of palladium/copper with similar systems (copper deposited on platinum and gold) indicates the same. Copper on platinum shows a relative increase of the selectivity towards NH_3 and copper on

gold towards NO at high copper coverages. This shows that the substrate has an influence on the selectivity of copper.

Electrolytes containing HClO₄ and H₂SO₄ show not only a large difference in activity, but also in selectivity. The difference in activity was attributed to the difference in the adsorption strength of the ions and would result in a difference in the concentration of NO₃⁻ ions at the surface. The result would be a different concentration of N-intermediates at the surface (step 2 in figure 8), and this would determine the selectivity. The way this influences the reaction is depicted in figure 8 as step 4. At low N-coverage NH₃ is formed, at high N-coverage N₂O. The N-species in acidic electrolytes is most likely NO, given the stability of NO on platinum [19,23], rhodium [23] and iridium [26] surfaces. This large effect of the anion on selectivity is not observed during the reduction of NO₂⁻, probably because NO and NO₂⁻ adsorb more strongly than NO₃⁻.

Between step 2 and 4 in figure 8 a desorption/readsorption step is included to bring NO to the palladium sites. Such a step is likely, since NO is formed on copper, but adsorbs weakly on copper and strongly on palladium.

The selectivity is also dependent on concentration, as the concentration increases the selectivity towards N₂O increases. The increase in selectivity to N₂O with concentration can be explained by an increase of the concentration N-species at the surface.

It should be noted that palladium at a high coverage of N-species would produce N₂, as can be seen during the reduction of NO (table 1). This explains the increase in selectivity to N₂ with decreasing copper coverage (figure 1b). This situation will however not occur during the NO₃⁻ reduction: palladium has little activity for the reduction of NO₃⁻, and therefore the N-coverage will be low at high palladium coverages (i.e. at low copper coverages).

4.3. Model for acidic electrolytes

The anion effect and the concentration effect on the selectivity show that the selectivity of the reaction is coupled to the activity of the reaction. To show the

relationship between activity and selectivity we propose a model based upon the coverage of N-species at the surface.

This model is shown in figure 8.

In step 1 adsorbs NO_3^- to the surface, hindered by SO_4^{2-} if present.

In step 2 NO_3^- reduces to NO_2^-/NO at the copper sites.

In step 3 NO_2^-/NO desorbs from the copper sites into the solution. Next it either adsorbs on a palladium site, on a copper site or diffuses into the bulk solution. Surface diffusion of the NO-species is also possible.

In step 4 NO is further reduced. NO at high coverage on palladium sites will be reduced to N_2 . NO at high coverage on copper sites will be reduced to N_2O . NO at low coverage on either palladium or copper will be reduced to NH_3 .

4.4. Alkaline solutions

The activity in alkaline electrolytes versus the copper coverage shows a change in slope between low and high coverages. It is unclear whether the slope becomes zero at high coverages. A possible explanation would be a shift in selectivity (from N_2 to NO_2^-) and therefore a decrease in electrons “consumed” per NO_3^- (5 to form N_2 and 2 for NO_2^-). The result would be a decrease in slope of 2/5 in the current versus copper coverage plot. The decrease in slope is however larger, so another effect must play a role as well.

The reduction shows only an anion effect when I^- is added and only slightly with Cl^- . This can be explained by assuming that OH^- bonds strongly to the surface.

As in acidic electrolytes the selectivity to N_2 decreases with increasing copper coverage in alkaline electrolytes.

A lower activity and selectivity for the reduction of NO_2^- on copper compared to palladium has been observed, similar to acidic electrolytes.

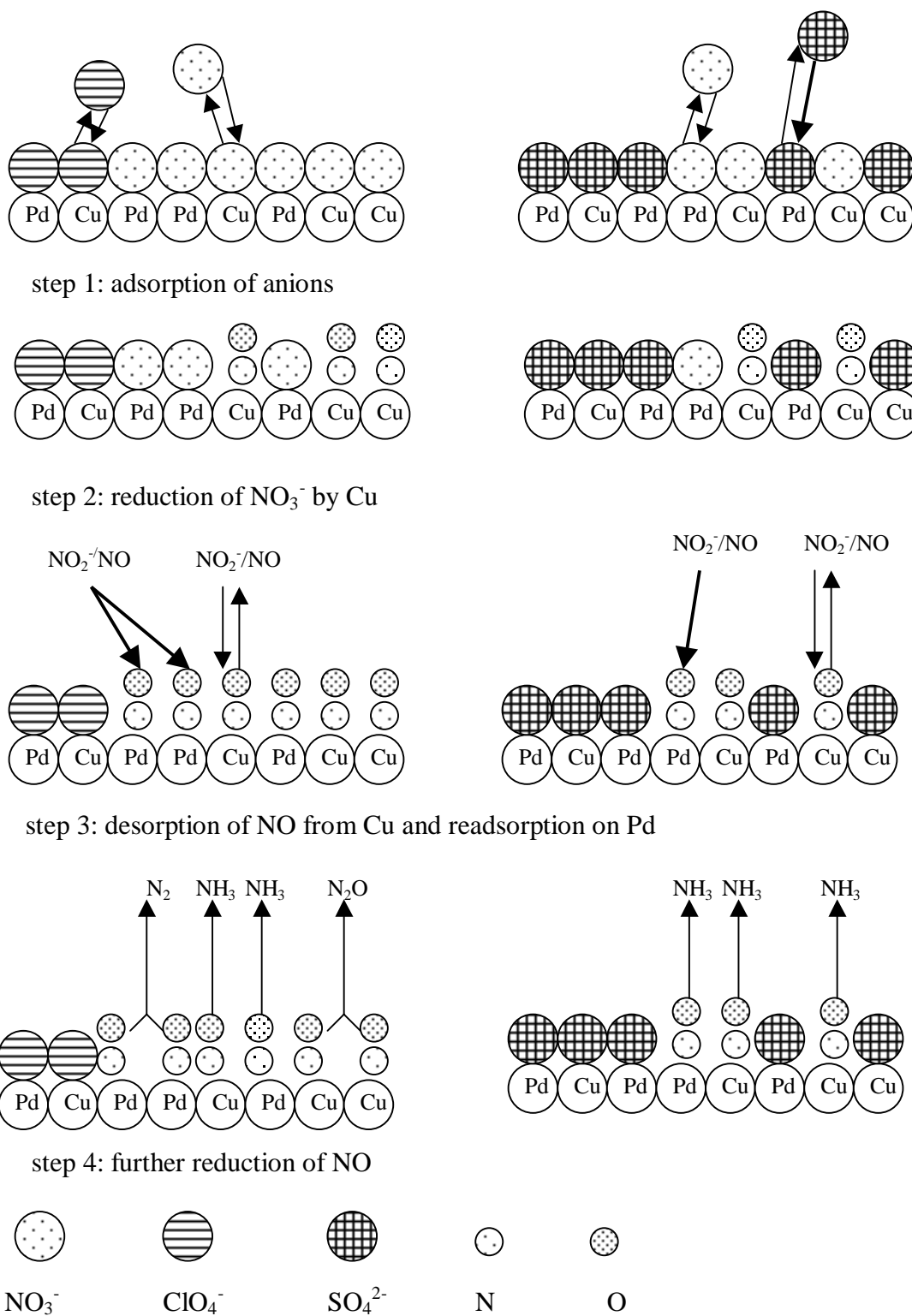


Figure 2.8: model for the reduction of NO_3^- on palladium/copper electrode.

The model proposed for acidic electrolytes will now be compared to the situation in alkaline electrolytes.

The adsorption as described in step 1 shows the anion effect like in acidic electrolytes, but only with very strongly adsorbing anions.

The rate determining step is the first electron transfer, similar to step 2 in the model. In both electrolytes a kinetic order to NO_3^- concentration of 0.7 is observed. The coverage dependence with copper is however different.

The desorption and readsorption of NO_2^- (step 3) is similar, NO_2^- can be detected at a ring electrode during RDE-experiments both in alkaline and acidic electrolytes.

Step 4, the further reduction of NO_2^- , shows the same decrease in selectivity to N_2 as in acidic electrolytes. The selectivity to N_2O however is virtually absent.

The similarities between the model in acidic electrolytes and the measurements in alkaline are too large to be ignored. It is likely the mechanism is the same, or has at least the same essential steps. There are however some differences which have not been explained yet. It is therefore not possible to prove that the mechanism is the same.

4.5. Reduction of NO to N_2

According to reaction scheme 1 N_2 can be formed by the reduction of N_2O and by a direct pathway from NO. If N_2 is formed by the reduction of N_2O sites should be available for producing N_2O and there should be sites available for reducing N_2O . It is observed that reduction of N_2O is relatively slow on copper and relatively fast on palladium, so it is possible that copper sites produce N_2O and palladium sites reduce N_2O to N_2 . Palladium sites have to be available, so the selectivity to N_2 would increase with the palladium coverage and the selectivity to N_2O would increase with copper coverage. This is consistent with the data produced in acidic electrolytes. This does not exclude parallel paths for the formation of N_2 , as also described in reaction scheme 1.

The reduction of N_2O in alkaline solutions starts at very positive potentials, even within the oxide regime, as has been reported earlier [27]. This could be an explanation for the low selectivity to N_2O in alkaline electrolytes as N_2O is easily further reduced to N_2 . It is expected from the measurements in acidic electrolytes that

at high coverages of copper the selectivity to N_2O would increase. If all the N_2O would reduce further, the selectivity to N_2 would increase since N_2 is the only product of N_2O reduction. In our case however we find a decrease in selectivity to N_2 with increasing copper coverages. This does not fit with N_2O as the intermediate for N_2 production; N_2 has to be produced by a pathway different from the reduction of N_2O .

This reasoning assumes the reaction follows the scheme as described in section 4.3 in both acidic and alkaline electrolytes. If the mechanism would change in alkaline electrolytes then the argumentation does not hold and the mechanism would have to be solved in both cases separately.

4.6. Comparison with drinking water purification catalysts

In this section we compare the predictions from our model for the mechanism with the data from the catalyst used for NO_3^- reduction in drinking water [1,3-5,7,9,14,29].

An increasing activity is observed with an increasing Cu:Pd ratio, as is predicted [1]. What is not predicted however is that at Cu:Pd ratios above 1:4 the activity decreases, but in alkaline solutions there was a decrease in slope of the activity versus copper coverage. It must be noted that the Cu:Pd ratios can not be translated directly to a Cu-coverage, the Cu-coverage depends on the preparation method [7,10]. The preparation method used in ref. [1] would give a relatively high Cu-coverage [7,10]. It might be that at Cu:Pd ratios of higher than 1:4 the surface is almost totally covered with copper and that the hydrogen dissociation becomes the rate limiting step instead of the NO_3^- reduction, which could not be the case during an electrochemical experiment.

At Cu:Pd ratios higher than 1:4 the selectivity to NO_2^- increased [14]. This is predicted in our model as well, especially if the surface coverage of copper becomes greater than 1, i.e. if bulk copper is formed at the surface. It would be important to check if bulk copper exists at the surface, because copper deposited on palladium reacts differently from bulk copper. The preparation method has to be chosen to avoid this problem.

Our model predicts that at a more negative potential the selectivity to NH_3 would be higher. A more negative potential corresponds to a higher partial pressure or

concentration of reductor. A higher selectivity to NH_3 at higher partial pressures of hydrogen has indeed been observed.

HCl is used as a neutralizer of the produced OH^- [1,3-5,7,9,14,29]. In acidic electrolytes this decreases the activity and selectivity to N_2 greatly, as is shown in figure 4. This is not the case for the drinking water catalyst however, where in neutral environments the addition of Cl^- shows an increase in activity and selectivity [29]. This is probably due to changes in the pH near the surface; during the reduction of NO_3^- the pH near the surface becomes more alkaline and this decreases both activity and selectivity to N_2 . During a reduction of NO_3^- in the presence of Cl^- the pH stayed lower than without Cl^- . Both SO_4^{2-} and HCO_3^- act as a pH-buffer and therefore improve the selectivity. As the solution becomes more alkaline more NH_3 is produced.

The catalyst for NO_3^- reduction in drinking water (pH between 5 and 9) shows similarities with a Pd/Cu-electrode in alkaline electrolytes. The selectivity to N_2O is in both cases very low [4]. Another resemblance is the absence of the anion-effect. It would be interesting to check the dependence of the activity of the drinking water catalyst with the copper coverage, but unfortunately the surface composition is unknown.

It should be noted that the value for the selectivity towards N_2 reported by Tacke [4] (>98%) is much higher than in our results (max. 60 %). Our model predicts that if palladium is added to the PdCu catalyst the intermediate NO_2^- will be reduced to N_2 , and this has indeed been observed [14]. It might be possible that the preparation method of the PdCu catalyst does not create uniform particles, but leaves some palladium uncovered. This will increase the selectivity compared to only PdCu catalyst. The increased selectivity can of course be attributed to other differences, like for instance the pH and experimental setup.

5. Conclusion

The role of copper in the Pd/Cu-catalyst is to enhance the reduction of NO_3^- to NO_2^- , both in the initial adsorption of NO_3^- and in the electron transfers. Copper has a negative influence on activity and selectivity after this step, and for this reason the yield of N_2 goes through a maximum. The reaction is very dependent on the electrolyte composition both as regards to pH and anions in the solution. The anion

dependence is explained in terms of the coverage of N-species at the surface; a high coverage of N-species gives high activity and selectivity to N₂ and N₂O, a low coverage of N-species gives NH₃.

References:

- [1] S. Hörold, K.-D. Vorlop, T. Tacke and M. Sell, *Catal. Today* 17 (1993) 21
- [2] J.F.E. Gootzen, P.G.J.M. Peeters, J.M.B. Dukers, W. Visscher and J.A.R. van Veen *J. Electroanal. Chem.* 434 (1997) 171
- [3] U. Prüsse, M. Kröger and K.-D. Vorlop, *Chem.-Ing.-Tech.* 69 (1997) 87
- [4] T. Tacke, dissertation, Techn. Univ. Braunschweig 1991 pg. 81
- [5] T. Tacke and K.-D. Vorlop, *Chem.-Ing.-Tech.* 65 (1993) 1500
- [6] G. Strukul, F. Pinna, M. Marella, L. Meregalli and M. Tomaselli, *Catal. Today* 27 (1996) 209
- [7] J. Batista, A. Pintar and M. Ceh, *Catal. Lett.* 43 (1997) 79
- [8] A. Pintar, J. Batista, J. Levec and T. Kajuchi, *Appl. Catal. B: Environ.* 11 (1996) 81
- [9] U. Prüsse, S. Hörold and K.-D. Vorlop, *Chem.-Ing.-Tech.* 69 (1997) 93
- [10] F. Skoda, M.P. Astier, G.M. Pajonk and M. Primet, *Catal. Lett.* 29 (1994) 159
- [11] T. Chierchie and C. Mayer, *Electrochim. Acta* 33 (1988) 341
- [12] J. Wärnä, I. Turunen, T. Salmi and T. Maunula, *Chem. Eng. Sci.* 49 (1994) 5763
- [13] N.E. Khomutov and U.S. Stamkulov, *Sov. Electrochem.* 7 (1971) 312
- [14] M. Hähnlein, U. Prüsse, S. Hörold and K.-D. Vorlop, *Chem.-Ing.-Tech.* 69 (1997) 90
- [15] M. Meierer, S. Harmgart and J. Fahlke, *VGB Kraftwerkstechnik* 75 (1995) 902
- [16] J. Willsau, and J. Heitbaum, *J. Electroanal. Chem.* 194 (1985) 27
- [17] manual mass spectrometer, Balzers AG (1991), Balzers Liechtenstein
- [18] W. Visscher, J.F.E. Gootzen, A.P. Cox and J.A.R. van Veen, *Electrochim. Acta* 43 (1998) 533
- [19] J.F.E. Gootzen, R.M. van Hardeveld, W. Visscher, R.A. van Santen and J.A.R. van Veen, *Recl. Trav. Chim. Pays-Bas* 115 (1996) 480
- [20] S. Ye and H. Kita, *J. Electroanal. Chem.* 346 (1993) 489
- [21] G. Horanyi and E.M. Rizmayer, *J. Electroanal. Chem.* 140 (1982) 347
- [22] A. Ahmadi, E. Bracey, R. Wyn Evans and G. Attard, *J. Electroanal. Chem.* 350 (1993) 297
- [23] A. Rodes, R. Gómez, J.M. Pérez, J.M. Feliu and A. Aldaz, *Electrochim. Acta* 41 (1996) 729-745
- [24] R.D. Ramsier, Q. Gao, H. Neergaard Waltenburg, K.-W. Lee, O.W. Nooi, L. Lefferts and J.T. Yates Jr. *Surf. Sci.* 320 (1994) 209
- [25] P. Dumas, M. Suhren, Y.J. Chabal, C.J. Hirschmugl and G.P. Williams, *Surf. Sci.* 371 (1997) 200
- [26] S. Zou, R. Gomez and M.J. Weaver, *Langmuir* 13 (1997) 6713
- [27] N. Furuya and H. Yoshiba, *J. Electroanal. Chem.* 303 (1991) 271
- [28] A. Pintar, M. Setinc and J. Levec, *J. Catal.* 174 (1998) 72

Chapter 3: Mechanistic Study of the Nitric Oxide Reduction on a Polycrystalline Platinum Electrode

Abstract

A systematic study was performed to determine the mechanism of the nitric oxide (NO) reduction on polycrystalline platinum. Both the reduction of NO in the presence of NO in the solution and the reduction of adsorbed NO in a clean electrolyte have been investigated.

The adsorbate reduction takes place through a combined proton/electron transfer in equilibrium followed by a rate determining chemical step. NH_3 is the only product in the absence of NO in solution.

The reduction in the presence of NO in the solution at potentials between 0.4 and 0.8 V vs. RHE yields N_2O as the only product. The mechanism of this reaction is not of the Langmuir-Hinshelwood type, but rather involves the combination of a surface-bonded NO molecule with a NO molecule from the solution and a simultaneous electron transfer. A protonation has to take place prior to this step. In alkaline solutions a chemical step appears to be partially rate determining. The continuous reduction of NO at potentials lower than 0.4 V yields mainly NH_3 . The mechanism of this reaction is the same as for the adsorbate reduction.

1. Introduction

The reduction of nitric oxide (NO) is an important reaction in environmental catalysis, since it determines the performance of wastewater treatment catalysts for nitrate, nitrite and NO removal. Platinum is known to be one of the best catalysts for the reduction of NO, both in the gas phase and at the electrochemical interface [1].

A variety of mechanisms and intermediates for the electrochemical reduction of NO have been suggested in the literature [2-7]. Based on the Tafel slope and the pH dependence, Colluci et al. [6] concluded that the rate determining reaction in the continuous reduction (i.e. in the presence of NO in solution) is $\text{NO}_{\text{ads}} + \text{H}^+ + \text{e}^- \rightarrow \text{NOH}_{\text{ads}}$. Recently Gootzen et al. [7] suggested that the reduction of NO in aqueous solutions could be similar to the reduction in gas phase, involving a NO dissociation step $\text{NO}_{\text{ads}} \rightarrow \text{N}_{\text{ads}} + \text{O}_{\text{ads}}$. Both groups assume that all the reacting species are adsorbed on the surface, except for protons and water. However, neither of the two mechanisms can explain why the products of the adsorbate reduction [7] and the continuous reduction are different [2] and why the continuous reduction starts ca. 400 mV more positive than the adsorbate reduction.

The objective of this article is to clarify these mechanistic aspects of both the continuous reduction and the adsorbate reduction of NO on polycrystalline platinum. To this end a systematic study is performed to determine the kinetic parameters and the selectivity, using the potential, pH, kinetic order in NO, H/D isotope effects, coverage and supporting electrolyte as variables.

2. Experimental

Rotating disk electrodes (RDE) of platinum were used in a homemade setup (real surface area 1.36 cm²). Adsorbate studies were performed on a platinum flag electrode (real surface area 4.40 cm²). The counter electrode in all cases consisted of a platinum flag. An AUTOLAB Pgstat 20 potentiostat was used for all RDE and adsorbate experiments. DEMS (Differential Electrochemical Mass Spectroscopy) measurements were performed on a Balzers Prisma QMS 200 mass spectrometer. Details of the setup are described elsewhere [8]. The DEMS signals of N₂, N₂O and NO were calibrated by oxidizing a monolayer of CO and measuring the amount of

CO₂. The signal was corrected for differences in sensitivity and fragmentation probability.

A Hg/HgSO₄ reference electrode was used for all measurements in H₂SO₄ except for the measurements at varying pH and in HClO₄ in which case a saturated PdH reference was used. In alkaline solutions a Hg/HgO reference electrode was used. All potentials reported in this chapter are converted to the RHE scale.

All glassware was cleaned in boiling H₂SO₄/HNO₃ to remove organic contaminations. Flag and DEMS electrodes were cleaned by flame annealing. RDE electrodes were cleaned by repeated cycling in the oxide region, after which the electrolyte was replaced. All measurements that were not reproducible within an accuracy of at least 10% were discarded.

All solutions were prepared with p.a. grade chemicals (Merck) and Millipore Gradient A20 water. D₂O (99.8 % deuterated, Merck) was distilled prior to the measurement to remove organic contaminations. All solutions were deaerated by purging with argon. NO was bubbled through two 2 M KOH washing flasks to remove NO₂ [3,6]. The solubility of NO is $1.4 \cdot 10^{-3}$ mol/l [6] in water at room temperature.

Adsorbate studies were performed by saturating the surface in a solution of saturated NO or 2 mM NaNO₂ under open circuit potential (OCP). NO adsorbates used for stripping in alkaline electrolytes were formed in a 0.1 M H₂SO₄ solution; NO adsorbates for stripping in acidic electrolytes were formed in a solution of the same composition as the electrolyte. At the beginning of the adsorption process an OCP of circa 0.4 V was observed. On a smooth electrode, after completion of the adsorption process, the OCP was 0.85 V when NO was used and 0.87 V when NO₂⁻ was used. On a rough electrode the OCP was 0.90 V upon completion when NO was used. When NaNO₂ was used the adsorption took place in a second cell and the electrode was transferred afterwards to a clean electrolyte. The electrode was protected by a droplet during the transfer. When NO was used the adsorption took place in the same cell as the adsorbate reduction, and the solution was replaced four times to remove NO from the solution. IR spectroscopy has shown that NO and NO₂⁻ yield the same adsorbate [9].

3. Results

3.1 NO adsorbate reduction in acidic solution

A typical stripping voltammogram of a platinum electrode saturated with NO in H₂SO₄ is given in figure 1, together with the DEMS signal for m/z = 44 (N₂O).

The absence of N₂O formation is in agreement with earlier observations of Gootzen et al. [7] and FTIR measurements by Rodes et al. on Pt (100) [10]. The charge involved in the reduction is 394 μC/cm² (corrected for hydrogen adsorption, as assessed from the voltammogram in the absence of NO adsorbates), which corresponds to a maximum coverage of 0.38. The voltammetric profile obtained in the positive sweep after NO reduction, is identical to that of the profile of a clean electrode in a clean solution, confirming that the NO adsorbate has been completely reduced and the surface is free of contaminations. The pH was observed to have no effect on the reduction profile on the RHE scale. The only product formed is NH₄⁺, as no N₂O and N₂ are detected using DEMS and no electroactive species (like H₂NOH) are detected during RRDE experiments [7]. NH₄⁺ is not electroactive [11].

When HClO₄ is used instead of H₂SO₄ the first reduction peak stays the same. The second peak is shifted 30 mV in the positive direction. The third peak has decreased to a shoulder on the second peak. The charge involved in the reduction is 379 μC/cm², which is similar to the value in H₂SO₄.

The influence of the initial NO coverage was studied by decreasing the adsorption time and the concentration of NO₂⁻. A typical profile is shown in figure 2 (solid line), together with the profile of the adsorbate at saturation coverage (line with triangles) and the blank profile (dotted line). In this case the coverage is 28 % of the saturation coverage.

The coverage was also decreased by partial reduction of a saturated layer of NO. The electrode was kept for 30 seconds at a potential of 0.15 V (i.e. at a potential between the first two peaks) and then stepped back to 0.6 V. The resulting profile is also shown in figure 2 (line with squares). The coverage is 26 % of the maximum coverage. A tenfold increase of the period at which the potential is held at 0.15 V has no influence on the profile.

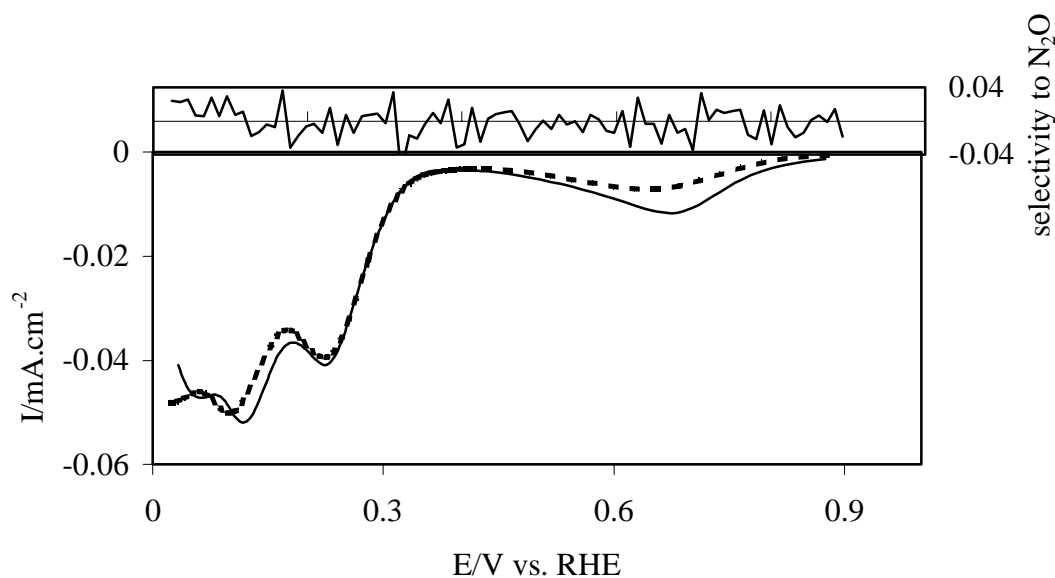


Figure 3.1: Reduction of adsorbed NO in H_2O and D_2O (lower part) and the selectivity to N_2O (upper part), 0.1 M H_2SO_4 , scan rate 20 mV/sec. Solid line H_2O , dotted line D_2O .

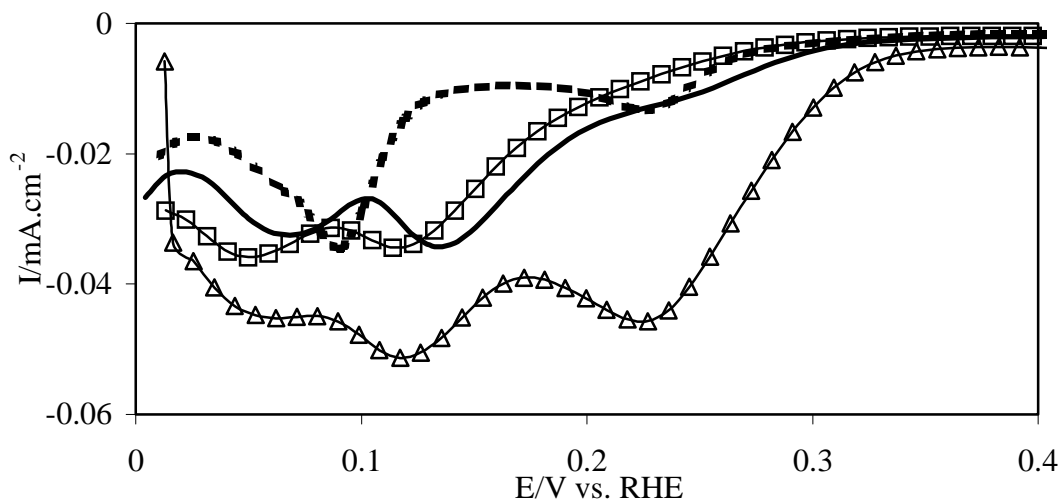


Figure 3.2: NO adsorbate reduction at low coverage, 0.1 M H_2SO_4 , scan rate 20 mV/sec. Dotted line is blank, line with triangles is at maximum NO coverage, solid line is NO adsorbed from a dilute solution, line with squares is NO partially reduced from maximum coverage

Both profiles at reduced coverage have the same general shape: only the most cathodic of the two main peaks is present. When the amount of NO is decreased by partial reduction the peak is at the same potential as at maximum coverage. When a

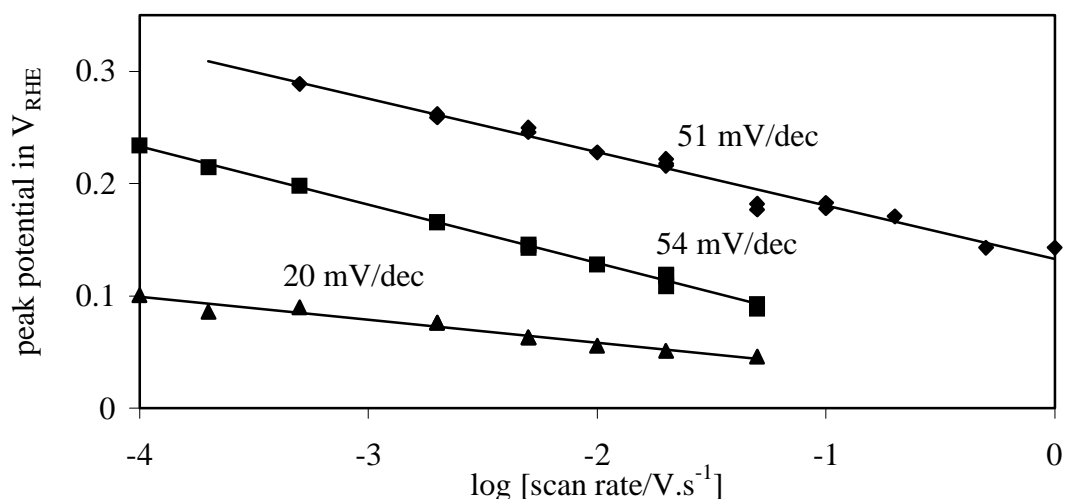


Figure 3.3: Tafel plot of NO adsorbate reduction, 0.1 M H₂SO₄. The three curves correspond to the three peaks in figure 1.

small amount of NO is adsorbed a small positive shift of 20 mV is observed compared to the maximum coverage.

The Tafel slope was estimated by plotting the stripping peak potential versus the logarithm of the scan rate ν . It has been shown that this plot indeed yields a Tafel slope if the rate of the reaction is first [12] or second order [13] in the coverage. We will argue in section 4.2 that there is strong evidence that the NO adsorbate reduction is first order in the NO coverage. Hence, in the following, we will refer to this $dE/d\log\nu$ as the Tafel slope.

The results are depicted in figure 3. The two main peaks show a Tafel slope of 51 resp. 54 mV/dec. The third peak shows a Tafel slope of 20 mV/dec. At scan rates higher than 50 mV/sec the second and the third peak start to overlap. Since all three peak potentials depend on the scan rate, typical for an irreversible process, we ascribe them to the NO reduction reaction, and not to the reversible hydrogen UPD process.

In order to test for a kinetic isotope effect the general shape of the stripping voltammetry and the Tafel slope have been measured in D₂O. The profiles at 20 mV/sec in H₂O and D₂O are compared in figure 1. The general shape remains the same, but the second main peak and the third peak have shifted 20 mV to negative potentials. The Tafel slopes corresponding to all three peaks are the same as in H₂O.

At the start of the reduction in figure 1 a small peak is seen at the same potential as that for the reduction of platinum oxides. This peak is observed only if NO_2^- is used for adsorbing NO at the surface, whereas it is not present when NO is used on a flat electrode. The peak is also observed when NO is adsorbed on a roughened platinum electrode; as mentioned in the experimental section the OCP after the adsorption is completed is 50 mV higher on a roughened electrode than on a smooth electrode.

Repeated measurements showed that the peak increases rapidly if trace amounts of oxygen are present. The adsorbate reduction itself does not change in the presence of trace amounts of oxygen.

3.2 *NO adsorbate reduction in alkaline solution*

The reductive stripping voltammetry of adsorbed NO in alkaline solutions shows only one peak. A typical profile is shown in figure 4, together with the profile in H_2SO_4 . No gaseous products are detectable during the reduction. It is unlikely that H_2NOH is formed, since acidic solutions show no electroactive species and the reduction of H_2NOH in alkaline solutions is faster than in acidic solutions [14]. The only product formed is therefore NH_3 . The (corrected) charge involved in the reduction is $367 \mu\text{C}/\text{cm}^2$, which corresponds to a maximum coverage of 0.34. The reduction peak shows a Tafel slope of 58 mV/dec, which is the same as in acidic electrolytes.

The stripping profile was measured in both 0.1 M and 1 M KOH to determine the pH dependence. The peak potential shifts 15 ± 5 mV in the positive direction on the RHE scale when the pH was increased, implying a more facile reduction in 1 M KOH.

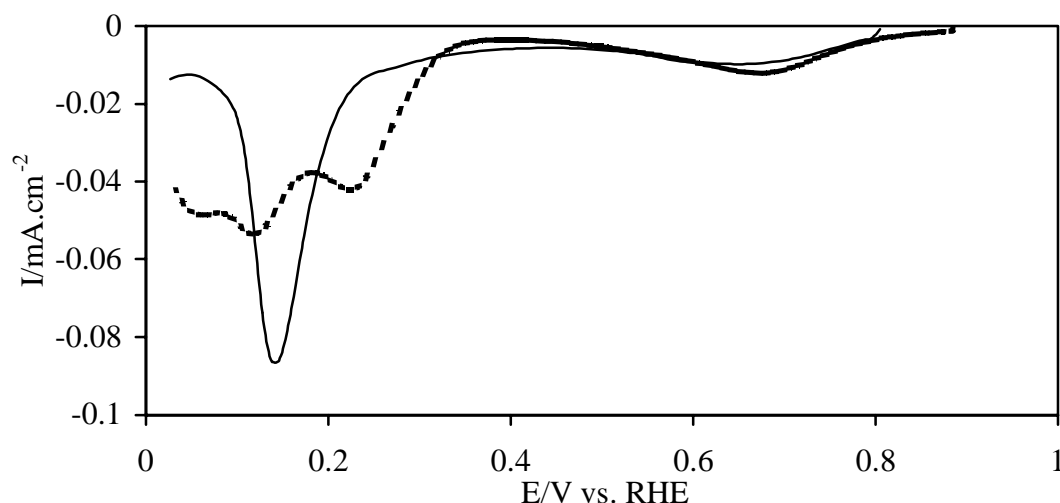


Figure 3.4: Reduction of adsorbed NO in KOH compared to H_2SO_4 , solid line 0.5 M KOH, dotted line 0.1 M H_2SO_4

3.3 Continuous reduction of NO in acidic solutions

The continuous reduction of NO was studied at platinum rotating disk electrodes. A typical steady-state polarisation curve at the lowest rotation frequency used is shown in figure 5a.

In figure 5b the number of electrons involved in the reduction process as extracted from the Levich equation is given [12].

$$\frac{1}{I} = \frac{1}{I_{kin}} + \frac{1}{0.62nFC^*D^{\frac{2}{3}}\nu^{-\frac{1}{6}}\omega^{\frac{1}{2}}}$$

To calculate the number of electrons the following values are used: $C^* = 1.40 \cdot 10^{-3}$ mol/dm³, $D = 2.5 \cdot 10^{-5}$ cm²s⁻¹ and $\nu = 8.5 \cdot 10^{-3}$ cm²s⁻¹ [6]. The same figure also shows the selectivity to N₂O determined using DEMS ($m/z = 44$), in which, clearly, the mass transport conditions are different from the RDE setup. At potentials lower than 0.3 V the number of electrons consumed per NO molecule starts to change, and at this point the DEMS measurements indicate a decrease in the selectivity to N₂O. Little N₂ is detected at any potential. At low potentials the main product is NH₃, since 5 electrons are consumed per NO molecule. It is known that at potentials lower than 0.3 V

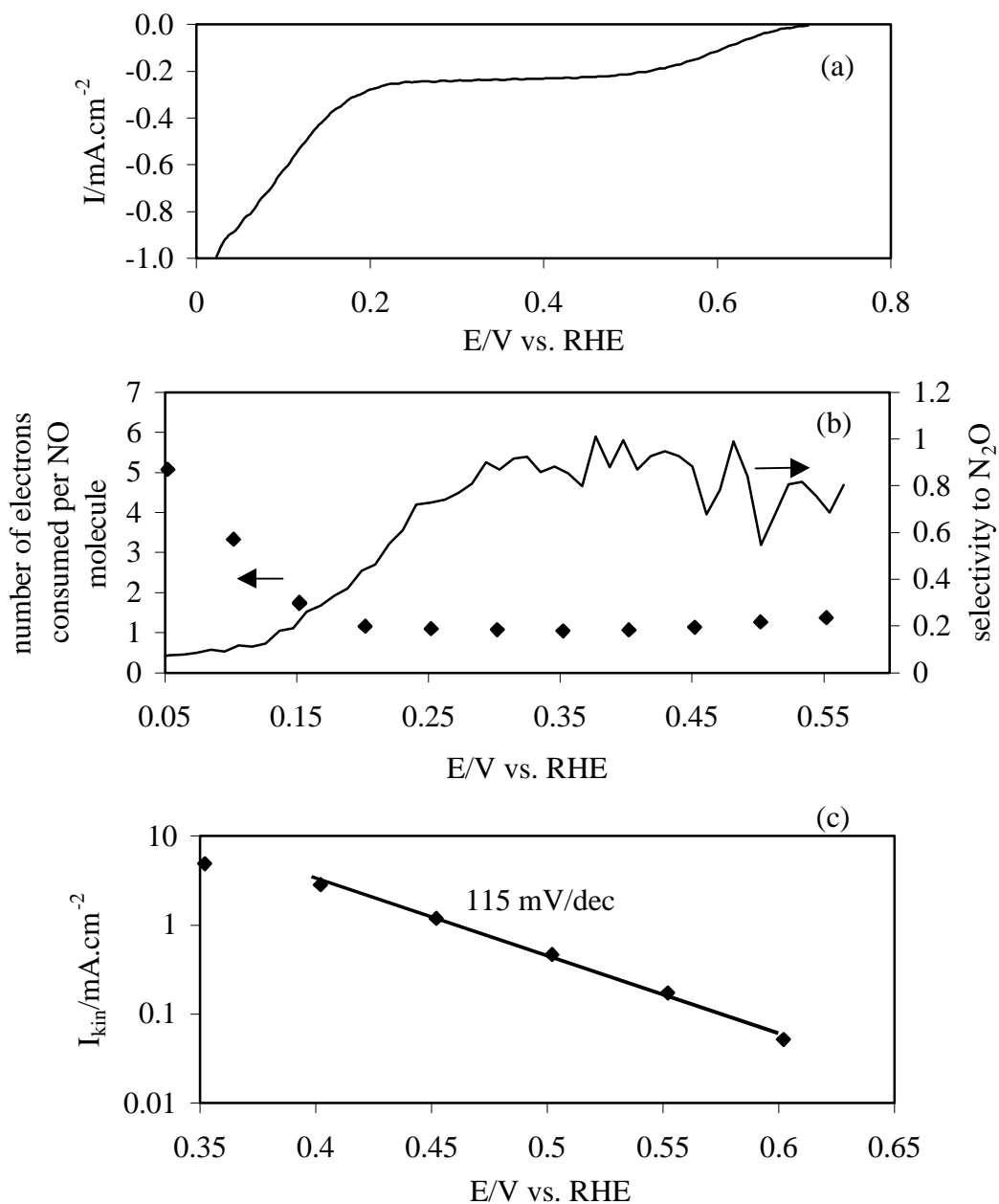


Figure 3.5, a: Typical polarisation curve, $\omega = 2 \text{ Hz}$, solution saturated with NO. b: Selectivity dependence of the continuous NO reduction on potential, $0.1 \text{ M H}_2\text{SO}_4$, solution saturated with NO. c: Kinetic limited current vs. potential, solution saturated with NO, $0.1 \text{ M H}_2\text{SO}_4$

H_2NOH can also be formed [2], but at very low potentials the selectivity to H_2NOH decreases [5]. At potentials lower than 0.35 V the Levich plot shows a curved instead of a straight line (figure 6), and the kinetically limited current can not be determined, although the number of electrons per NO molecule can still be estimated.

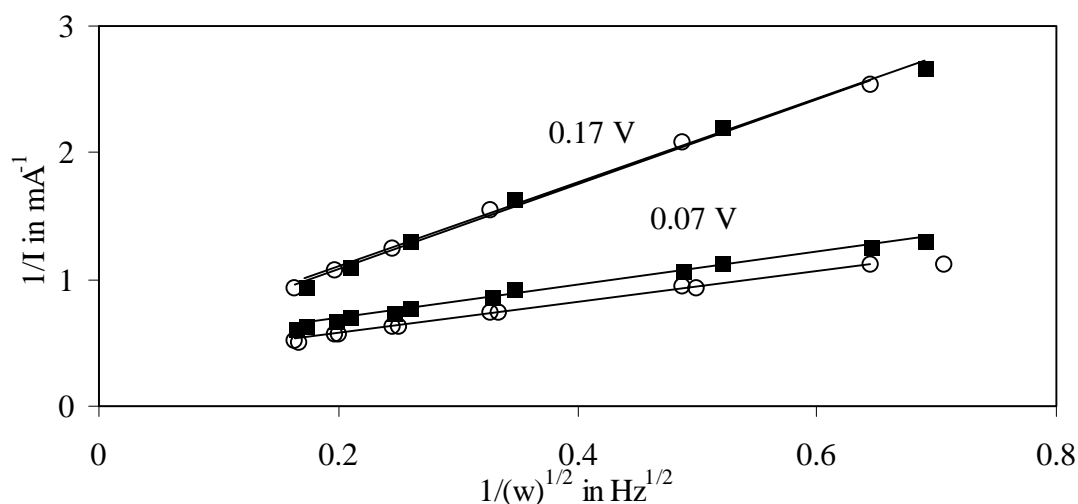


Figure 3.6: Levich plots of the NO reduction in H₂O and D₂O at 0.17 and 0.07 V, 0.1 M H₂SO₄, solution saturated with NO, open circles H₂O, closed squares D₂O

The Tafel slope, as determined from the kinetically limited current, in the region from 0.4 to 0.65 V is 115 mV/dec (figure 5c). As for the adsorbate reduction the pH was observed to have no effect on the reduction profile on the RHE scale.

When deuterated water (D₂O) was used instead of H₂O the activity at potentials higher than 0.1 V did not change compared to H₂O. At lower potentials a small decrease in activity was observed. A comparison of the Levich plots at 0.17 and 0.07 V in H₂O and D₂O is given in figure 6, illustrating this observation.

The kinetic order in NO was determined by diluting a saturated solution of NO with clean base electrolyte, and measuring the kinetic limited current in the usual way. Figure 7 shows the results and clearly illustrates that the kinetic order in solution NO in the N₂O producing region is 1.

In the ammonia producing potential region this procedure for determining the kinetic reaction order did not work because of the non-linear Levich plots. Here a qualitative idea of the reaction order was obtained by bubbling NO through the clean electrolyte in the DEMS setup, and plotting the measured current vs. the NO mass signal. Figure 8 shows results in both the N₂O producing region (0.4 V) and the NH₃ producing region (0.0 V). Fig. 8a confirms the first-order kinetics in NO in producing

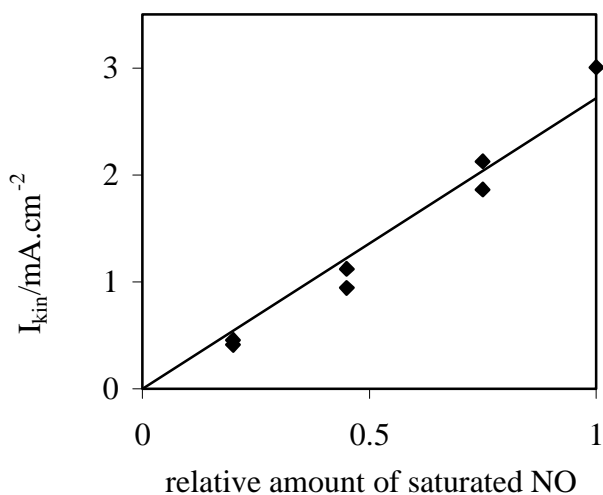


Figure 3.7: kinetic limited current of NO reduction in a saturated solution of NO diluted with clean electrolyte, 0.1 M H_2SO_4 , 0.4 V

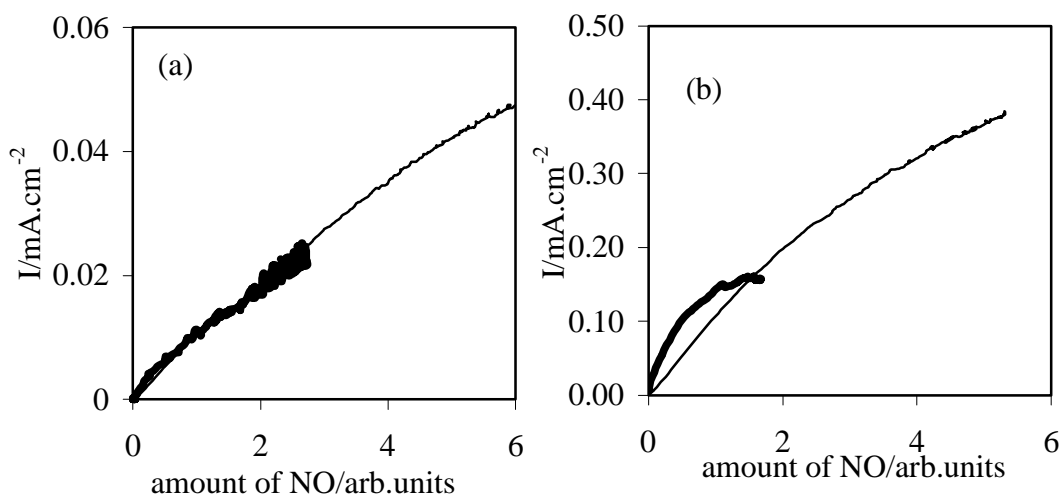


Figure 3.8: Kinetic order of NO from DEMS experiments at 0.4 V (figure a) and 0 V (figure b), thick line 0.5 M KOH, thin line 0.1 M H_2SO_4

N_2O , whereas the measurements at 0.0 V (fig. 8b) suggest a kinetic order significantly lower than one when producing NH_3 .

3.4 Continuous reduction of NO in alkaline solutions

The continuous reduction was studied in alkaline solutions using the RDE setup, similar to the measurements in acidic electrolytes.

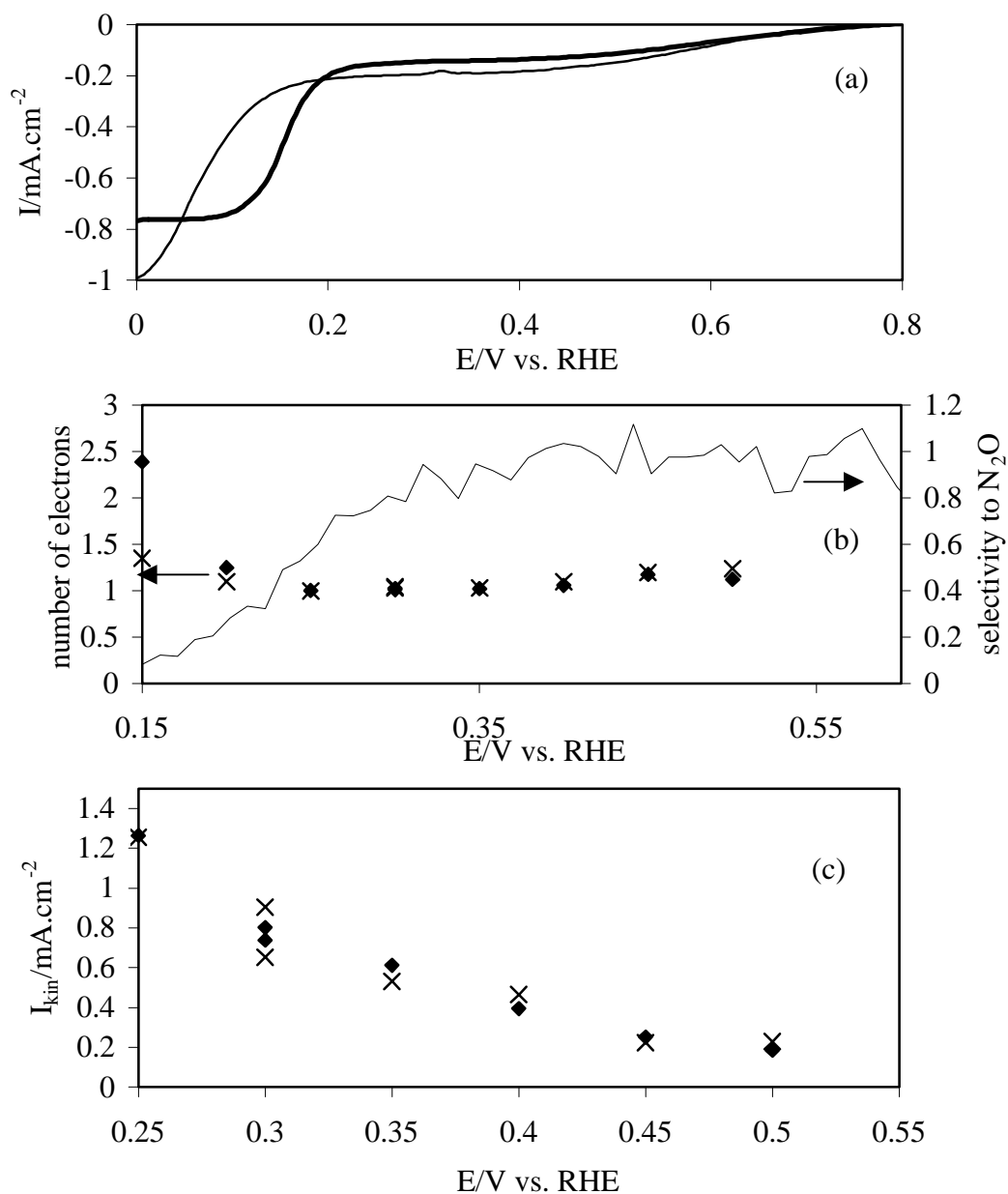


Figure 3.9, a: Typical polarisation curve, $\omega = 2$ Hz, solution saturated with NO, thick line 1 M KOH, thin line 0.1 M KOH. b: Dependence of the selectivity measured by RDE and DEMS of the NO reduction on the potential in 0.1 M and 1 M KOH, solution saturated with NO. c: Kinetically limited current of the NO reduction in 0.1 and 1 M KOH versus potential, solution saturated with NO, crosses 0.1 M KOH, solid diamonds 1 M KOH

A typical steady-state polarisation curve in 1M and 0.1 M KOH at the lowest rotation frequency used is shown in figure 9a. The number of electrons consumed per NO molecule and the DEMS signal for $m/z = 44$ in a 1 M KOH solution are plotted in

figure 9b. The general shape and the selectivity are similar to acidic electrolytes, and the potential at which the selectivity changes is the same. Like in acidic electrolytes the data at low potentials (lower than 0.2 V) suffer from the fact that the Levich plots are non-linear. In figure 9c the kinetic limited current derived from the RDE experiments in between 0.25 and 0.5 V is plotted. The current in figure 9c is only weakly dependent on potential; an approximate Tafel slope of 300 mV/dec is obtained.

The pH dependence was measured by comparing the reduction in 0.1 M and 1 M KOH. To compare the Levich slopes in 0.1 M and 1 M KOH a correction had to be made for the difference in viscosity and the diffusion coefficient. The correction was made by assuming that the selectivity at high potentials (0.4-0.6 V) is always 100 % to N₂O.

The data points in figure 9c in the N₂O producing region are the same in 0.1 M and 1 M KOH on the RHE scale, so the reaction shows the usual pH dependence in this potential region. It is observed that at 0.05 V the kinetically limited current in 1 M KOH is about 20 times higher than in 0.1 M KOH. An increased activity is observed throughout the potential region where NH₃ is formed both in the cyclic voltammetry and the RDE experiments. The point at which the selectivity changes from N₂O to NH₃ is shifted ca. 40 mV in the positive direction upon going from 0.1 M to 1 M KOH.

The kinetic order in NO at 0.4 V and 0.0 V was estimated using the DEMS setup, and is shown in figure 8 (thick line). At 0.4 V the kinetic order of the reaction rate (both current and N₂O production) in NO is one whereas at 0.0 V, in the NH₃ producing region, the order becomes much less than one.

4. Discussion

4.1 Adsorption of NO

When the adsorption of NO and NO₂⁻ on smooth electrodes are compared, it appears that some platinum oxides are formed in the case of NO₂⁻, presumably

according to $\text{HNO}_2(\text{aq}) \rightarrow \text{NO}_{\text{ads}} + \text{OH}_{\text{ads}}$. This is inferred from the small reduction peak at ca. 0.65 V, observed during the adsorbate stripping (figs. 1 and 4). The increase in the OCP after adsorption of NO_2^- compared to NO is consistent with an increase in the amount of platinum oxides. It must be noted that the OCP is well within the region where platinum oxides are formed, but no platinum oxides are detected in the case of NO. Apparently NO adsorption blocks the formation of surface oxides.

However, when NO is adsorbed on a roughened electrode, platinum oxides are detected very similar to those observed of the HNO_2 decomposition on the surface. Gootzen et al. [7] have previously ascribed this observation to NO dissociation, but since it is not observed on a smooth electrode, a different mechanism seems more likely. Possibly, on a smooth surface the NO surface concentration is homogeneous, whereas on a substantially roughened surface, it is not unlikely that the NO concentration at certain places is higher than at others, which in turn may set up local cells with NO reduction as the cathodic branch and platinum oxidation as the anodic branch. The overall reaction $2 \text{NO}(\text{aq}) + \text{H}_2\text{O} \rightarrow \text{N}_2\text{O}(\text{aq}) + 2 \text{OH}_{\text{ads}}$ is irreversible and possible since the OCP during adsorption is in the potential region where NO can be reduced to N_2O . The end result is a slight oxidation of the platinum surface, reflected in a small positive shift of the NO adsorption potential.

It should be noted that the presence or absence of platinum oxide reduction peak at 0.65 V has no influence on the NO stripping voltammetry.

4.2 Reduction of NO adsorbate

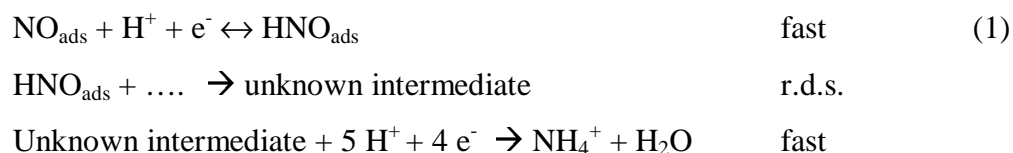
The stripping voltammetry of adsorbed NO in acidic solutions exhibits three peaks. We will refer to the peak at most positive potentials as the first peak, and to the peak at most negative potentials as the third peak. The third peak is absent in HClO_4 and has a Tafel slope deviating from the other two. This peak is apparently affected by anion adsorption.

The second peak is formed at all coverages of NO, whereas the first peak is seen only at high coverage. This suggests that two types of surface-bonded NO exist, conveniently referred to as strongly and weakly bonded NO. The fact that it is possible to reduce the adsorbate corresponding to the first peak without affecting the second peak confirms this. The individual peaks can not simply be assigned to a

single crystal face; most single crystal faces themselves show multiple peaks when adsorbed NO is stripped off reductively [9].

A small difference is seen when a low amount of NO is adsorbed or when an adlayer at maximum coverage is partially reduced. The difference indicates that NO adsorbs randomly with a preference for the strongly bonded sites, whereas partial reduction leaves only strongly bonded NO. NO does not seem to diffuse to the sites where it is weakly bonded, since no difference is observed in the amount of strongly bonded NO when the duration of the partial reduction was made ten times larger.

The Tafel slope of the first two peaks in the adsorbate reduction is ca. 60 mV/dec., typical for an electrochemical equilibrium, followed by a rate-determining potential-independent chemical step. The reaction is first order in H^+ , implying that a protonation takes place. However the position of the first peak does not change when H_2O is replaced by D_2O , so that apparently the protonation is not involved in the rate-determining step. The protonation should therefore take place before the rate-determining step. Combining these facts leads to the following simplified reaction scheme:



The reason HNO and not NOH is suggested as the hydrogenated intermediate is that gas phase HNO is about 100 kJ/mol more stable than gas phase NOH [15], but admittedly the stability of the surface-bonded species is not known. No species other than NO have been detected using IR-spectroscopy in the potential region where NO is reduced [10,16]. It might be that the coverage of HNO is very low (below the detection limit) or that its vibrations coincide with either the water or the NO vibrations (the NO stretch vibration of HNO is 1570 cm^{-1} [17]). The exact nature of the chemical step remains unknown at present, though a dissociation step seems a likely candidate.

The second peak shows both an anion effect and a small kinetic isotope effect. However, since the Tafel slope and the pH dependence are the same for the first and

second peak we believe that the above reaction scheme should apply to strongly bonded NO as well.

Mechanism 1 presumably also holds for NO adsorbate reduction in alkaline solutions, although the peak potential changes slightly with the pH. The shift is less than 59 mV on the RHE scale, which would be expected if the reaction were independent of pH.

4.3 Continuous reduction of NO

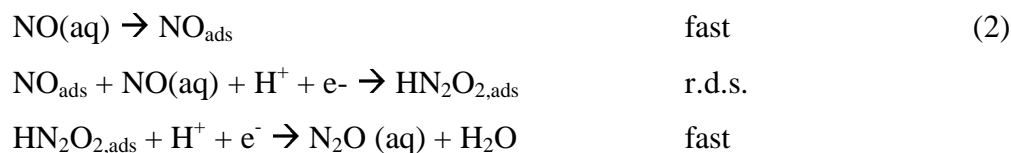
The selectivity of the continuous reduction of NO is markedly different from the adsorbate reduction, as the continuous reduction can produce N₂O at potentials higher than 0.4 V. At potentials lower than 0.4 V mainly NH₄⁺ is produced in acidic solutions.

The continuous reduction to N₂O is first order in H⁺ but shows no isotope effect. Similar to the adsorbate reduction this suggests that a protonation takes place prior to the rate-determining step. The Tafel slope in acidic solutions is 120 mV/dec.; hence, in contrast to the adsorbate reduction, the first electron transfer is rate determining.

It is tempting to assume that the reaction follows a Langmuir-Hinshelwood type mechanism with NO_{ads} as the reacting species, as proposed by Colluci et al. [6] and Gootzen et al. [7]. There are three arguments why we believe such a mechanism cannot be operative. The first argument is that the continuous reduction starts 400 mV positive to the potential where the adsorbate reduction starts. If NO_{ads} would be the only reacting species such a large difference would be hard to explain. Secondly N₂O is formed during the continuous reduction, whereas no N₂O is formed during the adsorbate reduction. The third argument is related to the fact that the rate of the reaction is first order in the concentration of solution NO. A Langmuir-Hinshelwood type of mechanism could only explain this if the coverage of NO_{ads} would be low. This is very unlikely, since the turn-over frequency of the reaction is low (ca. 1 NO per Pt per sec.), the adsorption energy of NO is high [e.g. 18] and no change in NO coverage is detected using IR-spectroscopy in the presence or absence of NO [9]. The

rate-determining step in the mechanism must therefore include a second NO molecule coming from the solution.

Pulling these arguments together the simplest conceivable mechanism consistent with the experimental data is the following:



The protonation and electron transfer are apparently not concerted, since no isotope effect is detected. This suggests that the rate-determining step in mechanism 2 consists in fact of a pre-equilibrium involving the protonation followed by a rate determining electron transfer. The rate-determining step in mechanism 2 is indeed first order in NO(aq) since the adsorption of NO is fast, and hence the concentration of NO_{ads} is zero-th order in NO(aq).

The continuous reduction to N₂O in alkaline electrolytes shows first-order kinetics in H⁺ and in NO, similar to acidic electrolytes. The major difference is the Tafel slope which is much higher. This might suggest that the protonation reaction is not in equilibrium but is partially rate determining.

The reduction of NO in the gas phase shows a negative kinetic order in the partial pressure of NO [19] at low temperature. This is consistent with a Langmuir-Hinshelwood mechanism with a high coverage of NO, the negative kinetic order being caused by NO blocking the sites for H₂ dissociation. In the liquid phase no sites are needed for H₂ to dissociate, since the reduction takes place electrochemically, and therefore the kinetic order in NO can be positive. We believe that this is an illustrative example of how the mechanisms in liquid and gas phase can be very different.

In the potential range where the continuous reduction of NO leads to NH₃ one observes a number of similarities with the adsorbate reduction. The change from N₂O to NH₃ as the main product starts at the same potential as the start of the adsorbate reduction, for which NH₃ is the only product. The effect of replacing H₂O with D₂O on the adsorbate reduction and the continuous reduction at low potentials is similar: in

both cases a change is observed at potentials lower than 0.1 V and no change is observed at higher potentials. Colluci et al. reported a Tafel slope of the continuous reduction to NH_3 of 73 mV/dec. [6], which is close to the Tafel slope of 60 mV/dec. for the adsorbate reduction. The kinetic order in NO is lower than one, which suggests that the amount of NO_{ads} determines the rate of the reaction. These similarities lead us to the conclusion that the mechanisms of the continuous reduction of NO to NH_3 and the adsorbate reduction are likely to be the same.

The continuous reduction to NH_3 in 1 M KOH has a higher activity compared to 0.1 M KOH than expected from the standard 59 mV/pH as obtained in acidic solutions. This is also true for the adsorbate reduction, although the effect is not as pronounced as for the continuous reduction. The reason for this difference is unclear.

5. Summary

A systematic study of the kinetics of the electrochemical reduction of NO has been performed in order to clarify the mechanism of the reaction. Both the reduction of adsorbed NO and the continuous reduction of NO have been studied.

During the reduction of adsorbed NO a combined proton/electron transfer takes place prior to the rate-determining chemical step. After the rate-determining step NH_3 is formed as the only product.

The continuous reduction of NO at potentials higher than 0.4 V yields N_2O . The rate-determining step is the combination of a NO molecule at the surface with a NO molecule from the solution involving a simultaneous electron transfer. The continuous reduction of NO at potentials lower than 0.4 V yields NH_3 . The mechanism for NH_3 formation is likely to be the same as the mechanism of the adsorbate reduction.

References:

- [1] K. Hara, M. Kamata, N. Sonoyama and T. Sakata *J. Electroanal. Chem.* 451 (1998) 181
- [2] R.R. Gadde and S. Bruckenstein *J. Electroanal. Chem.* 50 (1974) 163
- [3] L.J.J. Jansen, M.M.J. Pieterse and E. Barendrecht *Electrochim. Acta* 22 (1977) 27
- [4] B.G. Snider and D.C. Johnson *Anal. Chim. Acta* 105 (1979) 9
- [5] I. Paseka and J. Voříková *Electrochim. Acta* 25 (1980) 1251

- [6] J.A. Colucci, M.J. Foral and S.H. Langer *Electrochim. Acta* 30 (1985) 521
- [7] J.F.E. Gootzen, R.M. van Hardeveld, W. Visscher, R.A. van Santen and J.A.R. van Veen *Recl. Trav. Chim. Pays-Bas* 115 (1996) 480
- [8] J. Willsau, and J. Heitbaum, *J. Electroanal. Chem.* 194 (1985) 27
- [9] A. Rodes, R. Gomez, J.M. Perez, J.M. Feliu and A. Aldaz *Electrochim. Acta* 41 (1996) 729
- [10] A. Rodes, R. Gomez, J.M. Orts, J.M. Feliu, J.M. Perez and A. Aldaz *Langmuir* 11 (1995) 3549
- [11] A. Rodes, R. Gomez, J.M. Orts, J.M. Feliu and A. Aldaz *J. Electroanal. Chem.* 359 (1993) 315
- [12] P.A. Christensen and A. Hamnett *Techniques and Mechanisms in Electrochemistry*, Blackie Academic and Professional: Glasgow (1994) 61
- [13] M.T.M. Koper, A.P.J. Jansen, R.A. van Santen, J.J. Lukkien and P.A.J. Hilbers *J. Chem. Phys.* 109 (1998) 6051
- [14] D. Möller and K.-H. Heckner *Z. Phys. Chemie.* 1 (1974) 33
- [15] P.J. Bruna *Chem. Phys.* 49 (1980) 39
- [16] M.J. Weaver, S. Zou and C. Tang *J. Chem. Phys.* 111 (1999) 368
- [17] C.E. Dateo, T.J. Lee and D.W. Schwenke *J. Chem. Phys.* 101 (1994) 5853
- [18] Y.Y. Yeo, L. Vattuone and D.A. King *J. Chem. Phys.* 104 (1996) 3810
- [19] G. Papapolymerou, A.G. Botis, A.D. Papargyris and X.D. Spiliotis *J. Molec Catal.* 84 (1993) 267

Chapter 4: Mechanistic Study on the Electrocatalytic Reduction of Nitric Oxide on Transition-Metal Electrodes

Abstract

The mechanism of the electrochemical reduction of nitric oxide (NO) on a series of metals (Pd, Rh, Ru, Ir and Au) has been studied, both for the reduction of adsorbed NO and for the continuous NO reduction. All metals show a high selectivity to N₂O at high potentials and a high selectivity to NH₃ at low potentials, whereas N₂ is formed at intermediate potentials (although gold forms mainly N₂O, and very little NH₃). The behaviour of the transition metals is very similar to platinum, suggesting that the reaction schemes are essentially the same (especially the potential windows in which the products are formed are similar). The mechanism that leads to N₂O, is believed to involve the formation of a weakly adsorbed NO-dimer intermediate, similar to recent suggestions made for the gas phase reduction of NO. The reduction of adsorbed NO leads only to formation of NH₃ and not to N₂O or N₂. The electrochemical measurements suggest that NH₃ formation involves a combined electron-proton transfer in equilibrium, followed by a non-electrochemical rate-determining step. The formation of N₂, produced at potentials between the formation of N₂O and NH₃, most likely takes place formed by the reduction of previously formed N₂O.

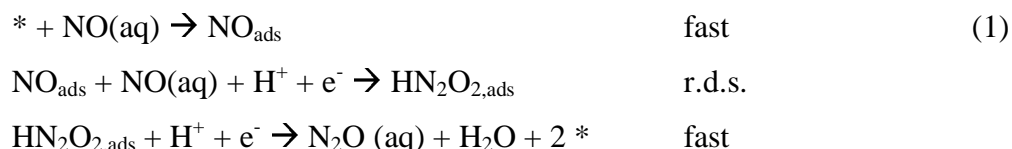
1. Introduction

The reduction of nitric oxide (NO) is an important reaction in environmental catalysis, since it determines the performance of wastewater treatment catalysts for nitrate, nitrite and NO removal [1], and the scrubbing of NO from gas streams [2]. Nitric oxide reduction has also been investigated as the cathodic reaction in fuel cells [3], because of its high reduction potential.

The electrodes employed in the electrochemical reduction of NO are usually noble transition metals, because they are the most active catalysts [4] and show the least formation of metal oxides. Palladium has the highest activity and selectivity to N₂ [3], and therefore is the catalyst of choice. Other metals form, depending on potential, undesirable products such as N₂O and/or NH₃.

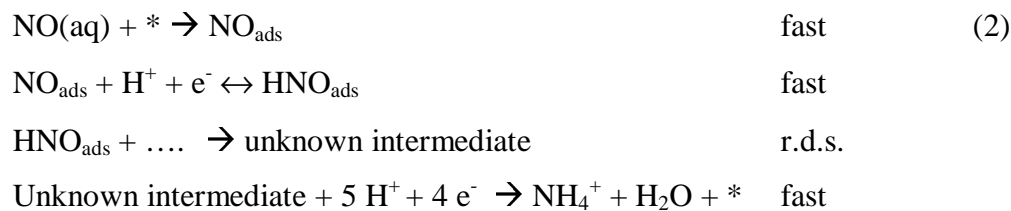
There is as yet little mechanistic insight as to why palladium is the best catalyst in the selective reduction of NO to N₂. The only metal for which reasonably detailed mechanistic information is presently available, is platinum [5].

Summarising the results of chapter 3, we found that there are two major reaction paths for NO reduction on platinum, one at high potentials (0.3 – 0.7 V vs. RHE) which leads to nitrous oxide (N₂O), and one at low potentials (0 – 0.3 V) which leads mainly to ammonia (NH₃). The formation of N₂O was observed to take place only in the presence of NO in the solution. From the Tafel slope, the pH-dependence and the kinetic order in NO solution concentration, the following reaction scheme was suggested:



where * denotes a free site at the surface. The most remarkable feature of this scheme is the rate-determining step, in which we proposed a surface-bonded NO to combine with a solution-phase NO. The latter may also be interpreted as a weakly bonded NO, as long as its concentration is first-order in solution NO to explain the experimentally observed NO kinetics in NO solution concentration.

The reaction scheme suggested for the formation of NH₃ proceeds through the reduction of adsorbed NO_{ads}:



Presumably, the rate-determining step in this scheme involves a breaking of the N-O bond.

Some nitrogen (N_2) is formed in the intermediate potential region (0.2 – 0.4 V vs. RHE), but we did not discuss the mechanism of its formation in our previous work. However, given the fact that N_2 is the most desirable product and that its selective formation is apparently quite sensitive to the nature of the electrode surface, more detailed investigations into the N_2 formation pathway are clearly of interest.

In this chapter, we study the electrocatalytic reduction of NO on five transition-metal surfaces, Ru, Rh, Ir, Pd and Pt, as well as on Au. We will show that the two separate pathways for N_2O and NH_3 exist for all these electrodes, and we will argue that they take place via reaction schemes similar to those on Pt. Most importantly, we will present more detailed results on the formation of N_2 on the different metal electrodes. From these results, we will suggest that the key intermediate in the N_2 formation is N_2O rather than surface bonded N_{ads} .

2. Experimental

Rotating disk electrodes (RDE) were used in a homemade setup. Platinum, palladium and gold were pretreated by repeated cycling in the hydrogen and oxygen evolution region in 0.1 M H_2SO_4 , after which the electrolyte was replaced with clean electrolyte. Rhodium, iridium and ruthenium were electrodeposited from the metal trichloride solution at 0.1 V (vs. RHE) prior to a measurement in the electrochemical cell, and traces of chloride were removed by thorough rinsing while the electrode was kept at -0.2 V. Iridium was deposited at ca. 80 °C. The blank cyclic voltammogram of the disk electrode was compared to that of a flag electrode, to check for the absence of contaminations and surface oxides.

Adsorbate studies were performed on a flag electrode of the pure metal. Differential Electrochemical Mass Spectroscopy (DEMS) electrodes consisted of platinum gauzes with the metal of interest electrodeposited onto it, except for gold, in which case a gold gauze was used. All flag electrodes were flame annealed prior to each measurement, except for gold, which was cleaned by repeated cycling between the hydrogen and oxygen evolution regions. The electrodes were quenched in clean water under an argon atmosphere, except for ruthenium, which was quenched in an argon/hydrogen atmosphere. The cyclic voltammogram in a clean solution was taken to check for the absence of surface oxides and contaminations.

The counter electrode in all cases consisted of a platinum flag. An AUTOLAB Pgstat 20 potentiostat was used for all RDE and adsorbate experiments. DEMS (Differential Electrochemical Mass Spectroscopy) measurements were performed employing a Balzers Prisma QMS 200 mass spectrometer. Details of the setup are described elsewhere [6]. The DEMS signals of N_2 , N_2O and NO were calibrated by oxidizing a monolayer of CO and measuring the amount of CO_2 . The signal was corrected for differences in sensitivity and fragmentation probability [7].

A $Hg/HgSO_4$ reference electrode was used for all measurements in acidic solutions. In alkaline solutions a Hg/HgO reference electrode was used. All potentials reported in this chapter, however, are converted to the RHE scale.

All glassware was cleaned in boiling H_2SO_4/HNO_3 to remove organic contaminations. All solutions were prepared with p.a. grade chemicals (Merck) and Millipore Gradient A20 water. All solutions were deaerated by purging with argon. NO was bubbled through two 2 M KOH washing flasks in order to remove NO_2 [8].

Adsorbate studies were performed by saturating the surface in a solution of saturated NO or 2 mM $NaNO_2$ under potential control (usually 0.37 V) in a 0.1 M H_2SO_4 solution in order to avoid oxidation of the surface by NO [9].

3. Results and discussion

3.1. Selectivity of the NO reduction

We will first discuss the various products of the NO reduction and the potential dependence of their transformation. The selectivity of the NO reduction in the presence of NO in the solution has been measured both in the DEMS setup by

measuring the amount of N₂O and N₂ formed, and in the RDE setup by determining the number of electrons transferred per NO molecule from the Levich equation:

$$\frac{1}{I} = \frac{1}{I_{kin}} + \frac{1}{0.62 n F C^* D^{\frac{2}{3}} \nu^{\frac{1}{6}} \omega^{\frac{1}{2}}}$$

In this equation, I_{kin} is the kinetic limited current, n is the number of electrons per NO molecule, C^* is the bulk concentration of NO, D is the diffusion constant of NO in water, and ν is the kinematic viscosity. The following values were used: $C^* = 1.40 \cdot 10^{-6} \text{ mol/cm}^3$, $D = 2.5 \cdot 10^{-5} \text{ cm}^2\text{s}^{-1}$ and $\nu = 8.5 \cdot 10^{-3} \text{ cm}^2\text{s}^{-1}$ [10], which allows the determination of n .

On all metals the potential window in which NO reduction takes place can be divided into three regions: at high potentials (0.4 – 0.7 V) N₂O is the main product, N₂ is formed with varying selectivity at intermediate potentials (0.2 – 0.4 V), whereas NH₃ is the main product at low potentials (0 – 0.3 V). It is known that hydroxylamine (H₂NOH) can be formed as a minor product at low potentials (0 V) on platinum [11], however, since a quantitative determination is quite complicated and it is only a minor product, we will exclude H₂NOH formation from our discussion. Figure 1 shows the selectivity to N₂O and N₂ of the six metals studied in this chapter, as obtained from the DEMS measurements. The amount of N₂ produced varies with the metals used, as do the boundaries of the three potential regions. The selectivity to N₂ on palladium, for instance, is very high and covers a larger potential window than on the other metals. As will be further discussed below, we believe that the similarities in selectivity are an indication that the reaction mechanism is similar on all transition metals.

The results will be discussed in three separate sections, according to the three potential regions.

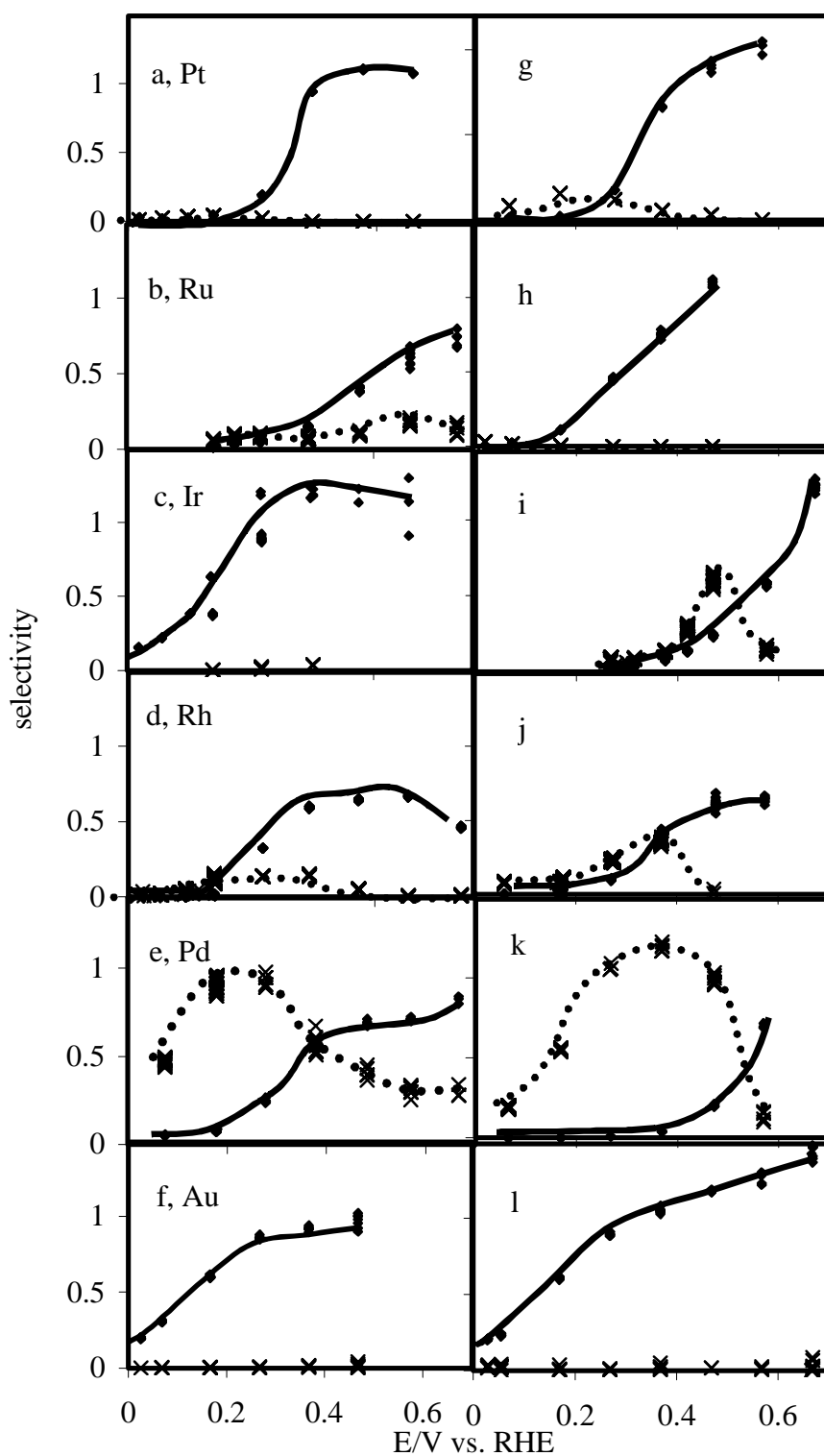


Figure 4.1: selectivity of the reduction of NO in the solution. Solution saturated with NO, a-f 0.1 M H₂SO₄, g-l 0.1 M KOH, a,g Pt, b,h Ru, c,i Ir, d,j Rh, e,k Pd, f,l Au. Solid lines and diamonds selectivity to N₂O, dotted lines and crosses selectivity to N₂

3.2. Reduction of NO to NH₃

The reduction of NO to NH₃ can be studied by continuous NO reduction in the potential region 0 – 0.3 V, or by the reduction of an NO adsorbate layer in a clean NO-free electrolyte. In the latter case, information about the rate-determining step in the overall reaction scheme can be obtained relatively easily by measuring a so-called Tafel plot, which gives the potential dependence of the overall reaction rate. Under the assumption that the reduction rate is first [12] or second order [13] in the adsorbate coverage, it can be shown that a plot of the peak potential (i.e. the potential at which a maximum current is measured during the reductive stripping voltammetry) vs. the logarithm of the scan rate is equivalent to a Tafel plot.

Table 1: Tafel slope of the adsorbed NO reduction, in mV/dec

	Pt	Rh	Ir	Ru
0.1 M H ₂ SO ₄	54 ± 3 [q]	70 ± 3	76 ± 5	66 ± 10
0.1 M KOH	58 ± 3 [q]	106 ± 3	88 ± 5	63 ± 1

Table 1 summarises the slopes of the Tafel plots obtained for the NO adsorbate reduction on Pt, Rh, Ir and Ru in acidic and alkaline solution. The maximum coverage of NO is in all cases similar (0.4 – 0.5 monolayer), and similar to values reported for single crystal surfaces [14,15,16]. Pd and Au are not included, as in the case of palladium the peak potential overlaps with the hydrogen evolution reaction, and in the case of gold because no NO adsorbate layer is formed. A typical Tafel plot for the NO reduction of Ru in acidic solution is shown in figure 2. A value of ca. 60 mV/dec indicates the existence of an electron-transfer step in equilibrium, followed by a rate-determining chemical (potential-independent) step. Together with the observed pH dependence, this has led us to suggest that the NO reduction on platinum follows scheme 2 discussed in the Introduction. The very similar Tafel slopes observed for the other metals may be interpreted according to a similar scheme, where a higher Tafel slope could point towards a slower first electron-transfer step.

We believe that the continuous reduction of NO to NH₃ in the potential range of 0 – 0.3 V takes place through the same mechanism as the adsorbate reduction, as

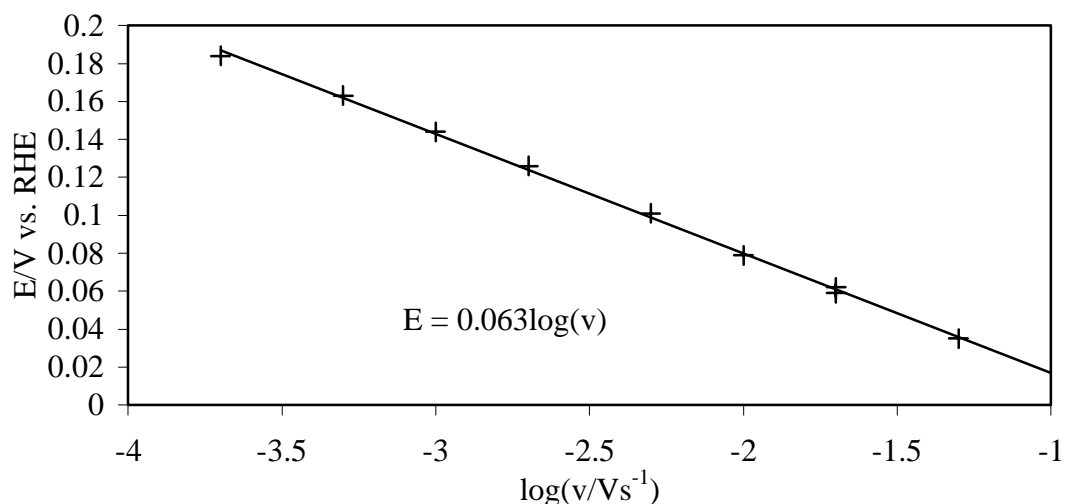


Figure 4.2: Dependency of the peak position of the NO reduction with the scan rate on ruthenium in 0.1 M H₂SO₄. Surface at maximum NO coverage.

the onset in NH₃ production in the continuous reduction occurs at roughly the same potentials as the adsorbate reduction (table 2). It is difficult to obtain kinetic information however, as the selectivity to NH₃ at 0.2 – 0.3 V is not 100 %.

Table 2: Peak potential of the NO adsorbate reduction at 5 mV/sec., compared to the potential at which the selectivity of the reduction of solution NO changes according to the RDE

		Pt	Pd	Rh	Ir	Ru
0.1 M H ₂ SO ₄	E _{peak}	0.21	0.01 ¹	0.11	0.17	0.102
	RDE	0.25	²	0.2	0.25	²
0.1 M KOH	E _{peak}	0.18	0.03 ¹	0.14	0.10	0.101
	RDE	0.2	²	0.15	0.15	0.2

¹ measured on a gold electrode with a thin (2-3 ML) palladium overlayer, and at 1 mV/sec.

² there is no change in the selectivity

Two metals behave differently from the other metals and have to be discussed separately, namely palladium and gold. On palladium the reduction of adsorbed NO takes place at significantly lower potentials than on the other noble metals (ca. 0 V). Also, the potential at which NH₃ is formed in the continuous reduction is low

compared to the other metals (ca. 0.1 V). On gold the selectivity to N_2O does not drop to zero, as on the other noble metals, since the adsorption of NO on gold is weak and little formation of NH_3 is observed.

In scheme 2, the dissociation of the N-O bond is assumed to take place after the protonation. However, NO is known to dissociate at room temperature on metals like rhodium, iridium and ruthenium, and hence we must consider this possibility in the overall reaction scheme. Since NO dissociation is also an important mechanistic issue in N_2O and N_2 formation, we postpone its discussion to section 3.5, where we will discuss a number of general mechanistic features in relation to the gas-phase reduction.

3.3. Reduction of NO to N_2O

The Tafel slopes of the NO reduction to N_2O on the various metals, as derived from the kinetic limiting current of the RDE measurements, are given in table 3. The Tafel slope was found to be close to 120 mV/dec in three cases: platinum and ruthenium in acidic solutions, and iridium in alkaline solutions. This implies that the first electron transfer is rate determining in these three cases. In all other cases the Tafel slope was found to be significantly higher than 120 mV/dec, indicating that the rate-determining step is a chemical step prior to the electrochemical steps. The values given in table 3 are significantly different from those given by Colucci et al. [8] (78, 116 and 408 mV/dec on resp. Pd, Rh and Ru in acidic solutions), as determined from voltammetry at stationary electrodes. Since reactions with mass-transport limitations should preferably be studied at rotating electrodes, and because we took extreme care to avoid surface oxidation of the less noble transition metals [17,18], we believe our values reflect more accurately the “real” Tafel slopes.

Table 3: Tafel slopes of the NO reduction between 0.4 – 0.7 V in a solution saturated with NO, in mV/dec.

	Pt	Pd	Rh	Ir	Ru	Au
0.1 M H_2SO_4	117± 4	160±18	436±32	201±39	133±13	356±16
0.1 M KOH	322±23	246±26	201±39	113±34	242±21	207±18

Table 4: current density of the NO reduction in saturated NO at 0.42 V, in mA/cm²

	Pt	Pd	Rh	Ir	Ru	Au
0.1 M H ₂ SO ₄	0.49	0.55	0.08	0.48	0.11	0.20
0.1 M KOH	0.28	0.52	0.33	0.54	0.43	0.62

Colucci et al. [8] suggested that the mechanism of the NO reduction to N₂O on platinum, palladium, rhodium and ruthenium includes only species which are adsorbed at the surface. Gootzen et al. [19] suggested for platinum electrodes, that the key step in the N₂O formation is the dissociation of NO, which also implies that only adsorbed species are involved in the formation of N₂O. However, we find that NO from the solution must be involved in the reaction scheme for two reasons. The first reason is that the potential window in which the reduction of adsorbed NO takes place (0 – 0.3 V) is much lower than the potential window considered here (0.4 – 0.7 V). Secondly, N₂O is not produced during the reduction of adsorbed NO. Since the only difference between the reduction of adsorbed NO and the reduction of NO at high potentials is the presence of dissolved NO, solution NO *must* be involved in the reaction sequence to produce N₂O. Since these observations hold for all metals studied here, we suggest that reaction scheme 1, proposed for platinum, is also valid for the other metals. The higher Tafel slopes observed for some of the systems could be explained by assuming that the first electron transfer shifts to a later stage in the scheme, and the surface dimerisation reaction becomes the rate-determining chemical step.

It is unclear whether dissolved NO reacts directly from the solution, or from a weakly adsorbed state at the surface. Either possibility will lead to the same N₂O formation kinetics and the same adsorbate reduction kinetics, since this weakly adsorbed NO will desorb when the solution is replaced with clean electrolyte.

Finally, we note that reaction scheme 1 predicts the rate of the reaction to be first order in the concentration of solution NO, because the surface is always covered with NO_{ads} and hence only the amount of NO(aq) changes with the NO concentration. A kinetic order of unity has indeed been observed on platinum in acidic solutions. Due to the large error bars in the determination of the kinetic limited current (table 3), we have not pursued these measurements for the other systems, but both DEMS

measurements and an analysis of the RDE data for palladium, using the procedure suggested by Markovic et al. [20], suggest a kinetic order close to one.

3.4. Reduction of NO to N₂

As mentioned in the Introduction, there is only scant mechanistic information available on the formation of N₂ from the electrocatalytic NO reduction. However, it seems that one may assume two alternative working hypotheses. The first hypothesis is that N₂ is formed by the reduction of N₂O, i.e. in series with the N₂O formation. This is a known reaction in electrocatalysis, that has been studied by a number of authors [21,22,23,24,25]. The second hypothesis is that N₂ is formed by a reaction of surface species (such as NO_{ads}, N_{ads}, NOH_{ads} or other yet unidentified species), i.e. in parallel with the N₂O formation.

If the first hypothesis would be true, i.e. N₂ would be formed from the reduction of N₂O, one would expect a correlation between N₂O reduction activity and the selectivity towards N₂ in the reduction of NO. Figure 3 gives the activity of the various metals in the N₂O reduction in acidic and alkaline solutions. The activity found in alkaline solutions increases in the order Au < Ru << Ir < Rh ≈ Pt << Pd, with the onset of the reaction being 0, 0.1, 0.4, 0.45, 0.45 and 0.6 V, resp. (figure 3). This ordering is comparable to the production of N₂ in alkaline solutions shown in figure 1, the potentials of the onset showing a reasonable agreement with the onset of the N₂O reduction (Au ≈ Ru << Pt < Rh < Ir << Pd, the onset of the reaction being 0, 0, 0.45, 0.45, 0.55 and 0.6 V resp.). Iridium is more active in the N₂ production than suggested by its N₂O reduction activity, which makes it an exception.

To compare the activity and selectivity in acidic solutions is more problematic, since the N₂O reduction is known to be very sensitive to the competitive adsorption of SO₄²⁻ anions [21,22]. The measurements should therefore be carried out in an HClO₄ solution instead of H₂SO₄. Unfortunately the activity of rhodium and iridium can not be obtained in HClO₄, since these metals can reduce ClO₄⁻ to Cl⁻ [26], which is known to adsorb strongly. In general, however, the series for the N₂ production from NO in acidic solutions is similar to the series of the N₂O reduction activity. Gold, for instance, is inactive in both cases, followed by iridium, rhodium and ruthenium, whereas palladium is very active. Platinum does not fit in the series, as the rate in N₂O

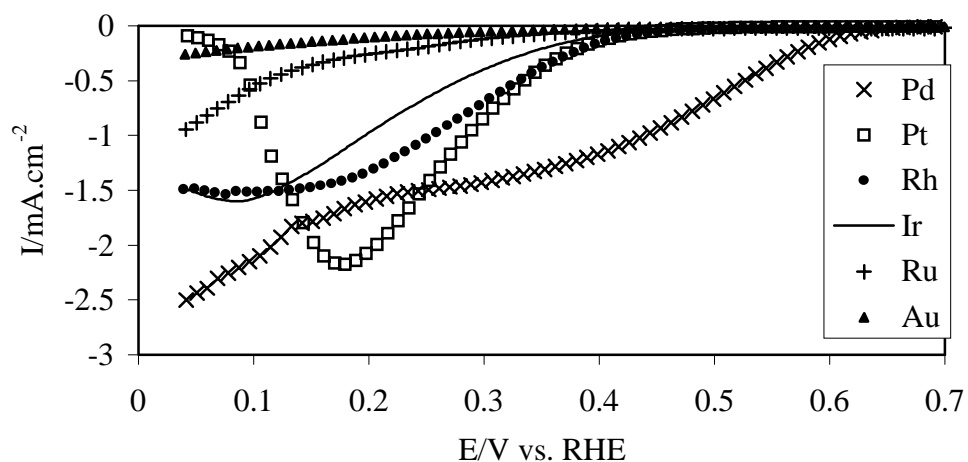


Figure 4.3: activity of the transition metals and gold in the N_2O reduction. 0.1 M KOH saturated with N_2O . crosses Pd, squares Pt, circles Rh, thick solid line Ir, plusses Ru, triangles Au.

reduction in both $HClO_4$ and H_2SO_4 is higher than on palladium, whereas palladium is more active in the selective formation of N_2 from NO.

The qualitative agreement between the N_2O reduction activity and the selectivity in the NO reduction to N_2 is a strong argument in favor of the “ N_2O serial pathway”. Also the fact that no N_2 is produced during the NO adsorbate reduction in the absence of NO in the solution disfavors the “adsorbate parallel pathway”. In fact, the NO adsorbate is generally not reactive at all at potentials for which N_2 is produced during the continuous NO reduction.

3.5 Mechanistic issues and comparison to gas phase reduction of NO

3.5.1 NO dissociation

As noted in section 3.2, it is known that NO may dissociate at room temperature on metals such as Rh, Ir and Ru, whereas it is generally adsorbed molecularly on Pt and Pd. An overview of the NO dissociation behavior on metal surfaces was recently given by Brown and King [27]. At higher coverages, the NO dissociation process may be inhibited because of the lack of adjacent empty sites or because strong lateral interactions between the dissociation products render the molecular state more stable. The necessity of having empty surface sites for triggering NO dissociation has been shown recently in detailed UHV surface-science studies of

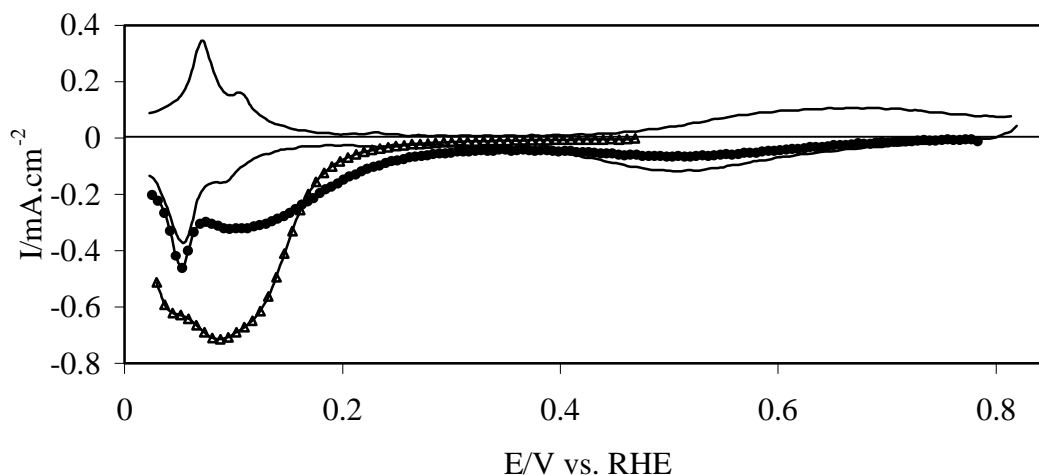


Figure 4.4: reduction of adsorbed NO on rhodium, scan rate $20 \text{ mV}\cdot\text{s}^{-1}$, open triangles NO adsorbed at 0.45 V, filled circles NO adsorbed at OCP (0.8 V), solid line blank

NO reactivity on Rh [28,29]. In most UHV studies, the N_{ads} species is considered as an intermediate in the N_2O , N_2 and NH_3 formation. Hence, we will have to consider the possibility of NO dissociation on Rh, Ru and Ir in the electrochemical context.

It is difficult to obtain any direct evidence for NO dissociation from electrochemical experiments. Gootzen et al. [19] suggested that the observation of an oxide reduction peak after NO adsorption on Pt at open-circuit potential (OCP) was due to the reduction of the adsorbed oxygen formed from NO dissociation. However, we showed recently that the peak is only observed on roughened electrodes [5], suggesting quite a different mechanism, and in keeping with gas-phase situation where NO adsorbs molecularly on Pt at room temperature. Interestingly, an oxide reduction peak is observed, at ca. 0.5 V, on a smooth flame-annealed Rh electrode after adsorption of NO at OCP (ca. 0.8 V), as illustrated in figure 4. When NO is adsorbed at 0.45 V, no oxide reduction peak is observed, and a much higher NO reduction charge is measured (see figure 4), indicating a higher coverage of NO under these conditions. However, these observations still do not prove the occurrence of NO dissociation. On Rh, surface oxides are known to be more stable than on Pt, and therefore on Rh, certainly at a potential of 0.8 V, a more competitive co-adsorption of oxides and NO is expected than on Pt. The peak at 0.5 V can hence be explained by the reduction of co-adsorbed oxides, which are not formed by NO dissociation.

An interesting observation to be made from figure 4 that could point towards the role of NO dissociation is the fact that the apparently lower coverage of NO formed at 0.8 V starts to be reduced at a significantly less negative potential than a saturated layer formed at 0.45 V. This could mean that the surface sites that become available after reduction of the surface oxides trigger the NO dissociation. The saturated NO adlayer is not or much less reactive at these potentials, as is also evidenced by the observation of a stable NO stretching peak in FTIR experiments of NO on single-crystal Rh [14]. A similar – though less pronounced - shift in the reduction peak is observed when a non-saturated NO adlayer is formed at 0.45 V by dosing from a less concentrated NO solution. These observations are in stark contrast with the coverage effects observed for the NO adsorbate reduction on Pt, where no such positive shifts in reduction potential with lower NO coverage are observed.

If NO dissociation plays a role on Rh, Ir, and Ru, then the observed Tafel slopes for the adsorbate reduction may suggest that it is not the rate-determining step in the ammonia formation. However, it should be realized that it is not *a priori* clear to what extent the NO dissociation has to be considered as potential or even pH dependent, as the *overall* NO dissociation process at electrochemical interfaces involves protonation of the oxygen:



It is obvious that the above experiments are not decisive in pinning down the possible role of NO dissociation on the less-noble transition metals Ru, Ir and Rh. More direct spectroscopic information is clearly needed. The results in Fig.5 do suggest, however, that at high NO coverages, which seems the relevant surface condition for the continuous NO reduction experiments, NO dissociation is not likely to take place at potentials above 0.3 V. Hence, it is suggested that NO dissociation does not play a significant role during N₂O and N₂ formation. Evidence for alternative mechanisms, in relation to gas-phase and UHV experiments, is discussed in the next two sections.

3.5.2 NO dimerization

The reaction scheme (1) suggested for the N₂O formation on Pt involves the formation of a (protonated) surface-bonded (NO)₂ dimer. The very similar conditions under which N₂O is formed on the other metals is suggestive of a more general applicability of this reaction scheme.

In fact, there is a growing surface-science literature on the formation of NO dimers on silver, copper, molybdenum, tungsten, and palladium, and it has also been suggested to exist on platinum and rhodium [27]. It has been shown that on silver the NO dimer is the key intermediate in the N₂O formation. NO is adsorbed weakly on Ag [27]. Apparently, strongly adsorbed NO is not required for the formation of the NO dimer or the production of N₂O. Theoretical DFT studies have also supported the existence of the NO dimer on Ag [30].

Even though we are not aware of similar UHV-based evidence for the NO dimer on Au, the generic similarity between Ag and Au suggest that it is reasonable to assume a similar N₂O formation mechanism on Au. This would certainly explain the unique selectivity of Au in reducing NO to N₂O as observed in our electrochemical study. Silver in fact has a similarly high selectivity towards N₂O in the electrochemical NO reduction [31]. Also, this weakly adsorbed state of NO involved in the dimer formation may explain the first-order kinetics in the NO solution concentration, as mentioned in the Introduction. Interestingly, there is no clear catalytic effect of any metal in reducing NO to N₂O, as is illustrated by the very similar activities observed for all metals as collected in Table 4. This also strongly suggests the involvement of weakly adsorbed intermediates in the key step of the reaction scheme. As mentioned in the previous section, under these conditions of high surface coverage, NO dissociation does not seem very likely.

The idea that N₂O formation takes place through the formation of a weakly-adsorbed NO dimer offers a consistent explanation of our observations. It would certainly explain why the reaction is so similar on all the different metals. However, spectroscopic proof of the existence of NO dimers under electrochemical conditions is certainly necessary to validate our interpretation.

3.5.3 N₂O as intermediate in N₂ formation

The data presented in section 3.4 offered evidence for the formation of N₂ from N₂O, i.e. in a serial pathway, rather than from other NO-derived adsorbates in a parallel pathway. This interpretation is based on the observations that there is a correlation between the selectivity of a given metal in producing N₂ from NO and its activity in reducing N₂O, and that no N₂, nor N₂O, is formed during the NO adsorbate reduction.

Interestingly, there is a very similar suggestion in the recent gas-phase literature. The formation of N₂O has not been observed under UHV conditions. However, Zaera and Gopinath [32] have suggested on the basis of isotope exchange measurements that the formation of N₂ under a constant flux of NO, is not due to the recombination of two N adatoms, but rather via an N₂O-type intermediate formed by the combination of an NO adsorbate and N adatom. According to Zaera and Gopinath, this reaction would only take place under conditions of a high gas-phase pressure of NO.

4. Conclusions

In this chapter, we have studied the mechanism of the electrocatalytic reduction of NO on Ru, Rh, Pd, Ir, Pt and Au electrodes by a combination of electrochemical measurements and on-line mass spectrometry. Our objectives were to assess to what extent the mechanistic schemes for N₂O and NH₃ formation recently suggested for the NO reduction on platinum, can also be applied to the other metals. In addition, we have studied the mechanism of N₂ production from NO.

All transition metals show a high selectivity towards N₂O at high potentials and, with the exception of Au, a high selectivity towards NH₃ at low potentials. At intermediate potentials, all metals, again with the exception of Au, produce N₂, though with varying selectivity.

The NO reduction to N₂O is suggested to take place by a mechanism similar to reaction scheme (1) suggested for Pt. The varying Tafel slopes found for the different metals may reflect a shift in the rate-determining step with the metal, or, more precisely, a shift in the occurrence of the first electron-transfer step in this mechanism. More importantly, however, the data for all metals are consistent with the

involvement of a weakly adsorbed NO dimer as the key intermediate in N₂O formation. The existence of an NO dimer has been proved on various metal surfaces in UHV. Moreover, its weak adsorption strength would explain why all metals show a similar activity in the NO reduction to N₂O.

We have also presented evidence that the mechanism of formation of N₂ is similar on all metals (except for Au, which does not produce N₂), and involves N₂O as the key intermediate. This deduction was based on the correlation between the selectivity of a certain metal towards producing N₂ from NO and its activity in reducing N₂O. Metals that actively reduce N₂O also produce more N₂ in their NO reduction. Moreover, no N₂ and N₂O are formed in the NO adsorbate reduction in the absence of NO in solution, suggesting that there is no parallel pathway for N₂ formation.

The situation for NH₃ formation is less clear. Certainly for the reduction of the NO adsorbate on Rh (and presumably also Ru and Ir) we cannot exclude the role of NO dissociation, which was not considered for Pt. Tafel slope measurements nevertheless suggest an electron-transfer step to be involved in, or prior to, the rate-determining step. At high NO coverages, NO reactivity on Rh is lower, suggesting a suppression of the NO dissociation by the blocking of free sites.

Finally, the best electrocatalyst for the selective reduction of NO to N₂ is palladium. At high potentials this is related to its high activity in reducing N₂O to N₂. At low potentials this is related to its low activity in the reduction of adsorbed NO to NH₃.

References:

- [1] A.C.A. de Vooy, R.A. van Santen and J.A.R. van Veen, *J. Mol. Catal. A.* 154 (2000) 203
- [2] J.H. Macneil, P.A. Berseth, G. Westwood and W.C. Troglor, *Environ. Sci. Technol.* 32 (1998) 876
- [3] M. Shibata, K. Murase and N. Furuya, *J. Appl. Electrochem.* 28 (1998) 1121
- [4] K. Hara, M. Kamata, N. Sonoyama and T. Sakata, *J. Electroanal. Chem.* 451 (1998) 181
- [5] A.C.A. de Vooy, M.T.M. Koper, R.A. van Santen and J.A.R. van Veen, *Electrochim. Acta* 46 (2001) 923
- [6] J. Willsau and J. Heitbaum, *J. Electroanal. Chem.* 194 (1985) 27
- [7] *Manual Mass Spectrometer*, A.G. Balzers, Balzers Liechtenstein, 1991
- [8] J.A. Colucci, M.J. Foral and S.H. Langer, *Electrochim. Acta* 30 (1985) 1675
- [9] R. Gomez and M.J. Weaver, *Langmuir* 14 (1998) 2525
- [10] J.A. Colucci, M.J. Foral and S.H. Langer *Electrochim. Acta* 30 (1985) 521

- [11] R.R. Gadde and S. Bruckenstein, *J. Electroanal. Chem.* 50 (1974) 163
- [12] P.A. Christensen and A. Hamnett, in "Techniques and Mechanisms in Electrochemistry." Blackie Academic and Professional, Glasgow, 1994
- [13] M.T.M. Koper, A.P.J. Jansen, R.A. van Santen, J.J. Lukkien and P.A.J. Hilbers, *J. Chem. Phys.* 109 (1998) 6051
- [14] A. Rodes, R. Gomez, J.M. Perez, J.M. Feliu and A. Aldaz, *Electrochim. Acta* 41 (1996) 729
- [15] B. Alvarez, A. Rodes, J.M. Perez, J.M. Feliu, J.L. Rodriguez and E. Pastor, *Langmuir* 16 (2000) 4695
- [16] R. Gomez and M.J. Weaver, *J. Phys. Chem. B* 102 (1998) 3754
- [17] M. Vukovic and D. Cukman, *J. Electroanal. Chem.* 474 (1999) 167
- [18] K. Iwayama and X. Wang, *Appl. Catal. B* 19 (1998) 137
- [19] J.F.E. Gootzen, R.M. van Hardeveld, W. Visscher, R.A. van Santen and J.A.R. van Veen, *Recl. Trav. Chim. Pays-Bas* 115, 480 (1996)
- [20] N.M. Markovic, R.R. Adzic, B.D. Cahan and E.B. Yeager, *J. Electroanal. Chem.* 377 (1994) 249
- [21] H.Ebert, R. Parsons, G. Ritzoulis and T. VanderNoot, *J. Electroanal. Chem.* 264 (1989) 181
- [22] A. Ahmani, E. Bracey, R.W. Evans and G. Attard, *J. Electroanal. Chem.* 350 (1993) 297
- [23] N. Furuya and H. Yoshida, *J. Electroanal. Chem.* 303 (1991) 271
- [24] G.A. Attard and A. Ahmadi, *J. Electroanal. Chem.* 389 (1995) 175
- [25] A. Kudo and A. Mine, *Appl. Surf. Sci.* 121/122 (1997) 538
- [26] A. Ahmani, R.W. Evans and G. Attard, *J. Electroanal. Chem.* 350 (1993) 279
- [27] W.A. Brown and D.A. King, *J. Phys. Chem.* 104 (2000) 2578
- [28] H.J. Borg, J.P.C.-J.M. Reijerse, R.A. van Santen and J.W. Niemantsverdriet, *J. Chem. Phys.* 101 (1994) 10052
- [29] M.J.P. Hopstaken and J.W. Niemantsverdriet, *J. Phys. Chem. B* 104 (2000) 3058
- [30] M. Perez-Jigato, D.A. King and A. Yoshimori, *Chem. Phys. Lett.* 300 (1999) 639
- [31] K. Hara, M. Kamata, N. Sonoyama and T. Sakata, *J. Electroanal. Chem.* 451 (1998) 181
- [32] F. Zaera and C.S. Gopinath, *Chem. Phys. Lett.* 332 (2000) 209

Chapter 5: Mechanistic Aspects of the Nitric Oxide Oxidation on Transition Metal Electrodes

Abstract

The electrochemical oxidation of nitric oxide (NO) was studied on various transition metals (Pt, Pd, Rh, Ru, Ir) and gold, both in the presence of solution NO and as adsorbed NO. In the oxidation of solution NO both HNO_2 and NO_3^- can be formed, depending on potential. The rate of the formation of NO_3^- is metal dependent, whereas the rate of the formation of HNO_2 is almost independent on the metal. It is suggested that strongly adsorbed NO is not included in the rate-determining step. The first electron transfer is the rate-determining step in the formation of HNO_2 . The oxidation of solution NO to HNO_2 on various metals shows similarities with the oxidation of CO on gold.

The oxidation of adsorbed NO occurs via an equilibrium between NO and HNO_2 prior to the rate-determining step, the subsequent non-electrochemical step is rate determining. The final product is NO_3^- . The curve of the adsorbate oxidation on platinum and rhodium almost overlap, indicating that the adsorbate oxidation is virtually metal-independent.

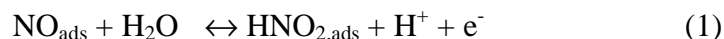
Surface oxides play a role both in the oxidation of solution NO and of adsorbed NO. The influence of surface oxides varies with the conditions: in the oxidation of adsorbed NO it inhibits the reaction, but it probably catalyses the oxidation of solution NO.

1. Introduction

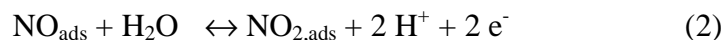
Our main motivation for research on the oxidation of NO is to get a complete overview on the electrochemical reactivity of NO. This is important because the standard equilibrium potential (E_0) of the NO reduction (1.59 V to N_2O , all potentials are vs. RHE) is higher than the E_0 of the NO oxidation (0.99 V to HNO_2 in acidic solutions and 0.37 V to NO_2^- in alkaline solutions), which indicates that thermodynamically NO can disproportionate to form N_2O and HNO_2 (or NO_2^-). In fact, there is a potential window in which both NO reduction and oxidation can occur on gold [1]. Also, the voltammetry on gold in a solution containing NO does not show a double layer region [1], i.e. a potential window with zero faradaic current, suggesting that both reactions occur simultaneously. An additional point of interest is the comparison of the NO oxidation with the CO oxidation, which is a well-known and well-studied reaction, as both reactions require an oxygen transfer from nearby water molecules.

Most research in the literature has used platinum as an electrode material. Dutta and Landolt [2] found that the oxidation of NO proceeds in two potential regions. From the relative currents in those regions it was suggested that in the first region HNO_2 is produced, and in the second region HNO_3 is produced. For the first potential region a Tafel slope of 110 mV/dec was observed, indicating that the first electron transfer is rate determining. Heckner and Schmid [3] have found that changing the electrode material from platinum to iridium or gold has no effect on the activity. They therefore suggested that the reactants are not adsorbed at the surface. Unfortunately both studies have been performed in strong (> 2 M) acidic solutions, and Snider and Johnson [4] have shown that the oxidation of NO and HNO_2 in strongly acidic solutions is different from those in diluted aqueous solutions.

Recent studies have focussed on the oxidation of NO adsorbed at the surface. Rodes et al. [5] have shown that the adsorption of HNO_2 leads to the formation of a NO adlayer at rhodium and platinum single crystal surfaces. Cyclic voltammetry showed that this adlayer can be reversibly oxidized on Pt(111) and Pt(100) in acidic solutions, whereas Pt(110) showed no reversible oxidation/reduction of NO. Based on coulometric data and the reversibility of the system, Rodes et al. [6] and Ye and Kita [7] ascribed this oxidation/reduction couple to reaction 1.



Momoi et al. [8] however, ascribed this couple to the reaction 2, based on STM and IRAS data.



The objective of this study is to obtain additional information on the reaction schemes of both the adsorbate oxidation and the oxidation in the presence of NO in the solution. We will study the role of the electrode material in the oxidation in the presence of NO, both in acidic and alkaline solutions. The findings in dilute aqueous solutions (0.1 M) will be compared to the strongly acidic solutions [2,3].

2. Experimental

Rotating disk electrodes (RDE) were used in a homemade setup. Platinum, palladium and gold were pretreated by repeated cycling in the hydrogen and oxygen evolution region in 0.1 M H₂SO₄ and subsequent replacing of the electrolyte. Rhodium, iridium and ruthenium were electrodeposited from the metal III chloride solution at 0.1 V each time prior to a measurement in the electrochemical cell and traces of chloride were removed by thorough rinsing while the electrode was kept at –0.2 V vs. RHE. Iridium was deposited at ca. 80 °C. The blank cyclic voltammogram was compared to that of a flag electrode, to check for contaminations and surface oxides.

Adsorbate studies were performed on a flag electrode of the pure metal. Differential Electrochemical Mass Spectroscopy (DEMS) electrodes consisted of platinum or gold gauzes. Platinum electrodes were flame annealed prior to each measurement. Gold electrodes were cleaned by repeated cycling in the hydrogen and oxygen evolution region. The cyclic voltammogram in a clean solution was taken to check for the absence of surface oxides and contaminations.

The counter electrode in all cases consisted of a platinum flag. An AUTOLAB Pgstat 20 potentiostat was used for all RDE and adsorbate experiments. DEMS (Differential Electrochemical Mass Spectroscopy) measurements were performed

employing a Balzers Prisma QMS 200 mass spectrometer. Details of the setup are described elsewhere [9]. The DEMS signals of NO and NO₂ were calibrated by oxidizing a monolayer of CO and measuring the amount of CO₂. The signal was corrected for differences in sensitivity and fragmentation probability [10].

A Hg/HgSO₄ reference electrode was used for all measurements in acidic solutions. In alkaline solutions a Hg/HgO reference electrode was used. All potentials reported in this chapter are converted to the RHE scale.

All glassware was cleaned in boiling H₂SO₄/HNO₃ to remove organic contaminations. All solutions were prepared with p.a. grade chemicals (Merck) and Millipore Gradient A20 water. All solutions were deaerated by purging with argon. NO was bubbled through two 2 M KOH washing flasks to remove NO₂ [2].

Adsorbate studies were performed by saturating the surface in a solution of saturated NO or 2 mM NaNO₂ under potential control (usually 0.37 V) in a 0.1 M H₂SO₄ solution to avoid oxidation of the surface by NO (chapter 3).

3. Results

3.1. Oxidation of NO in the solution.

When the cyclic voltammogram of the NO oxidation is obtained in acidic solutions, platinum, palladium and iridium show a difference between the scan going to high potentials (positive scan) and the subsequent scan going to low potentials (negative scan). The cyclic voltammogram of iridium is given as an example in figure 1; note that the current in the positive scan is lower than the negative scan. Gold, ruthenium and rhodium do not show this effect, the positive and negative scans virtually overlap. To compare the activity of the transition metals and gold, the negative scans obtained immediately after the positive scan, are shown in figure 2. Two waves can be distinguished, one from 0.85 – 1 V, and a second one starting at ca. 1.1 V, depending on the metal. Ruthenium is an exception, as only one wave can be distinguished.

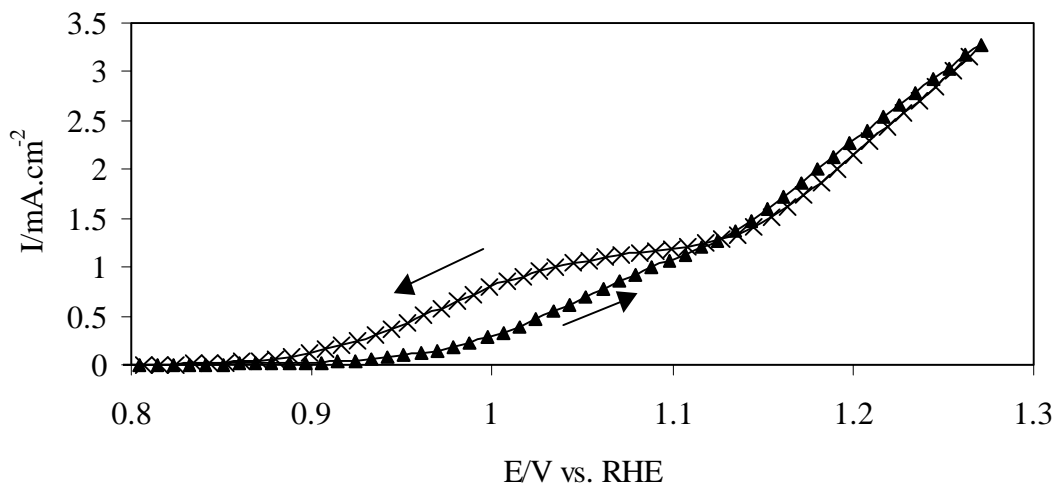


Figure 5.1: oxidation of solution NO on iridium, RDE setup 36 r.p.s., 0.1 M H_2SO_4 saturated with NO, triangles positive scan, crosses negative scan

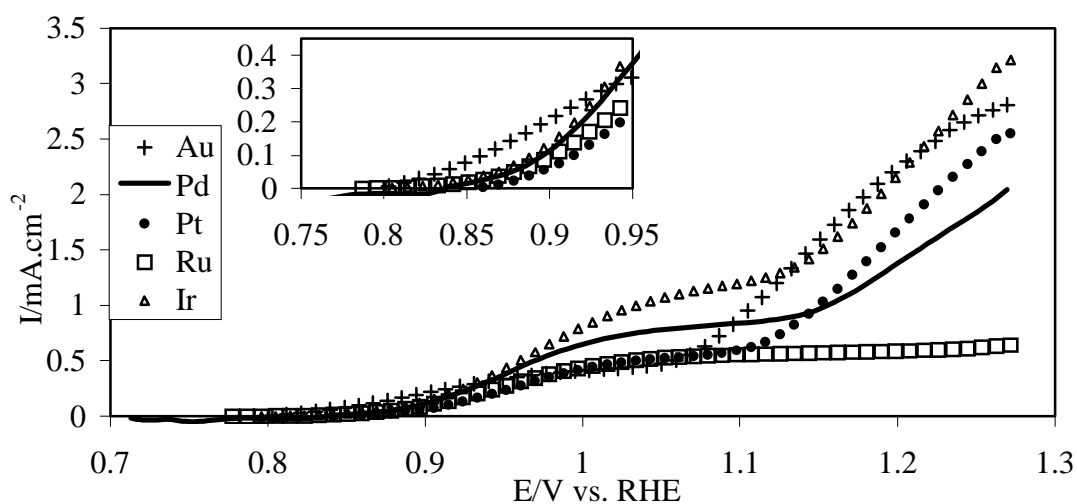


Figure 5.2: oxidation of solution NO on Au (crosses), Pd (thick solid line), Pt (circles), Ru (squares) and Ir (triangles). Inset is an enlargement of the currents between 0.75 and 0.95 V. Flag electrode, 0.1 M H_2SO_4 saturated with NO, $20 \text{ mV}\cdot\text{s}^{-1}$

The first wave in figure 2 is essentially independent of the nature of the electrode material (see inset in figure 2), similar to the oxidation in strongly acidic solutions, indicating that the reactive intermediate does not have a strong interaction with the electrode surface. The positive scans do show some changes with the choice of the metal, but, as the current shows a large statistical error (figure 3) and the differences are smaller than 100 mV, we infer that the metal dependence of the first wave is small. The onset of the potential curves in figure 2 is negative of the standard potential of reaction 1 (0.99 V vs. RHE [11]), showing that the overpotential for this reaction is small. The fact that gold is as active as the other metals, whereas NO is not

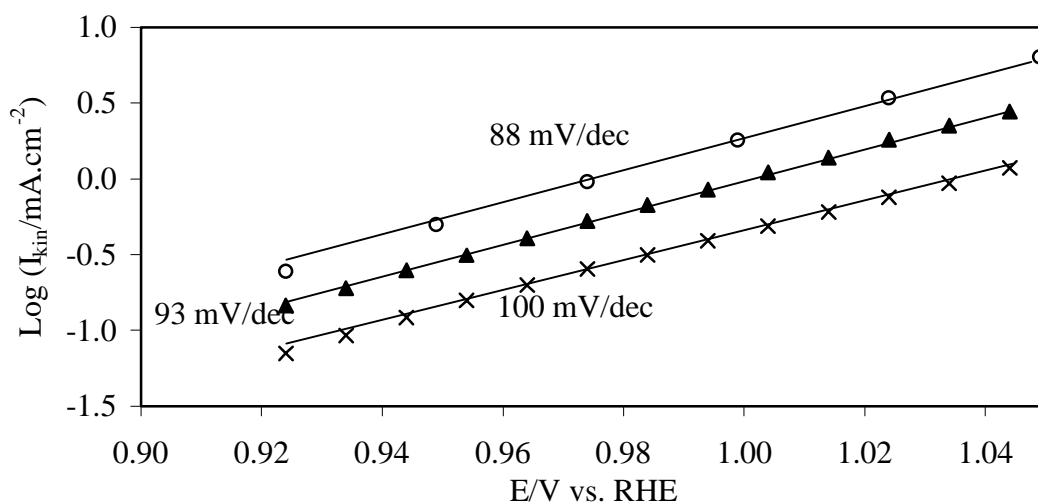
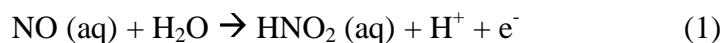


Figure 5.3: Tafel slope analysis of the kinetic limited current of the solution NO oxidation on platinum obtained from RDE experiments, 0.1 M H₂SO₄ saturated with NO. Circles, triangles and crosses are different runs under identical conditions

adsorbed on gold, is another indication that the reactive NO does not have a strong interaction with the surface in this potential region. The Tafel slope of the NO oxidation between 0.9 and 1 V is close to 120 mV/dec on platinum and gold, derived both from figure 2 and from RDE measurements (figure 3), indicating that the first electron transfer is rate determining. Figure 3 shows that the Tafel slope is reproducible within 10 %, even though the current density of the NO oxidation is not. The slope of the Levich plot (see appendix 1) between 0.9 and 1.1 V on both gold and platinum indicates that the total number of electrons produced per NO molecule is one, and the product therefore is HNO₂. Combining these facts we propose that the reaction equation for the first wave is:



The activity for NO and HNO₂ oxidation on gold are compared in figure 4. Figure 4 indicates that the second wave is the result of the oxidation of HNO₂ on gold, which suggests that the second wave is the oxidation of NO, via HNO₂, to NO₃⁻ on all metals. Previous RDE measurements [2] have shown that the ratio of the slopes of the Levich plots in the potential window of the first and second wave is 1:3, as expected when the products are HNO₂ (1 electron) and NO₃⁻ (3 electrons). However, there is no diffusion limited current in figure 1, which is the reason why the apparent ratio is not

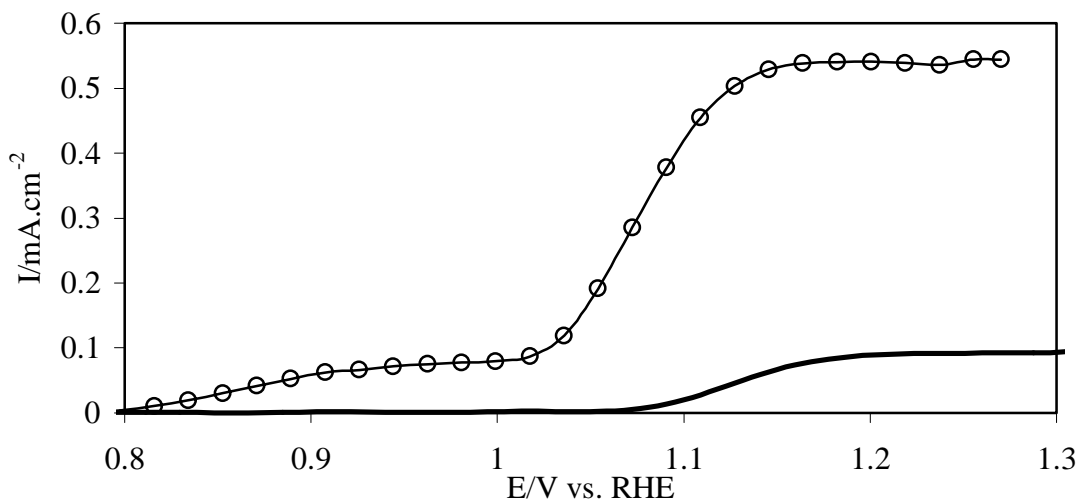


Figure 5.4: comparison of NO and HNO₂ oxidation on gold in 0.1 M H₂SO₄, circles solution saturated with NO, thick solid line 1 mM NaNO₂, RDE setup, 2 Hz

1:3. No attempt to detect NO₃⁻ has been made in a rotating ring-disk electrode (RRDE) setup, since no material is both active in the NO₃⁻ reduction and inactive in the NO reduction, and hence residual NO would interfere with the measurement. NO₂ can be excluded as a product, as it is not detected during DEMS measurements at any potential. When the voltammogram of the HNO₂ oxidation on gold in figure 4 between 1.05 and 1.12 V is plotted as a Tafel plot a value of 53 ± 7 mV/dec is found, suggesting a Nernstian equilibrium prior to a rate determining chemical step.

It is very difficult to obtain reliable kinetic information on the NO oxidation, especially when the RDE is used. Figure 3 shows three runs of the kinetic limited current as determined from RDE experiments of the NO oxidation on platinum from a 0.1 M H₂SO₄ saturated with NO under (supposedly) identical conditions. The currents found from the RDE measurements on gold are equally irreproducible. Problems in obtaining reliable data have been reported before: Dutta and Landolt [2] reported that the current at 1.3 V for the oxidation of solution NO on platinum was poorly reproducible. Figure 1 also shows that the current is poorly reproducible, as the positive and negative scan, for platinum, palladium and iridium, have different currents. Apparently, the state of the surface, which is determined by the exact history of the electrode, has a profound effect on the oxidation of solution NO. The problems in obtaining reliable data for the NO oxidation in alkaline solutions are even larger, which is the reason why those data are not presented in this chapter.

Figure 1 shows that for the oxidation of NO to HNO₂ on iridium the negative scan of voltammogram shows higher currents than the positive scan. The only difference between the positive and the negative scan is the possibility of surface oxides present during the negative scan, which could play a catalytic role in the NO oxidation. The subsequent reductive scan, however, does not show the typical metal-oxide reduction peak, which could prove the existence of surface oxides. The role of surface oxides in the oxidation to HNO₂ therefore remains unclear, but it would offer a plausible explanation for the poor reproducibility of the oxidation of solution NO.

The role of surface oxides in the oxidation to NO₃⁻ is different, as for instance all metals except gold deactivate when the potential is cycled repeatedly between 0.7 – 1.4 V in alkaline solutions. Hence, surface oxides hinder the NO oxidation under these conditions.

3.2. *NO adsorbate oxidation*

A typical plot for the oxidation of adsorbed NO, formed in a solution on HNO₂ at 0.37 V, on platinum, is shown in figure 5. The oxidation of NO is not complete, as after the oxidative scan a typical NO reduction feature can be seen. Even if the electrode is kept at 1.4 V for 15 minutes the oxidation is still not complete, showing that NO is surprisingly resistant to oxidation. The reductive scan shows, apart from the NO reduction at 0 - 0.3 V, also the oxide reduction peak at 0.7 V, showing that aside from NO oxidation also metal oxidation takes place. The presence of NO has no strong effect on the surface oxide reduction, since the surface oxide reduction peak is at the same position and has the same shape as in the blank voltammogram.

If we assume that NO_{ads} is oxidized to NO₃⁻, then the amount of NO_{ads} can be calculated by dividing the net charge of the oxidation (the charge of the NO oxidation plus surface oxide formation minus the charge of oxide reduction) by three (the oxidation of NO to NO₃⁻ produces 3 electrons per NO molecule). The total amount of NO_{ads} equals the amount of NO_{ads} oxidized plus the amount of NO_{ads} reduced in the subsequent reduction scan. The latter is equal to the net reduction charge, divided by five (the reduction of NO to NH₃ consumes 5 electrons per NO molecule). The amount of NO oxidized to NO₃⁻ is 0.28 monolayer. The amount of NO left at the

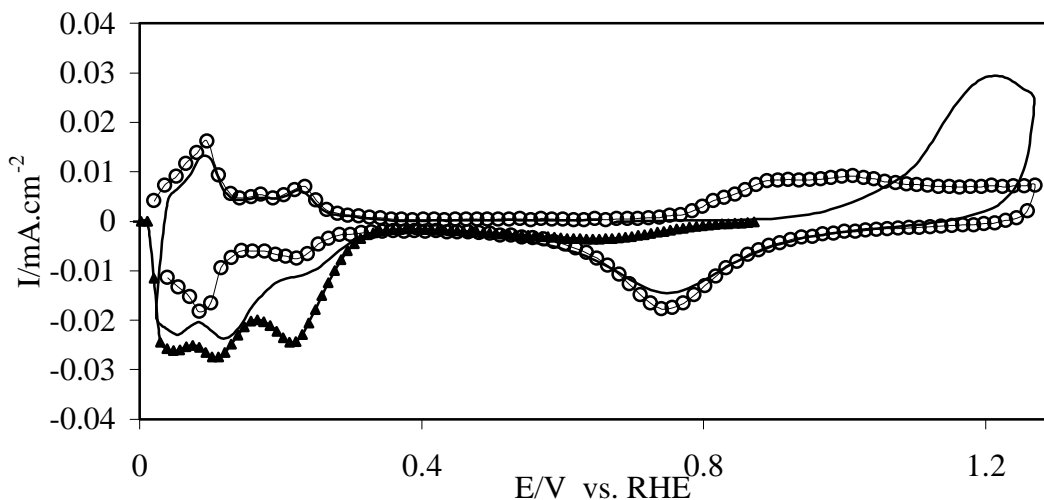


Figure 5.5: reduction and oxidation of adsorbed NO on platinum in 0.1 M H_2SO_4 , solid line NO oxidation and subsequent reduction (adsorption potential 0.67 V), circles blank, triangles NO reduction (adsorption under OCP (0.87 V))

surface, which is subsequently reduced to NH_3 , is 0.13, so the initial amount of NO is 0.41 monolayer. This is the same amount as obtained from the direct NO reduction (chapter 3), which shows that NO_3^- is in fact the product of the NO adsorbate oxidation.

When the scan rate of the oxidation is decreased the amount of NO oxidized increases slightly, showing that the final stages of the reaction are very slow. We attribute this to surface oxides, which somehow inhibit NO oxidation by stabilizing NO at the surface. The relationship between the oxidation of adsorbed NO and the formation of surface oxides is complex, since the presence of NO hinders the formation of surface oxides, as can be seen by comparing the adsorbate oxidation to the blank in figure 5. The role of surface oxides in the oxidation of adsorbed NO should be understood before an attempt at solving the mechanism can be made.

Under certain conditions, a plot of the peak potential of an adsorbate oxidation versus the logarithm of the scan rate yields the same information as a Tafel plot. This can be shown for a first [12] and second [13] order reaction. Based on the fact that in all cases the plot yields a straight line, we assume this procedure is also valid in the present case, and therefore we will refer to this slope as the Tafel slope of the adsorbate oxidation.

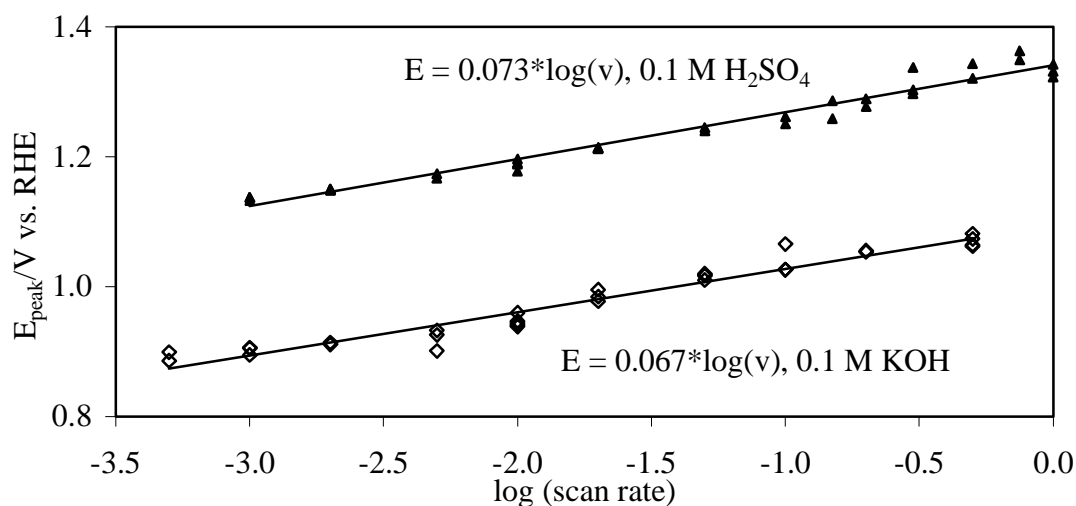


Figure 5.6: plot of the peak potential of the oxidation of adsorbed NO on platinum versus scan rate. Triangles 0.1 M H₂SO₄, diamonds 0.1 M KOH. NO at maximum coverage

Figure 6 shows the Tafel plot of the NO adsorbate oxidation on platinum both in acidic and alkaline solutions, the Tafel slope being close to 60 mV/dec, indicating the first electron transfer is in equilibrium, and a subsequent chemical step is rate determining. The electron transfer step is most likely reaction 1, following Rodes et al. [6] and Ye et al. [7]:



At present it is unclear what the subsequent non-electrochemical step would be, only that the final product is NO₃⁻. When the oxidation of NO adsorbed on platinum and on rhodium are compared (figure 7) the curves almost overlap, indicating that the onset of the reaction is similar. Comparison of figure 7 with the oxidation of solution NO to HNO₂ (figure 2) shows that both reactions occur in the same potential region, and when platinum is replaced by another metal the difference is in both cases small. This could indicate there is a relation between the oxidation of adsorbed NO and the oxidation of solution NO. However, both the potential-dependence, i.e. the Tafel slope, and the product, HNO₂ vs. NO₃⁻, are different. Also, it was concluded in the previous section that the oxidation of solution NO most likely involves weakly adsorbed intermediates. Both indicate that the relation between the

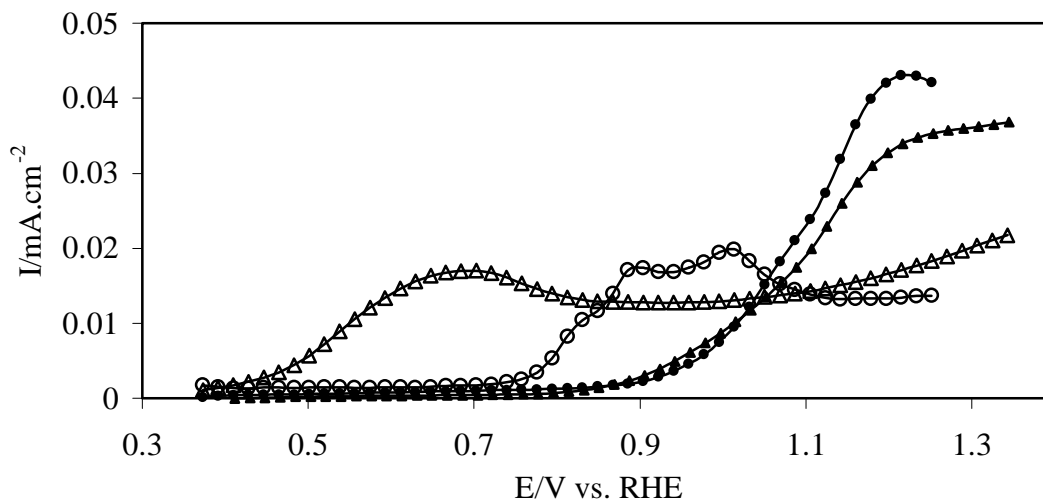


Figure 5.7: oxidation of adsorbed NO of rhodium (triangles) and platinum (circles), closed markers NO oxidation, open markers blank, flag electrode, 20 mV/s, 0.1 M H_2SO_4

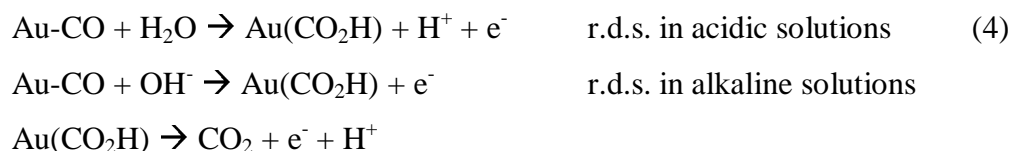
oxidation of adsorbed NO and the oxidation of solution NO is not a simple superposition. Therefore, it is unclear what the role of adsorbed NO is in the oxidation of solution NO, and this issue should be addressed in future research.

It is important to note that both on platinum and rhodium there is a slight shoulder at ca. 1.0 V on the oxidation peak (figure 7), indicating that there are multiple processes taking place at the surface.

3.3. Comparison with CO oxidation

There are a number of similarities between NO and CO. The heat of adsorption on platinum, for instance, is similar [14], and both oxidations require oxygen transfer from water, so the reaction scheme for the oxidation of NO might be similar to the oxidation of CO. In this section we will first compare the oxidation of solution NO will be compared to the oxidation of solution CO, then the oxidation of adsorbed NO will be compared to the oxidation of adsorbed CO.

It was suggested that NO is weakly adsorbed during the oxidation of solution NO. The oxidation of solution NO should therefore also be compared to CO oxidation on a metal where CO is weakly adsorbed, like gold [15]. It has been suggested that the CO oxidation on gold follows reaction scheme 4 [16]:



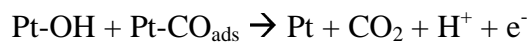
The rate-determining step in reaction scheme 4 is similar to scheme 1, in the sense that in both cases it is an reaction of an adsorbed molecule with water in a one-electron transfer. In both cases the Tafel slope indicates that this electron transfer reaction is rate determining.

The reaction rate of the CO oxidation on gold decreases in the potential region where surface oxides are formed, surface oxides therefore hinder the oxidation of CO. The same effect is suggested for the oxidation of NO to NO_3^- , but it is opposite to the catalytic effect of surface oxides suggested for the NO oxidation to HNO_2 . The role of surface oxides on the oxidation of NO can not be understood using only electrochemical methods.

The CO oxidation is not completely first order in the concentration of H^+ , i.e. there is a potential shift on the RHE scale. This is related to the reaction scheme, since an isotope-exchange experiment showed that in acidic solutions the rate decreased six-fold in D_2O , showing that an OH-bond is involved in the rate-determining step; in alkaline solutions the rate did not change when H_2O was replaced with D_2O . The oxidation of solution NO on gold is fully pH-dependent, i.e. does not shift on the RHE scale. However, a complex pH-dependence is also observed for the NO adsorbate oxidation: the pH-dependence of the reaction (250 mV shift over 12 decades) is between full dependence (no potential shift on the RHE scale) and no dependence (720 mV shift on the RHE scale). An isotope-exchange experiment might yield useful information on the NO oxidation as well, given the complex pH-dependence. However, it is important to note that HNO_2 is a weak acid, the pK_z is ca. 3 [17]. This could also result in a complex pH-dependence, as has already been shown for the oxidation of NO_2^- on platinum [17].

The oxidation of adsorbed NO and of adsorbed CO cannot be compared on gold, since neither is strongly adsorbed on gold. The comparison would have to be made on a metal like platinum, which strongly adsorbs both NO and CO [14].

However, the oxidation of CO on platinum, both CO in the solution and adsorbed CO, follows a completely different reaction scheme from gold [13,18]:



This reaction scheme shows some major differences with the oxidation of NO present in the solution. The most important difference is that the kinetic order in the concentration of CO is negative, since CO adsorbs more strongly on platinum than OH in the potential region of interest. The kinetic order in NO is positive, since the RDE measurements show an increase in the rate of the reaction as the rotation frequency increases, i.e. the concentration of NO near the surface increases. A second difference is the maximum coverage of CO (close to 0.8) and NO (0.4). Finally the potential at which the reactions take place is different. Each of these differences would have a large impact on the OH formation at the surface, the first step in scheme 5. The oxidation of adsorbed NO and CO are therefore difficult to compare. If no surface oxides would be present during the oxidation of adsorbed NO then their influence could be neglected. However, figure 5 shows that NO and OH can be co-adsorbed, showing that the role of surface oxides can not a priori be neglected.

Potential-step experiments (not shown), where the potential is increased instantly and the current is measured, do not yield a peak, but the current decreases continuously. This is unlike similar experiments on the CO oxidation [13, and references therein], where the current first increases and then decreases, yielding a current peak.

4. Summary

In the oxidation of solution NO both HNO_2 and NO_3^- can be formed, depending on potential. The rate of the formation of NO_3^- is metal dependent, whereas the rate of the formation of HNO_2 is almost independent on the metal. Since gold is as active as the other metals, and gold is known to adsorb NO weakly, it is suggested that strongly adsorbed NO is not included in the rate-determining step. The first

electron transfer is the rate-determining step in the formation of HNO_2 . The oxidation of NO to HNO_2 shows similarities with the oxidation of CO on gold.

Prior to the rate-determining step in the oxidation of adsorbed NO is an equilibrium between NO and HNO_2 , the subsequent chemical step is rate determining. The product is NO_3^- . The curve of the adsorbate oxidation on platinum and rhodium almost overlap, indicating that the reaction is virtually metal-independent.

Surface oxides are expected to play a role both in the oxidation of solution NO and of adsorbed NO . The influence of surface oxides varies with the conditions: in the oxidation of adsorbed NO it stabilizes NO at the surface, i.e. it inhibits the reaction, in the oxidation of solution NO it probably catalyses the reaction. The exact role can not be investigated using only electrochemical methods. We suggest spectroscopic techniques, and especially SERS, as a tool, since those techniques can detect surface oxides in situ.

References

- [1] S. Susuki, T. Nakato, H. Hattori and H. Kita, *J. Electroanal. Chem.* 396 (1995) 143
- [2] D. Dutta and D. Landolt, *J. Electrochem. Soc.* 119 (1972) 1320
- [3] H.N. Heckner and G. Schmid, *Electrochim. Acta* 16 (1971) 131
- [4] B.G. Snider and D.C. Johnson, *Anal. Chim. Acta* 105 (1979) 9
- [5] A. Rodes, R. Gomez, J.M. Perez, J.M. Feliu and A. Aldaz, *Electrochim. Acta* 41 (1996) 729
- [6] A. Rodes, R. Gomez, J.M. Orts, J.M. Feliu and A. Aldaz, *J. Electroanal. Chem.* 359 (1993) 315
- [7] S. Ye and H. Kida, *J. Electroanal. Chem.* 346 (1993) 489
- [8] K. Momoi, M.-B. Song and M. Ito, *J. Electroanal. Chem.* 473 (1999) 43
- [9] J. Willsau and J. Heitbaum, *J. Electroanal. Chem.* 194 (1985) 27
- [10] manual mass spectrometer, Balzers AG (1991), Balzers Liechtenstein
- [11] Handbook of chemistry and physics, 57th edition, R.C. Weast (Ed.), CRC press, Cleveland, 1976
- [12] P.A. Christensen and A. Hamnett, in "Techniques and Mechanisms in Electrochemistry." Blackie Academic and Professional, Glasgow, 1994
- [13] M.T.M. Koper, A.P.J. Jansen, R.A. van Santen, J.J. Lukkien, and P.A.J. Hilbers, *J. Chem. Phys.* 109 (1998) 6051
- [14] Y.Y. Yeo, L. Vattuone and D.A. King, *J. Chem. Phys.* 104 (1996) 3810
- [15] J.-D. Grunwaldt and A. Baiker, *J. Phys. Chem. B* (1999) 1002
- [16] G.J. Edens, A. Hamelin and M.J. Weaver, *J. Phys. Chem.* 100 (1996) 2322
- [17] R. Guidelli, F. Pergola and G. Raspi, *Anal. Chem.* 44 (1972) 745
- [18] S. Gilman, *J. Phys. Chem.* 68 (1964) 70

Chapter 6: The Role of Adsorbates in the Electrochemical Oxidation of Ammonia on Noble and Transition Metal Electrodes

Abstract

The activity for ammonia oxidation and the intermediates formed during the reaction have been studied on platinum, palladium, rhodium, ruthenium, iridium, copper, silver and gold electrodes. The activity in the selective oxidation to N_2 is directly related to the nature of the species at the surface: the electrode is active if NH_{ads} (or $NH_{2,ads}$) is present, and deactivates when N_{ads} is present. The potential at which NH_{ads} or N_{ads} are formed is metal dependent. The observed trend in the strength of adsorption of N_{ads} is $Ru > Rh > Pd > Ir > Pt >> Au, Ag, Cu$. This trend corresponds well with the trend observed in the calculated heat of adsorption of atomic nitrogen, with iridium being an exception.

Platinum is the best catalyst for this reaction because N_{ads} is formed at high potential, compared to rhodium and palladium, but seems to stabilize NH_{ads} rather well. Gold, silver and copper do not form NH_{ads} or N_{ads} , and show only an activity when the surface becomes oxidized. The metal electrodisolution is enhanced by ammonia under these conditions. Most metals produce oxygen containing products, like NO and N_2O , at potentials where the surface becomes oxidized.

1. Introduction

Ammonia is a common and highly toxic component in gaseous and aqueous waste streams, and its decomposition has therefore become a prominent topic in environmental catalysis [1]. Commonly aqueous ammonia is removed by bacterial degradation, but this process can be problematic due to high cost or low effectiveness [2]. Therefore there is an increased interest in oxidizing ammonia using metallic or oxidic catalysts in water.

The oxidation of ammonia on a platinum catalyst in water can take place either electrochemically [3] or using oxygen as an oxidizing agent [4]. In both cases the presence of oxides at the surface determines the selectivity of the reaction: if no surface oxides are present N_2 is formed, whereas oxygen-containing products, like N_2O and NO_2^- , are formed in the presence of surface oxides. At the electrochemical interface no surface oxides are formed at potentials lower than 0.8 V (versus RHE). In the case of oxidation with oxygen no oxides are formed when the supply of O_2 is diffusion limited. This suggests that the mechanism of ammonia oxidation in both cases should be similar, and that electrochemical methods can be used to obtain mechanistic information that is also relevant to the liquid-phase oxidation using oxygen, which would be the preferred method in a catalytic reactor.

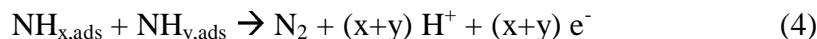
Several transition metal catalysts have been tested for the selective oxidation of ammonia to dinitrogen. Both liquid-phase oxidation methods using oxygen [4] and electrochemical methods [5] have shown that iridium is the most active catalyst in producing dinitrogen, but is also more prone to deactivation than platinum. Both palladium and ruthenium are less active in producing dinitrogen than platinum or iridium [4].

From the fundamental point of view, it is of interest to compare the ammonia oxidation at metal-liquid interfaces with the oxidation at the metal-gas interface. The activity of several metals in the gas phase has been reviewed by Il'chenko [6] and Papapolymerou et al. [7]. The noble transition metals (Pt, Pd, Rh and Ir) are found to be the most active catalysts. The coinage metals (Cu, Ag, and Au) were found to be less active than the noble transition metals, but more active than the other transition

metals and the metal oxides. Similar to the oxidation in water, the most active catalyst for the selective oxidation to dinitrogen is iridium [7,8].

More insight in the detailed mechanism of the gas-phase ammonia oxidation comes from UHV experiments at well-defined metal surfaces. Temperature programmed oxidation experiments on Pt(111) [9] and Pt(100) [10] showed that NH_3 is consecutively dehydrogenated to NH_2 , NH and finally to N . After these steps N_2 is formed by the combination of two N adatoms. Besides N_2 also NO is formed at high oxygen coverages [9,10], quite similar to the situation in the aqueous phase. On both Pt(111) and Pt(100) the combination of 2 N atoms to form N_2 takes place at a higher temperature (470 resp. 550 K) than the dehydrogenation reactions (ca. 350 K), implying that this reaction is the rate-determining step in the ammonia oxidation on single-crystal platinum surfaces.

At metal-liquid interfaces, essentially all of our current mechanistic understanding of the ammonia oxidation comes from electrochemical studies using platinum electrodes. These studies are all supportive of a mechanism for the dinitrogen formation originally suggested by Gerischer and Mauerer [11]:



with $x, y = 1$ or 2

From the observed Tafel slope of 39 mV/dec in the potential range of 0.45-0.6 V, Oswin and Salomon [12] concluded that the third step in this scheme is the rate determining reaction. At potentials higher than 0.6 V Gerischer and Mauerer observed that the platinum electrode deactivates. From an ex situ analysis of a deactivated electrode using temperature programmed desorption, only N_2 was detected and no H_2 . Hence these authors concluded that the deactivation of the electrode was related to the formation of N_{ads} . This inactivity of N_{ads} towards N_2 formation is in sharp contrast to the gas phase ammonia oxidation.

Gerischer and Mauerer also observed that between 0.45 and 0.6 V the kinetic order in the concentration of NH_3 is zero [11]. This indicates that the adsorption of NH_3 is fast, and the surface is saturated with ammonia adsorbates.

The mechanistic model of Gerischer and Mauerer was confirmed by coulometric experiments measuring the charge involved in the formation, oxidation or reduction of the adsorbate, giving information about its valency [3,13,14]. Wasmus et al. [3] observed that the adsorbate formed at relatively low potentials (< 0.6 V), where dinitrogen is formed, has a valency consistent with a hydrogenated nitrogen adsorbate like NH_{ads} or $\text{NH}_{2,\text{ads}}$. At higher potentials (> 0.6 V), the coulometric data of Gootzen et al. [13] suggested the presence of a fully dehydrogenated adsorbate, i.e. atomic nitrogen N_{ads} .

The question that naturally arises from the above discussion is whether the Gerischer-Mauerer mechanism also applies to other transition-metal and noble metal electrodes. It is then also of interest to investigate if the activity for dinitrogen production can be related to the relative stability of the various adsorbates on the different metals and their respective potential dependence.

It is our aim in this chapter to address these issues on five different polycrystalline transition-metal electrodes (Ru, Pd, Rh, Ir and Pt) and three polycrystalline coinage metal electrodes (Cu, Ag, Au). To this end, we will first return to platinum, and present detailed potential-dependent coulometric data on the oxidation and reduction of the ammonia adsorbate. These data will give us a more detailed picture of the nature and the amount of adsorbate as a function of electrode potential than the previous adsorbate studies. The methods applied to platinum will then be discussed for the other metals, and a relation will be established between the nature of the adsorbate, the potential of deactivation and the overall activity for dinitrogen formation. Finally, these trends will be compared to the stability of ammonia and atomic nitrogen on the various metals in vacuum as obtained from quantum-chemical density-functional theory calculations.

2. Methods

2.1. Experimental

Platinum, iridium, rhodium, palladium and ruthenium flag electrodes were flame annealed prior to each measurement. Surface oxides on platinum and palladium electrodes were reduced by taking a cyclic voltammogram prior to the measurement. Iridium and rhodium electrodes were cooled in an argon atmosphere and protected from air by a droplet of clean water to avoid the formation of surface oxides. Ruthenium electrodes were cooled in a hydrogen/argon mixture instead of pure argon. A blank cyclic voltammogram was recorded prior to each experiment to check the cleanliness of the surface and to reduce possible surface oxides. Gold and silver electrodes were cleaned by repeated cycling in the oxygen and hydrogen evolution region. Copper electrodes were prepared in situ by deposition from a 10 mM CuSO₄ solution onto a platinum electrode in 0.1 M H₂SO₄.

DEMS (Differential Electrochemical Mass Spectroscopy) measurements were performed on a Balzers Prisma QMS 200 mass spectrometer. Details of the setup are described elsewhere [15]. The DEMS signals of N₂, N₂O and NO were calibrated by oxidizing a monolayer of CO and measuring the amount of CO₂. The signal was corrected for differences in ionisation and fragmentation probability.

DEMS electrodes were prepared similarly to the flag electrodes except for rhodium and iridium, which were freshly prepared by deposition from a bath of 1 mM IrCl₃ or RhCl₃ in 0.1 M H₂SO₄ (iridium was deposited at 80 °C) on a platinum gauze. The solution was thoroughly rinsed while keeping the electrode at -0.2 V to remove chlorides from the surface.

The electrochemical quartz microbalance (ECQM) system consists of gold, silver or copper electrodeposited on a gold covered quartz crystal (5 MHz, Phelps electronics) in a teflon encasing [16]. The frequency was measured with a Philips PM 6680/016 frequency counter.

All chemicals are of p.a. quality (Merck) for the adsorbate experiments, whereas suprapure (Merck) chemicals were used for the oxidation of NH₃ with ammonia in the solution. Solutions were prepared using Millipore MilliQ water (resistance > 18.2 MΩ and total organics concentration 3 p.p.b. or lower). The

reference electrode was a Hg/HgO/KOH (1 M or 0.1 M) electrode, but all potentials will be referred to the RHE scale. Oxygen was removed from the solution by purging with argon (4.7, Hoekloos) prior to the measurement.

Adsorbate experiments were performed by allowing the adsorbate to be formed in a solution of 10 mM NH₃ in 0.1 M KOH at a fixed potential (the adsorption potential) for two minutes. The electrode was then transferred at the adsorption potential to a cell containing a deoxygenated 0.1 M KOH solution. The time during which the electrode was not under potential control was always less than 0.5 seconds, and the electrode was protected by a droplet of electrolyte during the transfer. In the DEMS setup the electrode could not be transferred, so that NH₃ was removed from the solution by rinsing with the blank electrolyte at least four times, while keeping the potential constant.

After the adsorbate was reduced, or oxidized and subsequently reduced, a second scan was taken. In all adsorbate experiments the absence of NH₃ in the solution was checked by comparing the second scan with the blank scan. The charge involved in the reduction of the adsorbate was corrected for the hydrogen UPD region in the case of platinum, iridium, rhodium and ruthenium. This was done because in the subsequent oxidation sweep the hydrogen UPD peaks are present, so they are formed in the reductive sweep and contribute to the total charge.

2.2. Computational

Adsorption energies of atomic nitrogen on the eight different metals under consideration in this chapter were calculated by the Vienna ab initio simulation package VASP [17], and based on a periodic slab-like representation of the metal surface using a plane-wave basis set and ultrasoft pseudopotentials. The electronic ground-state energy was computed by the density functional theory (DFT) method in the generalized gradient approximation proposed by Perdew and Wang [18,19]. This DFT method is known to yield quite accurate binding energies [20].

The (111) surface of all fcc metals was modeled as a three-layer slab with the atom-atom distance fixed at their experimental equilibrium values (obtained from [21]), whereas the hcp ruthenium surface was modeled as a three-layer slab of (0001) orientation. Even though this does not give an accurate geometric representation of the real surface, these approximations are known to still give fairly reliable binding

energies [20], with a minimal amount of computational cost. The nitrogen atom was adsorbed in the fcc hollow site of the (111) surface, and the nitrogen-metal distance was optimized in all calculations. The adsorption energy was obtained from the difference between the total energy of the (metal+adsorbate) system and the sum of the total energies of the clean metal surface and the uncoordinated atom in vacuum.

The nitrogen atom was adsorbed on a (2x2) unit cell of surface atoms, yielding a nitrogen adatom coverage of 0.25. In all cases the plane-wave expansion was truncated at a cut-off energy of 300 eV, and a grid of 7x7x1 Monkhorst-Pack special k-points was used to perform the Brillouin-zone integrations.

3. Results and discussion

3.1. Adsorption energies

It is quite obvious from the Gerischer-Mauerer mechanism discussed in the Introduction that the interaction of both ammonia and its dehydrogenated surface intermediates with the surface will greatly influence the activity of the metal surface as well as its tendency to deactivate. In this section we will briefly summarize the adsorption energies of ammonia from the gas phase, as obtained from the experimental literature, and atomic nitrogen, from the calculational procedures described in the previous section. Our purpose is to relate these energies to the observed experimental trends in activity, to be reported in the next sections.

The adsorption energies of ammonia from the gas phase or vacuum (as well as the experimental circumstances under which they were determined) are given in table 1. In general, the transition metals have a stronger affinity for ammonia than the coinage metals Cu, Ag and Au. We also note here that the adsorption energy of ammonia on transition-metal surfaces is higher than that of water, which typically has an adsorption energy of 40-50 kJ/mol on transition metal surfaces [28].

Table 2 gives the DFT-computed adsorption energies for atomic nitrogen. Not surprisingly, the trend in metal dependence is quite similar to that calculated previously for atomic oxygen [29]. Although at this point we do not want to anticipate on the electrochemical activity trends suggested by these data, we note that in general

Table 1: Desorption energy of NH_3 on selected noble metals in kJ/mol. If several adsorption states are possible the highest energy is given.

Pt	Pd	Rh	Cu	Ag
96 ¹		82 ²	62 ³	46 ⁴
70 ⁵	73 ⁵	71 ⁵		
110 ⁶			55 ⁷	

1. Pt (100), TPD in UHV [22]
2. Rh (111), TPD in UHV [23]
3. Cu (100), TPD in UHV [24]
4. Ag (110), TPD in UHV [25]
5. polycrystalline wire, obtained from fitting reaction parameters during the oxidation with O_2 [7]
6. DFT cluster calculations on Pt (111) [26]
7. DFT cluster calculations on Cu (100) [27]

Table 2: DFT calculated adsorption energy of atomic N on selected noble metals in kJ/mol

Ru	Ir	Rh	Pd	Pt	Cu	Au	Ag
-525	-453	-448	-398	-394	-318	-162	-156

for an oxidation reaction in which N_{ads} is formed (like reaction 5 in the Gerischer-Mauerer mechanism), one expects that a higher adsorption energy implies a lower (less positive) electrode potential at which the reaction takes place at a certain rate.

3.2. Platinum

Activity

A typical cyclic voltammogram of the oxidation of NH_3 on a polycrystalline platinum electrode is shown in figure 1. As reported before [11], the electrode deactivates at potentials above 0.6 V.

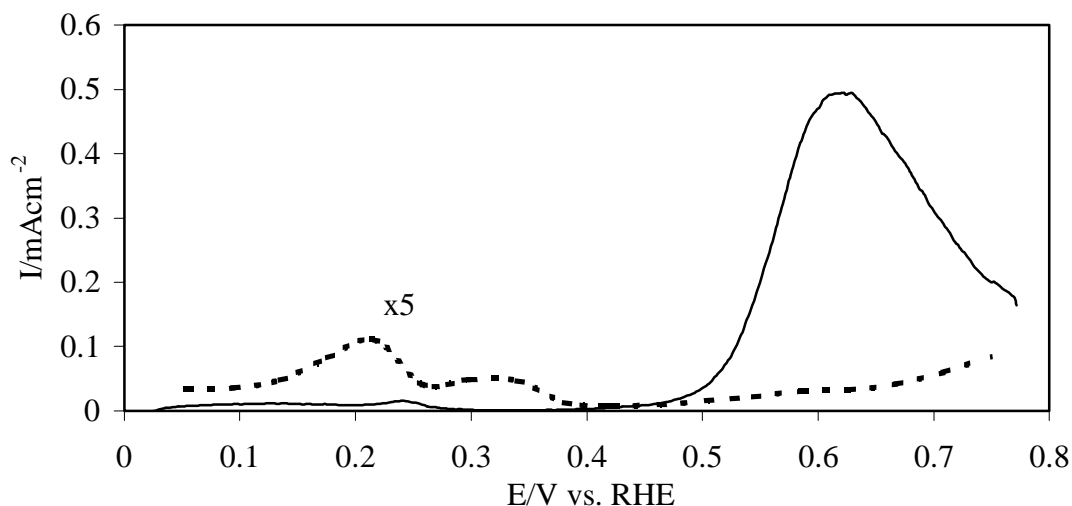


Figure 6.1: Voltammogram of platinum in the presence (solid line) and absence (dotted line) of 0.1 M NH₃, 1 M KOH, 20 mV/sec. The current of the blank voltammogram has been multiplied by a factor of 5 for clarity.

When the potential is increased stepwise the current quickly reaches a constant steady state current at potentials lower than 0.57 V, whereas at higher potentials the electrode deactivates with time (figure 2a). Figure 2b shows that a Tafel plot with a slope of 40 mV/dec is obtained in the potential range of 0.4 - 0.55 V, in agreement with earlier results of Oswin and Salomon [12]. Figure 2c shows that at 0.5 V the kinetic order in the concentration of NH₃ is close to zero. This value is measured in the entire potential window between 0.4 – 0.55 V, and is in agreement with the results of Gerischer and Mauerer [11].

DEMS experiments show that the selectivity to N₂ is 100 % at potentials lower than 0.8 V, whereas at higher potentials oxygen containing products like N₂O and NO are formed, as was already reported by Wasmus et al. [3].

Reduction of the adsorbate

To study the nature and coverage of the ammonia adsorbate, the adsorbate was formed at a certain adsorption potential, E_{ads} , in an ammonia-containing solution, and then transferred to another cell containing an ammonia-free electrolyte, where the adsorbate was stripped off to 0 V in a reductive scan. The coulometric charge obtained from this experiment, corrected for the hydrogen formation charge in the

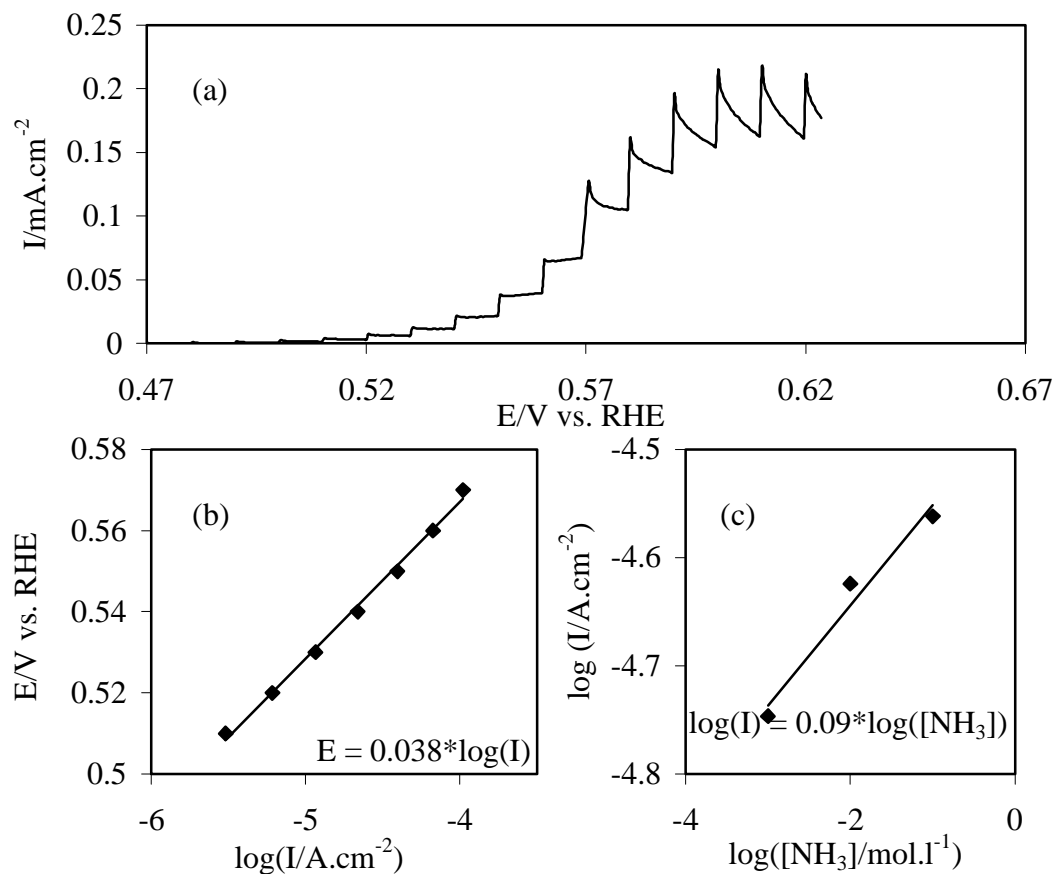


Figure 6.2, a: Activity of platinum in the NH_3 -oxidation, stepwise increase of the potential, 1 mM NH_3 in 1 M KOH, 10 sec. per step, b: Tafel plot, from data in figure 2a, c: kinetic order in the concentration of NH_3 on platinum, 0.5 V, 1 M KOH

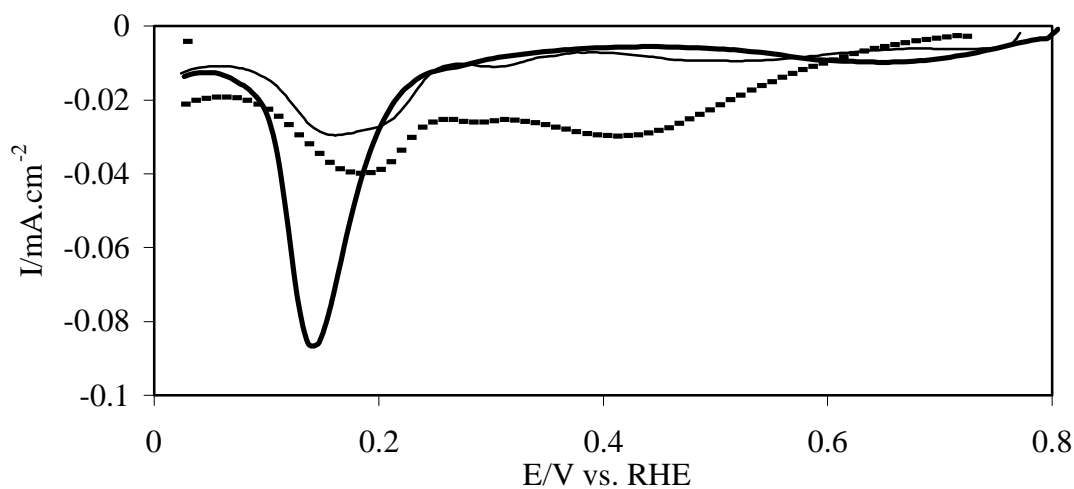


Figure 6.3: Comparison of adsorbate reduction from $E_{\text{ads}} = 0.77$ V (dotted line), NO reduction (thick line) and blank (thin line) on platinum, 1 M KOH, $v = 20$ mV/sec

blank voltammogram, is a measure for the amount and valency of the ammonia adsorbate formed at E_{ads} . The surface was free of ammonia adsorbates at 0 V, as evidenced by the fact that the positive-going scan after reductive stripping was identical to that of a clean blank voltammogram. No charge correction was made for anion (OH^-) adsorption, primarily because the amount of anion co-adsorbed with the ammonia adsorbate at a typical E_{ads} is difficult to estimate, but presumably small (see below).

A typical reduction profile is given in figure 3, together with the blank and the reduction profile of NO_{ads} . Since the reduction profile of the adsorbate is substantially different from the profile of NO_{ads} , it is unlikely that NO is formed during the adsorbate formation. As no gaseous products are detected during the reductive scan in the DEMS setup, and it is known that H_2NOH is reduced under these conditions [30], the product of the adsorbate reduction must be ammonia.

In figure 4 the charge obtained in the adsorbate reduction is plotted against E_{ads} . Three potential regions can be distinguished in figure 4: between 0.35 and 0.4 V the charge is close to zero, from 0.4 to 0.6 V the charge increases, whereas between 0.6 and 0.8 V the charge is constant. These three potential windows will be discussed separately.

Although the charge of the adsorbate reduction between 0.35 and 0.4 V is close to zero, adsorbates are nevertheless present. This can be concluded from figure 5, in which the cyclic voltammetry of a platinum electrode between 0 and 0.4 V in the presence and absence of NH_3 is compared. The profiles of the two curves are different, although the charge under the two curves is the same. Since no net charge is produced during the adsorbate reduction, nor during the formation, the different voltammetric profiles must be due to the adsorption of intact NH_3 from the ammonia containing solution. This would agree with the higher adsorption energy of ammonia on platinum compared to water (section 3.1).

In the potential window from 0.4 to 0.6 V the charge of the adsorbate reduction increases with E_{ads} . This is also the potential window in which the electrode produces N_2 without deactivation. It is therefore likely that the adsorbate in this potential window is the intermediate of the reaction, i.e. $\text{NH}_{2,\text{ads}}$ and/or NH_{ads} .

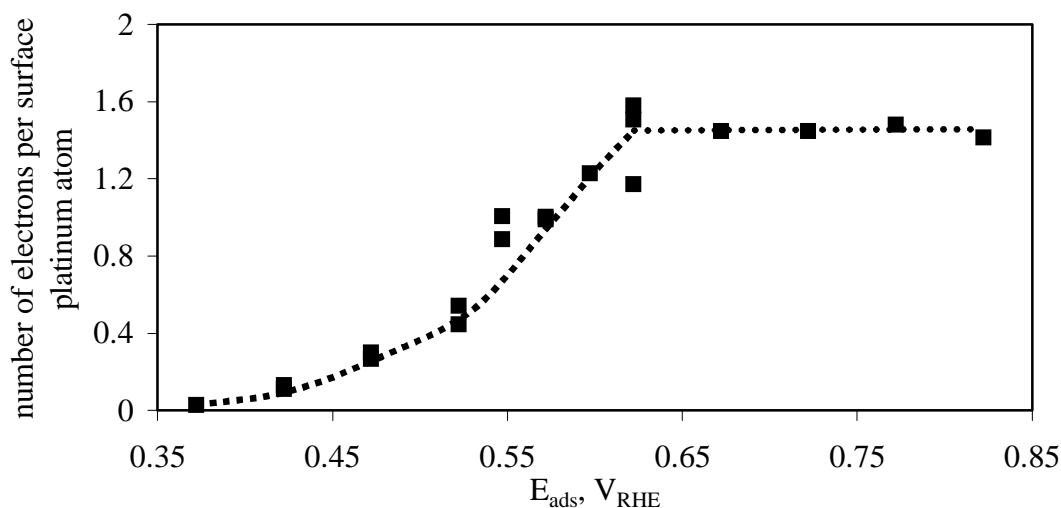


Figure 6.4: Integrated charge of the reduction of the ammonia adsorbate after formation at E_{ads} on platinum, 1 M KOH

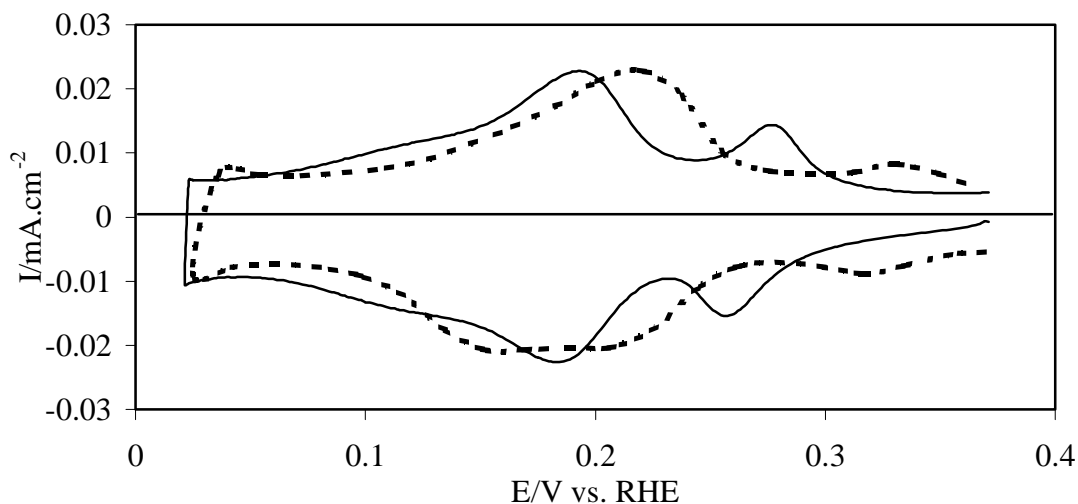


Figure 6.5: Hydrogen UPD region of platinum in the presence (solid line) and absence (dotted line) of NH_3 , 20 mV/sec, 1 mM NH_3 in 1 M KOH

In the potential window from 0.6 to 0.8 V the adsorbate reduction charge has a constant value of ca. $343 \mu\text{C}/\text{cm}^2$, which amounts to 1.63 electrons per surface platinum atom. Gootzen et al. [13] reported that the charge of the adsorbate formation is $325 \mu\text{C}/\text{cm}^2$, in good agreement with our data. Gootzen et al. already argued that this makes N_{ads} the most likely adsorbate at potentials between 0.6 and 0.8 V, as the charge would correspond to the most reasonable coverage of ca. 0.5. Other possible adsorbates, like NH_{ads} or $NH_{2,ads}$, would have coverages of 0.8 and 1.6 resp., which seem unreasonably high.

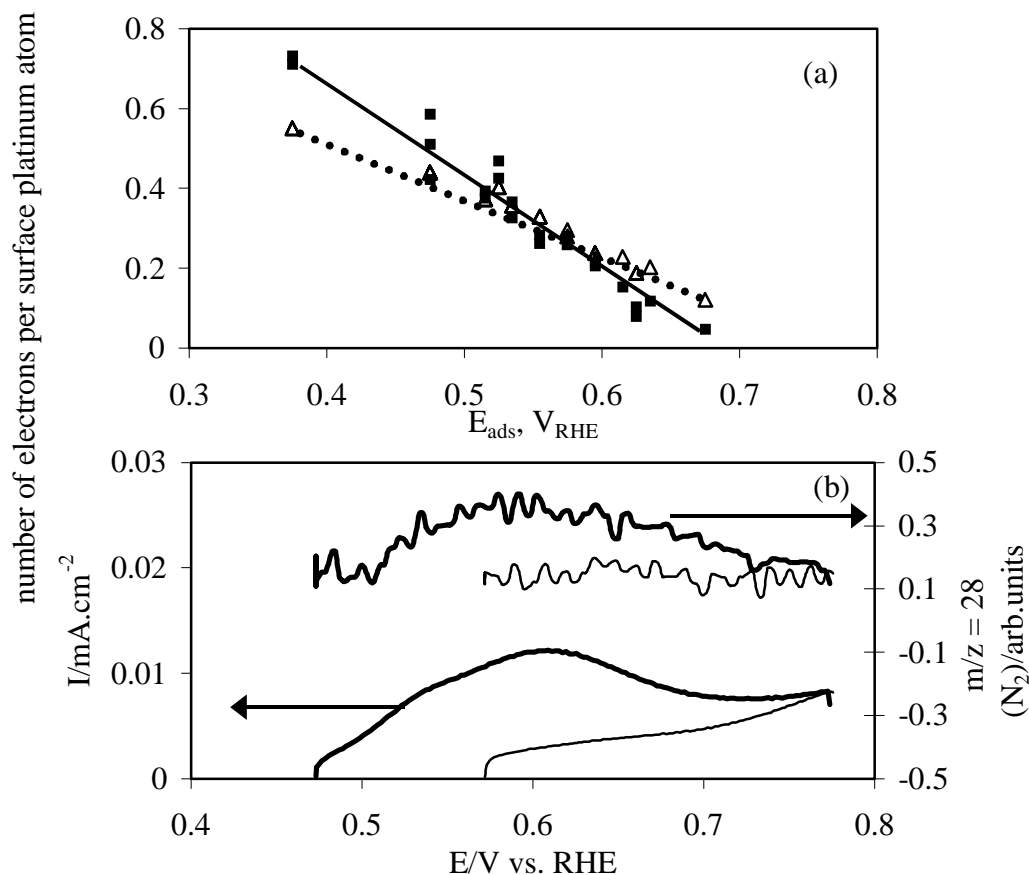


Figure 6.6, a: Charge of the oxidation of the ammonia adsorbate formed at E_{ads} to 0.77 V on platinum, filled squares ammonia adsorbate, open triangles blank, 1 M KOH, b: DEMS on ammonia adsorbate oxidation, E_{ads} 0.47 (thick line) and 0.57 V (thin line) on platinum, 1 M KOH

Oxidation of the adsorbate

The nature of the adsorbate formed at a certain E_{ads} was also studied by oxidizing it to a potential just negative of the onset of the platinum surface oxidation, so that the formation of nitrogen-oxygen compounds can be reasonably excluded (see below).

Figure 6a shows the charge involved in the oxidation of the adsorbate adsorbed at E_{ads} , to a potential of 0.77 V. The adsorbate oxidation charge is compared to the charge under the blank voltammogram between these two potentials. Interestingly, the adsorbate oxidation charge is lower than the “blank charge” for potentials higher than 0.57 V, whereas it is higher for lower potentials. This suggests that at potentials below 0.57 V, “oxidizable” adsorbates are formed, i.e. $NH_{2,ads}$ and/or

NH_{ads} , whereas above 0.57 V an “inert” species is the main adsorbate, i.e. N_{ads} . The lower charge then mainly stems from anion (OH^-) adsorption [31], which is partially blocked by the presence of the ammonia adsorbates.

When the same experiment is carried out in the DEMS setup, it is observed that oxidation of the adsorbate formed at $E_{\text{ads}} < 0.57$ V is accompanied by the formation of N_2 , whereas no N_2 is formed upon oxidation with $E_{\text{ads}} > 0.57$ V (figure 6b). This further supports the idea that the reactive intermediates in forming N_2 are $\text{NH}_{2,\text{ads}}$ or NH_{ads} , and N_{ads} is unreactive with respect to N_2 formation. The fact that the N_2 production gradually decreases toward higher potentials (figure 2) suggests there is a gradual change in the mixed “composition” of ammonia adsorbates. It is also interesting to note that the “transition potential” of 0.57 V observed in this adsorbate oxidation experiment coincides with the “deactivation potential” found in figure 2.

When the adsorbate formed at a certain $E_{\text{ads}} < 0.77$ V, is oxidized to 0.77 V, and subsequently reduced, a voltammetric profile is obtained which is the same as the profile for the adsorbate formed directly at 0.77 V. Therefore, the adsorbates studied in this section are the same as those studied during the adsorbate reduction, and likewise we may exclude the formation of oxygenated nitrogen adsorbates, such as NO, for potentials lower than 0.77 V.

However, when the adsorbate oxidation is carried out to higher potentials, new features appear in the subsequent reductive scan, as illustrated in figure 7, which shows the cyclic voltammogram of an adsorbate formed at $E_{\text{ads}} = 0.77$ V and oxidized to 1.4 V. First of all, there is a clear oxidation peak, which has a higher charge than the blank oxidation peak and is also shifted positively with respect to the blank surface oxidation peak. This suggests that the N_{ads} species is further oxidized in this potential region, as well as that it inhibits the metal surface oxidation.

The most distinct feature in the subsequent reductive scan is the enhanced irreversibility of the typical oxide reduction peak. We tentatively ascribe this feature to the formation of metal oxynitrides in the previous oxidative scan, which are more difficult, apparently, to reduce than the metal oxides in the blank profile. The irreversible formation of these oxynitrides is evidenced by the fact that keeping the electrode at 1.4 V for 15 minutes does not change appreciably the profile of the

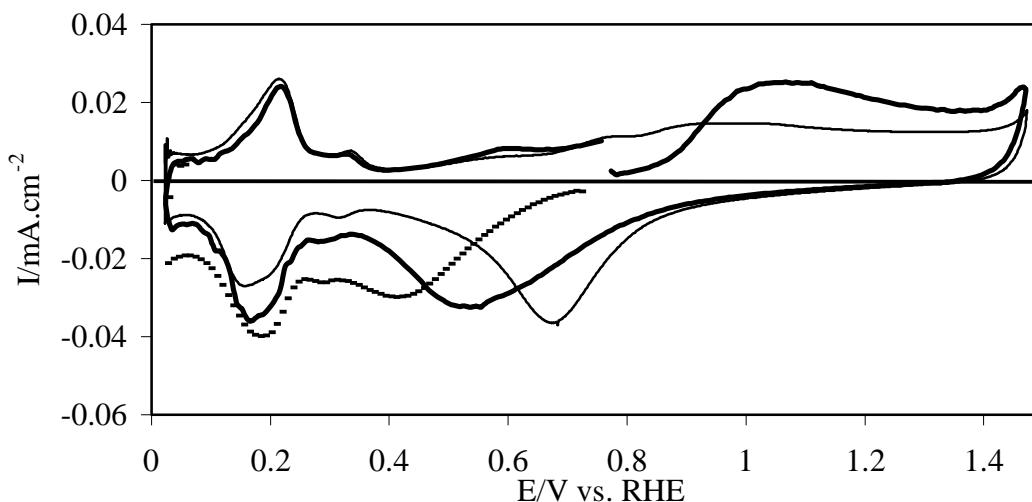


Figure 6.7: Comparison of the oxidation and subsequent reduction of the ammonia adsorbate ($E_{ads} = 0.77$ V) (thick line), reduction of the ammonia adsorbate ($E_{ads} = 0.77$ V) (dotted line) and blank (thin line) on platinum, 20 mV/sec, 1 M KOH

reduction peak. No N_2O or NO were detected in the DEMS setup. Hence, it is apparently difficult to oxidize these compounds further. Note that the reduction profile after oxidation is different from the reduction profile of the ammonia adsorbate, showing that the nature of the adsorbate has changed.

Since the adsorbate blocks anion adsorption it seems reasonable to assume that anion desorption does not play a very important role during the adsorbate reduction. This holds especially at potentials higher than 0.6 V, where the charge of the adsorbate oxidation is substantially lower than the charge of the anion adsorption. At low potentials (0.3 - 0.4 V, near the hydrogen UPD region), the anion adsorption is not substantial, and can therefore be disregarded. In the potential window from 0.4 - 0.6 V anion adsorption might play a role, but it is difficult to determine to what extent. For this reason the adsorbate reduction charge has not been corrected for OH^- desorption.

Concluding, the above results essentially confirm previous work on ammonia oxidation on platinum electrodes [3,11,12,13] and underscore the basic applicability of the mechanism suggested by Gerischer and Mauerer. In addition to the previous work, our potential-dependent coulometric data give a clear picture of how the nature

of the ammonia adsorbate changes with potential, and how this is related to the activity for the N_2 formation.

In the potential window of 0.3 – 0.4 V undissociated ammonia is the main adsorbate. The adsorbate should be relatively strongly adsorbed, to explain the low kinetic order observed. As the potential is increased above 0.4 V, the ammonia adsorbate is dehydrogenated to $NH_{2,ads}$ and NH_{ads} and N_2 is being produced. Hence, these adsorbates (most likely NH_{ads} , though we have no way to directly prove that) are the active intermediates in the selective oxidation to N_2 . At potentials higher than 0.6 V, the main adsorbate becomes N_{ads} , which is not active in the N_2 formation, and the electrode deactivates. Finally, as the potential is raised to potentials where platinum becomes oxidized, we found evidence for the formation of an oxynitride surface layer. At these potentials N_2O and NO are formed in the presence of ammonia, whereas no such products are formed during the adsorbate oxidation.

3.3. Iridium

A typical cyclic voltammogram of a polycrystalline iridium electrode in the presence and absence of NH_3 is given in figure 8. Increasing the potential stepwise, the activity is shown in figure 9a. The electrode is observed to deactivate slowly at potentials higher than 0.5 V, though the rate of deactivation is much more gradual than for platinum (figure 2). The Tafel slope in the potential window of 0.4 - 0.5 V is found to be 48 mV/dec (figure 9b), whereas the kinetic order in the concentration of ammonia at 0.45 V is 0.5 (figure 9c). DEMS experiments show that the selectivity to N_2 is 100 % at potentials below 0.8 V. The potential was always kept below 0.8 V to prevent the formation of poorly reducible surface oxides [32].

The charge corresponding to the reduction of the adsorbate formed at E_{ads} to 0 V is plotted in figure 10a. As for platinum, the charge was corrected for the hydrogen UPD adsorption, but not for any anion adsorption. Since the adsorbate reduction in the DEMS setup showed that no gaseous products are formed, we assume that the product was in all cases ammonia.

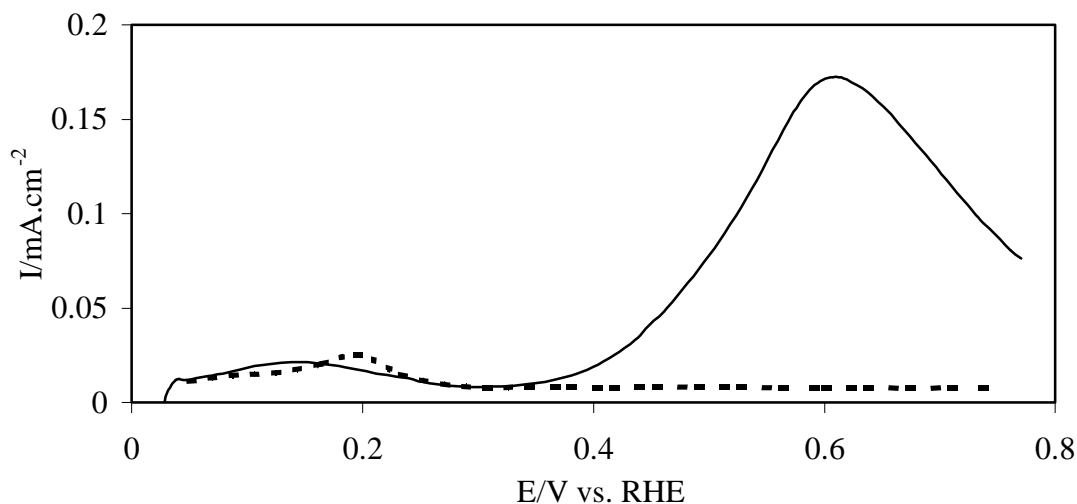


Figure 6.8: Voltammogram of iridium in the presence (solid line) and absence (dotted line) of 0.1 M NH_3 , $v = 20 \text{ mV/sec}$, 1 M KOH

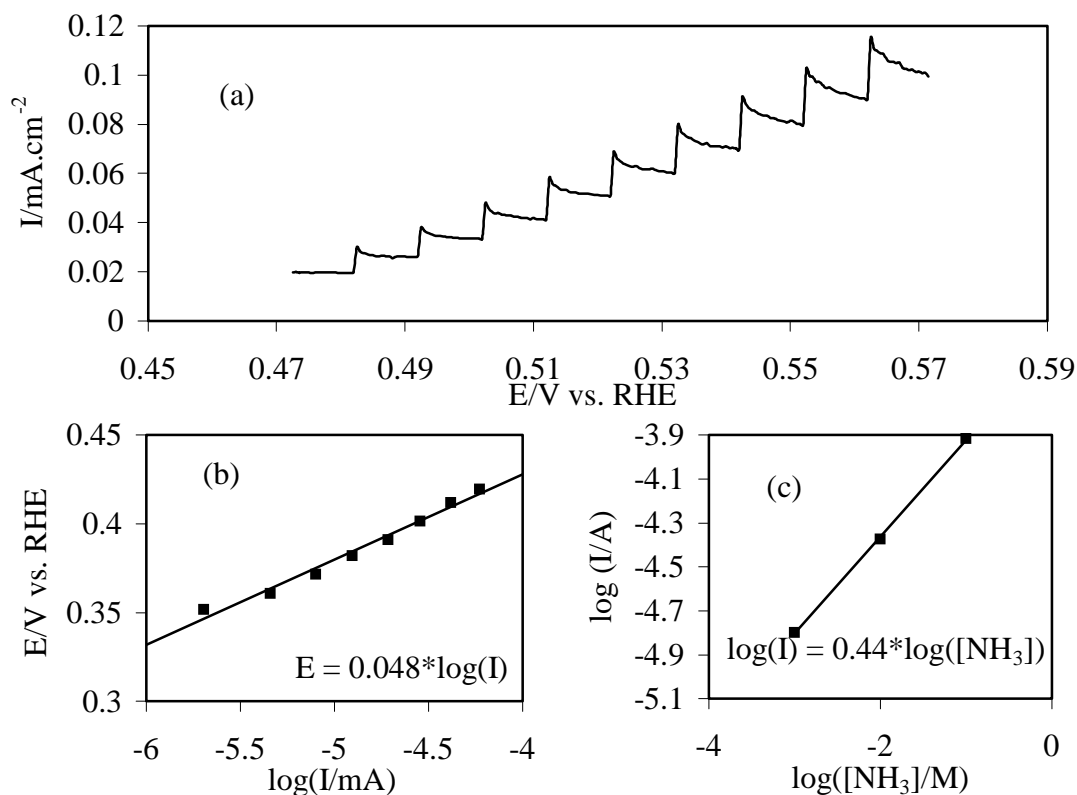


Figure 6.9 a: Activity of iridium in the NH_3 oxidation, stepwise increase of the potential, 1 mM NH_3 in 1 M KOH, 10 sec. per step, b: Tafel slope of the NH_3 oxidation on iridium, same data as used in figure 9a, c: Kinetic order in the concentration of NH_3 on iridium, 0.45 V, 1 M KOH

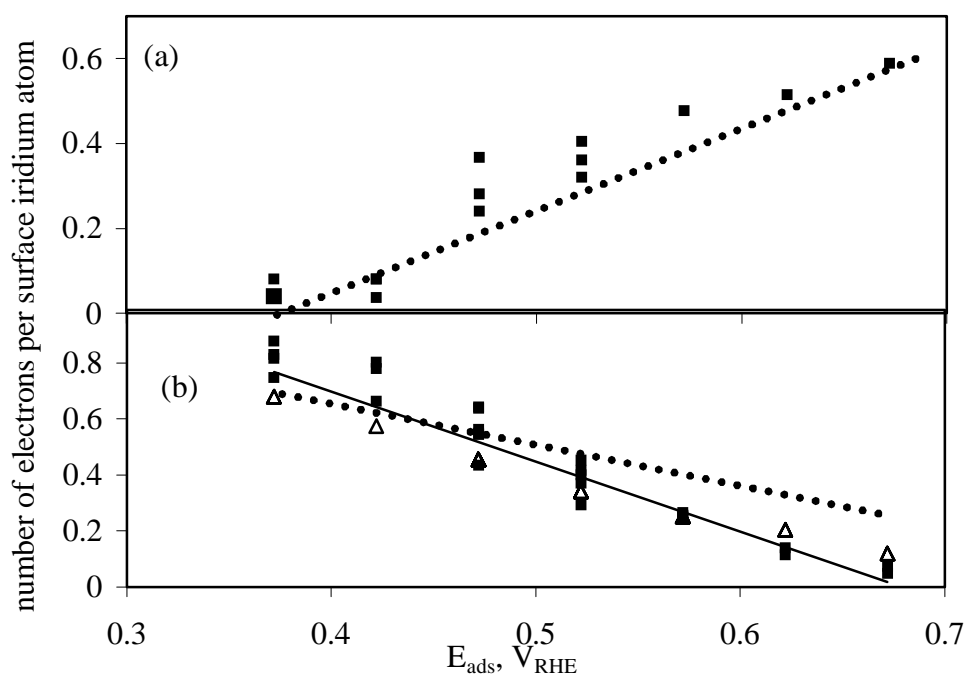


Figure 6.10 a: Integrated charge of the reduction of the ammonia adsorbate after formation at E_{ads} on iridium, 1 M KOH, b Charge of the oxidation of the ammonia adsorbate formed at E_{ads} to 0.77 V on iridium, filled squares ammonia adsorbate, open triangles blank, 1 M KOH

Between 0.35 and 0.45 V the charge of the adsorbate reduction is low, similar to the results for platinum. The presence of ammonia in the solution changes the shape of the cyclic voltammogram in the hydrogen UPD region without changing the total charge, indicating that ammonia is adsorbed in this potential window. The high kinetic order in ammonia suggests that ammonia is more weakly adsorbed on iridium than on platinum.

Between 0.45 and 0.55 V the amount of adsorbate increases, and this is also the potential window in which the electrode is active in the formation of N_2 . It is therefore likely that this adsorbate is the intermediate of the reaction.

Between 0.55 and 0.7 V the charge corresponding to the adsorbate reduction reaches a maximum value of 0.6 electrons per iridium surface atom. This value is significantly lower than that observed for platinum.

In contrast to platinum, iridium forms surface oxides at potentials lower than 0.77 V, which could lead to the formation of oxygen-nitrogen species at the surface. However, the shape of the reduction profile is in all cases very different from the reduction profile of NO_{ads} , indicating that no nitric oxide is formed. This statement

also applies for experiments in which the adsorbate was formed at $E_{\text{ads}} < 0.77$ and was subsequently oxidized to 0.77 V.

The nature of the ammonia adsorbate was also determined by measuring the charge involved in the oxidation from E_{ads} to 0.77 V and comparing it to the corresponding charge obtained from the blank cyclic voltammogram (10b), following the same procedure as described for platinum. Between 0.4 - 0.55 V the adsorbate is “oxidizable”, i.e. the charge of the adsorbate oxidation is higher than obtained from the blank, whereas between 0.55 - 0.7 V the adsorbate is “inert”, i.e. the adsorbate oxidation charge is lower than the blank. The same experiments performed in the DEMS setup showed that when E_{ads} is between 0.4 - 0.55 V some N_2 is formed during the oxidation, whereas when E_{ads} is between 0.55 and 0.7 V no N_2 is formed. Given the similarity between figures 6a and 10b, the DEMS results, and the fact that no nitric oxide is formed, we identify the “oxidizable” adsorbate as $\text{NH}_{2,\text{ads}}$ and/or NH_{ads} , and the “inert” adsorbate as N_{ads} .

The above results are clearly similar to platinum and consistent with the Gerischer-Mauerer mechanism, suggesting that also on iridium the partially dehydrogenated ammonia species $\text{NH}_{2,\text{ads}}$ and NH_{ads} are active in the formation of N_2 , whereas N_{ads} is an inactive surface poison. There are two notable differences with platinum, however. First of all, the kinetic order in ammonia is significantly higher for iridium compared to platinum, which we believe to be related to the weaker adsorption of ammonia on iridium versus platinum. Secondly, the maximum N_{ads} coverage is significantly lower than on platinum, estimated to be ca. 0.2 for iridium versus 0.5 for platinum. We have no clear explanation for this difference. The low N_{ads} coverages on iridium may render our assumption to neglect anion OH^- co-adsorption unjustified, but we believe the qualitative conclusions should still remain valid.

3.4. Ruthenium, rhodium and palladium

The 4d transition metals ruthenium, rhodium and palladium all show a similar inactivity towards N_2 production and therefore will be discussed in one section.

Figure 11 shows the voltammetry of the three 4d metals in the absence and presence of NH_3 in the solution. All three metals show a very low activity towards

NH_3 oxidation, as can be gathered from the faradaic currents flowing, which are an order of magnitude smaller than on platinum and iridium (figure 1 resp. 8). The steady-state current in the potential window from 0 to 0.8 V on all three metals is zero. DEMS experiments did not reveal any steady state production of N_2 at any of the three metals, though a small amount of N_2 was found on rhodium between 0.3 and 0.8 V and on ruthenium between 0.5 and 0.8 V during cyclic voltammetry. On palladium, some N_2O production was observed at potentials higher than 0.8 V, whereas no N_2O was observed on rhodium or ruthenium.

It can also be observed in figure 11b that on rhodium the faradaic oxidation charge found between 0 and 0.25 V (the “hydrogen UPD region”) is higher in the presence of NH_3 than in its absence. This is in contrast to iridium and platinum, and suggests that the oxidative dehydrogenation already takes place in this potential region. As is well known, on palladium there is no hydrogen UPD region due to the formation of bulk palladium hydrides below 0.25 V.

Figure 12 reports for the three metals the charge (in numbers of electrons per surface metal atom) obtained in the reduction of the ammonia adsorbate, following the procedure previously described for platinum and iridium. (The potential window on palladium was restricted from E_{ads} to 0.25 V, due to the formation of bulk hydrides.) The amount of adsorbate clearly increases with positive potentials and attains maximum values of ca. 1.7, 1.3 and 1.8 for ruthenium, rhodium and palladium, resp. On ruthenium and palladium, the potential at which a certain amount of adsorbate is present (for instance 1 electron per surface metal atom), is shifted ca. 100 – 150 mV negatively compared to platinum. On rhodium, this shift is smaller, ca. 50 mV. On all three metals, the adsorbate reduction profile was significantly different from the NO reduction profile, measured in a separate experiment.

Figure 13 reports for all three metals the charge obtained in the ammonia adsorbate, adsorbed at E_{ads} and oxidized to 0.77 V, compared to the charge obtained similarly for the blank solution. As for platinum and iridium, the two plots obtained in ammonia and blank solution intersect, and at potentials above this intersection point we assume the ammonia adsorbate to be inert (N_{ads}) and to block anion OH^- adsorption. For the 4d metals this intersection potential is considerably (ca. 200-300 mV) lower than for platinum and iridium. This indicates a stronger adsorption bond of N_{ads} on ruthenium, rhodium and palladium than on platinum and iridium. When the

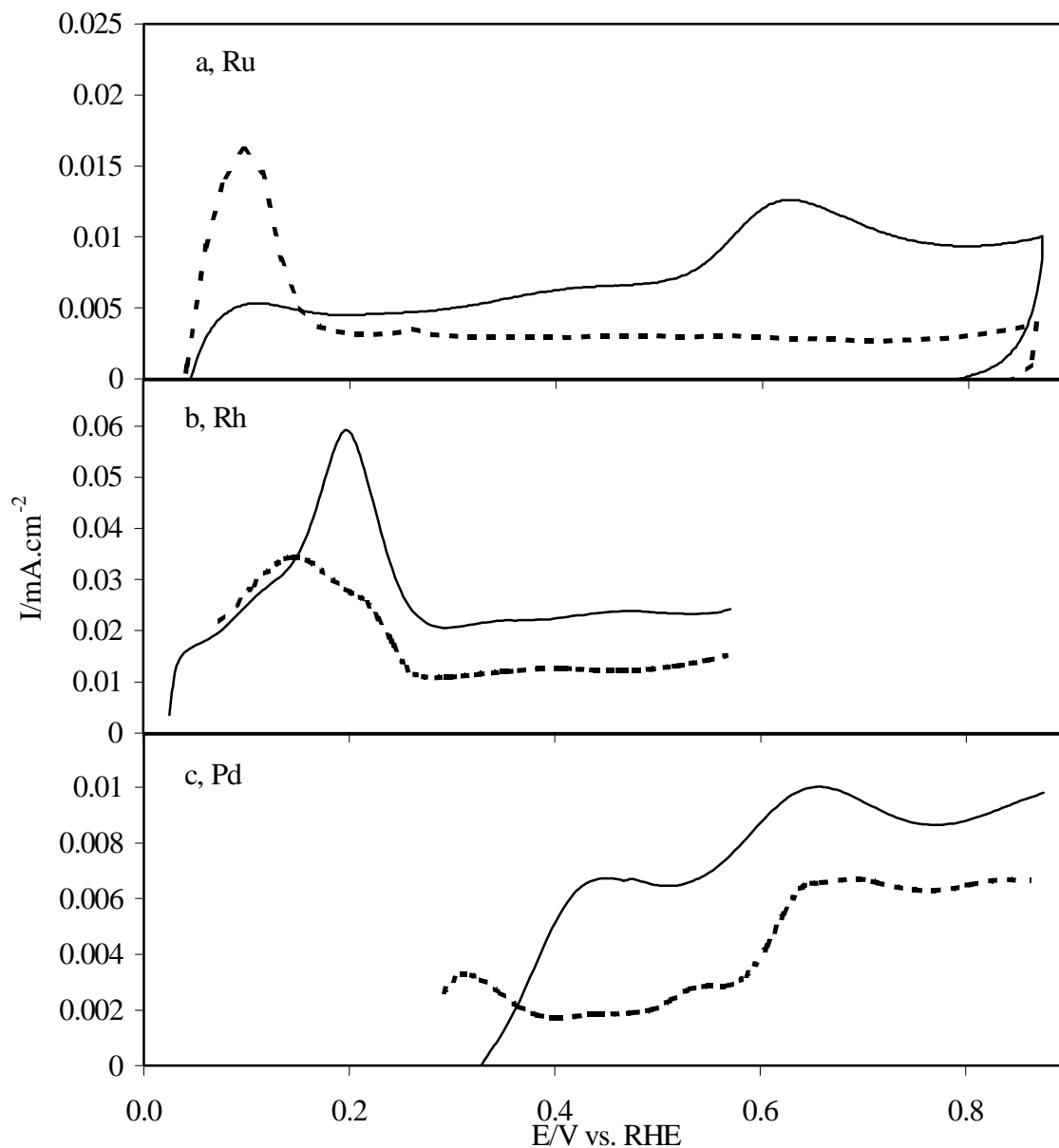


Figure 6.11: Voltammogram of ruthenium (a), rhodium (b) and palladium (c) in the presence (solid line) and absence (dotted line) of 0.1 M NH_3 , 1 M KOH , $v = 20\text{ mV/sec}$

same adsorbate oxidation experiment was carried out in the DEMS setup, no N_2 formation was observed for the 4d metals.

The above results clearly illustrate that on the 4d metals ammonia is dehydrogenated at significantly lower potentials than on platinum and iridium,

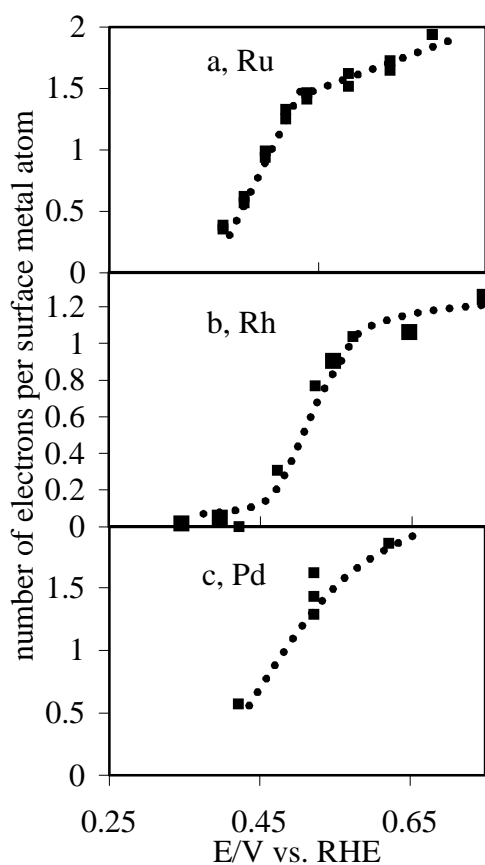


Figure 6.12: Integrated charge of the reduction of the adsorbate after formation at E_{ads} on ruthenium (a), rhodium (b) and palladium (c), 1 M KOH

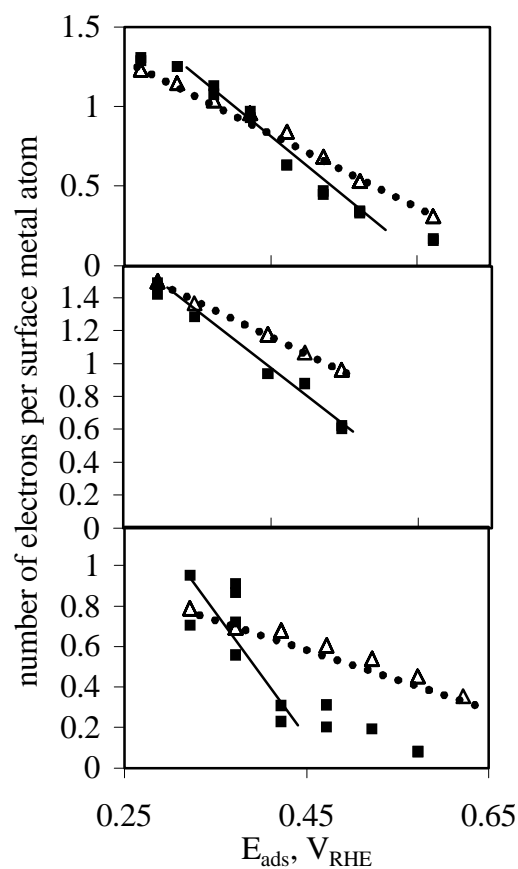


Figure 6.13: Charge involved in the oxidation of the ammonia adsorbate formed at E_{ads} to 0.77 V on ruthenium (a), rhodium (b), and palladium (c), filled squares ammonia adsorbate, open triangles blank, 1 M KOH

leading to the inert surface poison N_{ads} at much lower potentials than on platinum and iridium. This suppresses reaction (4) in the Gerischer-Mauerer mechanism and explains why ruthenium, rhodium and palladium are not active in the selective ammonia oxidation to N_2 .

3.5. Copper, silver and gold

The cyclic voltammetry of the coinage metals copper, silver and gold in the presence and absence of NH_3 is shown in figure 14. For all three metals, the activity is very low and an oxidation current is observed only in the potential region where the metal surface is oxidized. Electrochemical Quartz Microbalance experiments showed that all three metals exhibit an enhanced electrodisolution in the presence of ammonia.

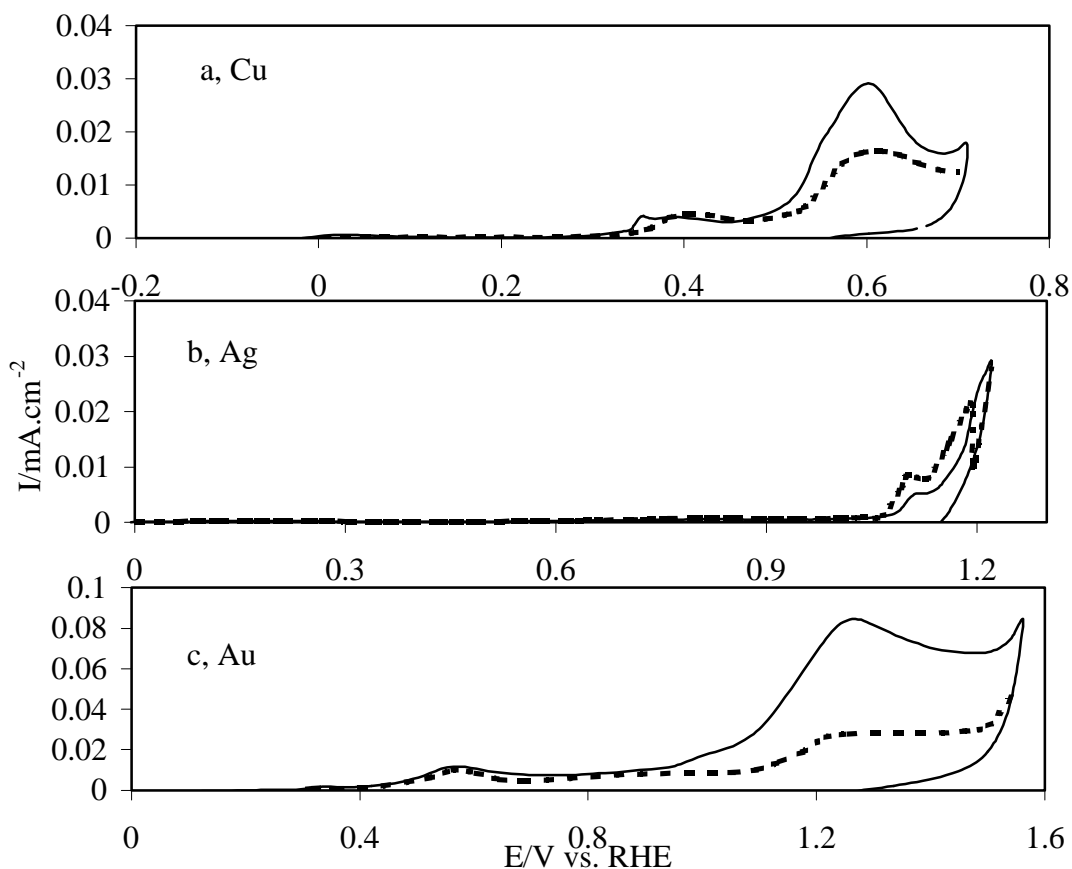


Figure 6.14: Cyclic voltammogram of copper (a), silver (b) and gold (c) in the presence (solid line) and absence (dotted line) of 0.1 M NH_3 , 1 M KOH, $\nu = 20$ mV/sec

In the case of copper, the current efficiency of this process was even 100 %, and DEMS experiments indeed showed no other (gaseous) products are formed on copper. On silver, DEMS experiments detected a small amount of NO, whereas on gold some N_2O formation was observed. The formation of N_2 was never observed on the coinage metals. According to the Pourbaix diagrams [33,34,35] the electrodisolution species formed are $\text{Cu}(\text{NH}_3)_2^+$, $\text{Ag}(\text{NH}_3)_2^+$ and $\text{Au}(\text{NH}_3)_2^+$.

As no faradaic current was observed in the double layer regions of all three coinage metals, there is no evidence for (oxidative) adsorption of ammonia on these surfaces. Hence, the Gerischer-Mauerer mechanism is not followed on these electrodes, and the main effect of ammonia is the enhancement of the electrodisolution through the formation of stable metal ion-ammonia complexes.

4. Conclusions and Summary

In this chapter, we have studied the electrocatalytic oxidation of ammonia from alkaline solution on a series of transition-metal and coinage-metal electrodes. The activity and selectivity towards N_2 was studied by a combination of voltammetry and on-line mass spectrometry, whereas the potential-dependent nature of the ammonia adsorbate was examined by reductive and oxidative stripping in an ammonia-free solution. Our main objective was to study the applicability of the ammonia oxidation mechanism originally suggested for platinum by Gerischer and Mauerer to the other metals, and to relate the experimentally observed patterns in activity and selectivity to the affinity of ammonia and atomic nitrogen to the different metals, as inferred from UHV experiments and quantum-chemical calculations.

Of the transition metals only the 5d metals platinum and iridium show a steady-state activity towards the selective formation of N_2 . The 4d transition metals ruthenium, rhodium and palladium show no, or at best only a transient formation of N_2 . The Gerischer-Mauerer mechanism explains this observation in terms of a high affinity of N_{ads} to the 4d metals surfaces: N_{ads} is an inert surface species under electrochemical conditions, whereas the active intermediate in the N_2 formation is a (partially) hydrogenated nitrogen species ($NH_{x,ads}$). The potential at which N_{ads} becomes the dominant ammonia adsorbate at the surface can be estimated from our oxidative stripping experiments. The point at which the charge of the oxidation to 0.77 V becomes smaller than the blank (suggesting the presence of an inert surface species) is ca. 0.55 V for iridium and platinum, but ca. 0.2 – 0.35 V lower on ruthenium, rhodium and palladium. This agrees well with our DFT calculations (section 3.1) which show that the binding energy of atomic nitrogen is significantly higher on the 4d metals than on platinum. Iridium seems to be an exception to this rule, as its affinity to N_{ads} is comparable to rhodium according to our DFT calculations. Iridium is exceptional in another sense, however, namely in its significantly lower N_{ads} saturation coverage compared to the other transition metals, as estimated from our coulometric data. The maximum coverage of N_{ads} on Ru, Rh, Pd and Pt is ca. 0.5, in good agreement with the UHV values on Pd(100) and Rh(100) [36]; for the much lower value (ca. 0.2) on iridium, we have no obvious explanation.

The coinage metals copper, silver and gold do not form any ammonia adsorbates, and their inability to dehydrogenate NH_3 under electrochemical conditions

is in agreement with the much lower DFT-calculated N_{ads} binding energies compared to the transition metals. Hence, these metals are inactive in the selective oxidation to N_2 , and the Gerischer-Mauerer does not apply. Rather, the presence of ammonia in the solution enhances their electrodisolution by the formation of stable metal ion-ammonia complexes.

Summarizing, the relationship between the activity of the electrode for the selective oxidation of ammonia to N_2 and the adsorption energy of atomic nitrogen can be comprehended according to the Sabatier principle. Metals with a low affinity for N_{ads} , and hence a low dehydrogenation capacity, such as the coinage metals, will not produce N_2 since the active intermediates are not formed. Metals with a high affinity for N_{ads} , such as ruthenium, rhodium and palladium, do not produce N_2 since the active intermediates are not stable with respect to atomic nitrogen. Only platinum and iridium seem to combine a good dehydrogenation capacity with a sufficiently low affinity for the formation of N_{ads} to lead to a steady-state production of the active intermediates needed to form N_2 .

Our DEMS experiments have also confirmed that oxygenated nitrogen species (such as NO and N_2O) may be formed only when the electrode surface becomes oxidized. For platinum, we have also found evidence for the formation of an oxynitride surface layer when the electrode potential is made sufficiently positive.

The above results provide convincing evidence, we believe, for the applicability of the Gerischer-Mauerer mechanism for the ammonia oxidation on transition-metal electrodes, and for the identification of N_{ads} as an inactive surface poison under electrochemical conditions. However, a complete model of the reaction mechanism should also establish the identification of the active intermediates, i.e. the exact nature of the N_2 formation step. It is clear that it must involve a hydrogenated nitrogen species, but its exact valency remains elusive. It seems that we may not even exclude a reaction of the type $NH_{\text{ads}} + N_{\text{ads}} \rightarrow N_2 + H^+ + e^-$, i.e. a step involving a hydrogenated surface species and atomic nitrogen. Also the exact role of the co-adsorbing OH^- ions should be established. We believe that such a more detailed model would enable a better understanding and design of bimetallic catalysts, such as platinum-iridium [37], the activity of which is higher than of the individual metals. This kind of insight would also allow a pre-selection of test catalysts.

References:

- [1] M. Bischoff, G. Strauss, E. Schultz, *Offenlegungsschrift Bundesrepublik Deutschland*, no. 40 20 (1992) 914 A1
- [2] L.J. Sealock Jr., D.C. Elliott, E.G. Baker, A.G. Fassbender, L.J. Silva, *Ind. Eng. Chem. Res.* 35 (1996) 4111
- [3] S. Wasmus, E.J. Vasini, M. Krausa, H.T. Mishima, W. Vielstich, *Electrochim. Acta* 39 (1994) 23
- [4] R. Ukropec, B.F.M. Kuster, J.C. Schouten, R.A. van Santen, *Appl. Catal. B* 23 (1999) 45
- [5] B.A. López de Mishima, D. Lescano, T. Molina Holgado, H.T. Mishima, *Electrochim. Acta* 43 (1998) 395
- [6] N.I. Il'chenko, *Russ. Chem. Rev.* 45 (1976) 1119
- [7] G. Papapolymerou, V. Bontozoglou, *J. Mol. Cat. A* 120 (1997) 165
- [8] A.C.M. van den Broek, J. van Grondelle, R.A. van Santen, *J. Catal.* 185 (1999) 297
- [9] W.D. Miehler, W. Ho, *Surf. Sci.* 322 (1995) 151
- [10] J.M. Bradley, A. Hopkinson, D.A. King, *J. Phys. Chem.* 99 (1995) 17032
- [11] H. Gerischer, A. Mauerer, *J. Electroanal. Chem.* 25 (1970) 421
- [12] H.G. Oswin, M. Salomon, *Can. J. of Chem.* 41 (1963) 1686
- [13] J.F.E. Gootzen, A.W. Wonders, W. Visscher, R.A. van Santen, J.A.R. van Veen, *Electrochim. Acta* 43 (1998) 1851
- [14] K.Sasaki, Y. Hisatomi, *J. Electrochem. Soc.* 117 (1970) 758
- [15] J. Willsau and J. Heitbaum, *J. Electroanal. Chem.* 194 (1985) 27
- [16] W. Visscher, J.F.E. Gootzen, A.P. Cox, J.A.R. van Veen, *Electrochim. Acta* 43 (1998) 533
- [17] G.Kresse, J.Hafner, *Phys.Rev.B* 47 (1993) 558; 48 (1993) 13115; 49 (1994) 14251.
- [18] S.J.Vosko, L.Wilk, M.Nusair, *Can.J.Phys.* 58 (1980) 1200
- [19] J.P.Perdew, J.A. Chevary, S.H. Vosko, K.A. Jackson, M.R. Pederson, D.J. Singh, C. Fiolhais, *Phys. Rev. B* 46 (1992) 6671.
- [20] B.Hammer, J.K.Norskov, in R.M.Lambert, G.Pacchioni (Ed), *Chemisorption and Reactivity on Supported Clusters and Thin Films*, Kluwer Academic, Dordrecht, 1997, 285
- [21] N.W.Ashcroft, N.D.Mermin, *Solid State Physics*, Saunders College Publishing, Fort Worth, 1976
- [22] J.M. Bradley, A. Hopkinson, D.A.King, *Surf. Sci.* 371 (1997) 255
- [23] R.M. van Hardeveld, R.A. van Santen, J.W. Niemantsverdriet, *Surf. Sci.* 369 (1996) 23
- [24] T.J. Chuang, H. Seti, I. Hussla, *Surf. Sci.* 158 (1985) 525
- [25] D.M. Thornburg, R.J. Madix, *Surf. Sci.* 220 (1989) 268
- [26] M. Garcia-Hernandez, N. Lopez, I. de P.R. Moreira, J.C. Paniagua, F. Illas, *Surf. Sci.* 430 (1999) 18
- [27] A.M. Marquez, N. Lopez, M. Garcia-Hernandez, F. Illas, *Surf. Sci.* 342 (1999) 463
- [28] P.A. Thiel, T.E. Madey, *Surf. Sci. Rep.* 7 (1987) 211
- [29] L.M.M. de Souza, F.P. Kong, F.R. McLarnon, R.H. Muller, *Electrochim. Acta* 42 (1997) 1253
- [30] G. Kokkinidis, *J. Electroanal. Chem.* 189 (1985) 155
- [31] N.S. Marinković, N.M. Marković, R.R. Adžić, *J. Electroanal. Chem.* 330 (1992) 433
- [32] P.P. Pickup, V.I. Birss, *J. Electrochem. Soc.* 135 (1988) 126

- [33] G. Trejo, A.F. Gil, I. Gonzalez, *J. Electrochem. Soc.* 142 (1995) 3404
- [34] I. Texier, S. Remita, P. Archirel, M. Mostafavi, *J. Phys. Chem.* 100 (1996) 12472
- [35] C. Nila, I. Gonzalez, *J. Electroanal. Chem.* 401 (1996) 171
- [36] K. Tanaka, T. Yamada, B.E. Nieuwenhuys, *Surf. Sci.* 242 (1991) 503
- [37] D.W. McKee, A.J. Scarpellino Jr., I.F. Danzig, M.S. Pak, *J. Electrochem. Soc.* 116 (1969) 562

Chapter 7: The nature of Chemisorbates formed from Ammonia on Gold and Palladium electrodes as discerned from Surface-Enhanced Raman Spectroscopy

Abstract

The chemisorbates formed from ammonia-containing alkaline electrolyte on gold and palladium electrodes have been identified using Surface-Enhanced Raman Spectroscopy (SERS). On gold, a potential-dependent band at ca. $365\text{-}385\text{ cm}^{-1}$ is observed, consistent with the metal-nitrogen stretch for molecular adsorbed ammonia on the basis of the frequency redshift observed upon deuteration. A similar feature is also observed on palladium, at $440\text{-}455\text{ cm}^{-1}$, again consistent with chemisorbed ammonia on the basis of the H/D shift. On palladium, but not on gold, however, transfer of the electrode to ammonia-free electrolyte yielded a vibrational band at $455\text{-}465\text{ cm}^{-1}$. The near-zero H/D frequency shift obtained for this irreversibly adsorbed component indicates the formation of chemisorbed atomic nitrogen on palladium. This finding is discussed in terms of the mechanism for ammonia electro-oxidation.

1. Introduction

The electrochemical oxidation of ammonia (NH_3) has received attention in the context of its possible application as an anode reaction in fuel cells [1], and more recently in relation to its heterogeneously catalyzed selective oxidation to dinitrogen (N_2) from aqueous waste-water streams using oxygen as an oxidant [2]. The kinetics of the electrochemical oxidation of ammonia on platinum have been examined by a number of authors [1,3-6]. In the mechanism originally suggested by Gerischer and Mauerer [3], the active intermediate in the selective oxidation to N_2 is a partly dehydrogenated ammonia adsorbate, $\text{NH}_{2,\text{ads}}$ or NH_{ads} . The atomic nitrogen adsorbate N_{ads} , which is apparently formed at more positive potentials, is inactive towards N_2 production at room temperature. These conclusions were later supported by electrochemical studies combined with on-line mass spectrometry [4-6]. The electrochemical oxidation mechanism is therefore distinctly different from those proposed for heterogeneous gas-phase oxidation [7], in which N_2 is usually formed from the combination of two N_{ads} species [8], albeit at temperatures higher than 300 K. On the other hand, v.d.Broek et al. [9] proposed that a NH_x species had to be activated to produce N_2 .

Recently, the Eindhoven group has studied in detail the applicability of the Gerischer-Mauerer mechanism to ammonia oxidation on a series of polycrystalline transition-metal and noble-metal electrodes by a combination of voltammetry, coulometry, and on-line differential electrochemical mass spectrometry (DEMS) [6]. In agreement with the Gerischer-Mauerer mechanism, it was found that metals with a high propensity for atomic nitrogen formation, such as ruthenium, rhodium, and palladium, show no, or at most only a transient, activity towards N_2 production. Metals with a low dehydrogenation capacity or weak affinity for N_{ads} , such as the coinage metals copper, silver, and gold, also do not produce any N_2 ; rather, the presence of ammonia in the electrolyte enhances their electrodisolution by the formation of metal-ion-ammonia complexes. Only platinum and iridium electrodes exhibit steady-state N_2 production at potentials at which no surface oxides are formed. According to the Sabatier principle [10], therefore, these two metals combine a relatively strong dehydrogenation capacity with a relatively weak affinity for atomic nitrogen.

Despite the rather convincing nature of the electrochemical data, direct in situ evidence on the molecular identity of the adsorbates involved in the ammonia oxidation is still lacking. In their original paper [3], Gerischer and Mauerer presented results of an ex situ temperature-programmed desorption study of a deactivated platinum electrode in the presence of an inert gas. Mainly N₂ was detected with only trace amounts of hydrogen. On the basis of this observation, Gerischer and Mauerer suggested N_{ads} to be the inactive surface species responsible for the deactivation of the platinum electrode at higher potentials.

A suitable technique for obtaining in situ information on the identity of the adsorbates formed in electrochemical surface reactions is Surface-Enhanced Raman Spectroscopy (SERS) [11]. The Purdue group has shown that by employing overlayer deposition strategies, SERS may be harnessed for the ultrasensitive in situ vibrational characterization of numerous electrode-electrolyte interfaces, including platinum-group transition metals, thereby extending its applicability beyond the traditional SERS-active metals copper, silver, and gold [11-13]. Combining the ability of SERS to access the low-wavenumber range, typical for metal-adsorbate vibrations, with hydrogen-deuterium isotope exchange tactics, the technique should enable us to assess the extent of hydrogenation of the ammonia adsorbate on the various metal electrode surfaces in relation to their selectivity for N₂ production.

In this communication we report the findings of a SERS study of the adsorbates formed at gold and palladium electrodes in ammonia-containing alkaline electrolyte. These metals were chosen in view of their resistance to surface oxidation, enabling ammonia adsorbates to be examined in alkaline media without major interference from oxide formation. Our results provide the first in situ spectroscopic evidence for the inactivity of N_{ads} for N₂ production on transition-metal electrodes, a finding that is in agreement with the Gerischer-Mauerer mechanism.

2. Experimental

The details of the experimental setup are described in ref. [14]. A Spectra Physics Stabilite (Model 2017) Kr⁺ laser provided the Raman excitation at 647.1 nm. with ca. 30 mW incident power on the surface. Scattered light was collected into a SPEX Triplemate spectrometer equipped with a Photometrics CCD detector. The gold electrode was a 0.4 cm. diameter rod sheathed in Teflon and roughened in 0.1 M KCl

as described in ref. [15]. Three to five monolayers of palladium were deposited onto gold from a 5 mM PdCl₂ solution to obtain a SERS-active palladium electrode.

The electrodes were thoroughly rinsed, the removal of residual adsorbed chloride being checked by the absence of the metal-Cl band at 335 cm⁻¹ [16]. Ammonia (25%) and KOH.H₂O were of suprapure quality (Merck) and perchloric acid of p.a. quality. All solutions were made with Millipore MilliQ water (>18.2 MΩ). During all measurements a saturated calomel reference electrode (SCE) was used, but all potentials will be referred instead to the reversible hydrogen electrode (RHE).

3. Results and discussion

Gold

Figure 1 shows a typical cyclic voltammogram on gold (20 mV s⁻¹) in 0.1 M KOH containing 0.1 M ammonia (solid trace). The dotted trace is a corresponding voltammogram obtained in 0.1 M KOH alone. We have previously shown that the increased current observed in the positive-going potential scan in the presence of ammonia above 0.9 V is largely due to enhanced electrodisolution of the gold surface, along with the formation of some N₂O [6]. The negative potential shifts of the subsequent reduction peaks are related to the higher stability of the gold-ion-ammonia complexes formed during the dissolution. When the electrode was transferred from an ammonia-containing electrolyte to an ammonia-free solution at 0.7 V, and the potential subsequently cycled between 0 and 1.4 V, no difference with the blank cyclic voltammogram was observed. This suggests that no irreversibly adsorbed ammonia species are formed at the gold electrode.

A set of potential-dependent SER spectra on gold in ammonia-containing electrolyte is shown in Figure 2A. A clear band at 365 to 385 cm⁻¹, the frequency blueshifting with increasing potential, is observed for potentials higher than ca. 0.3 V.

This feature is absent in ammonia-free solution. The band frequency, along with its potential dependence, is consistent with a metal-ammonia stretching vibration (ν_{M-NH_3}). While this mode is seldom observable in electron energy-loss spectra (EELS) of ammonia at metal-vacuum interfaces [17,18], an intense SERS ν_{M-NH_3} band

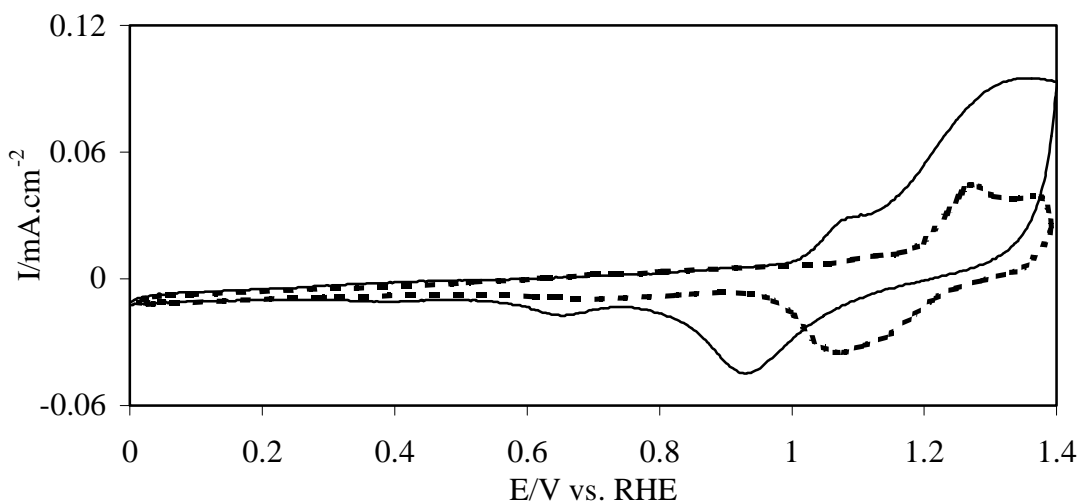


Figure 7.1: Anodic-cathodic cyclic voltammograms (20 mV s^{-1}) on gold in 0.1 M KOH in the presence (solid trace) and absence (dotted trace) of 0.1 M NH_3 .

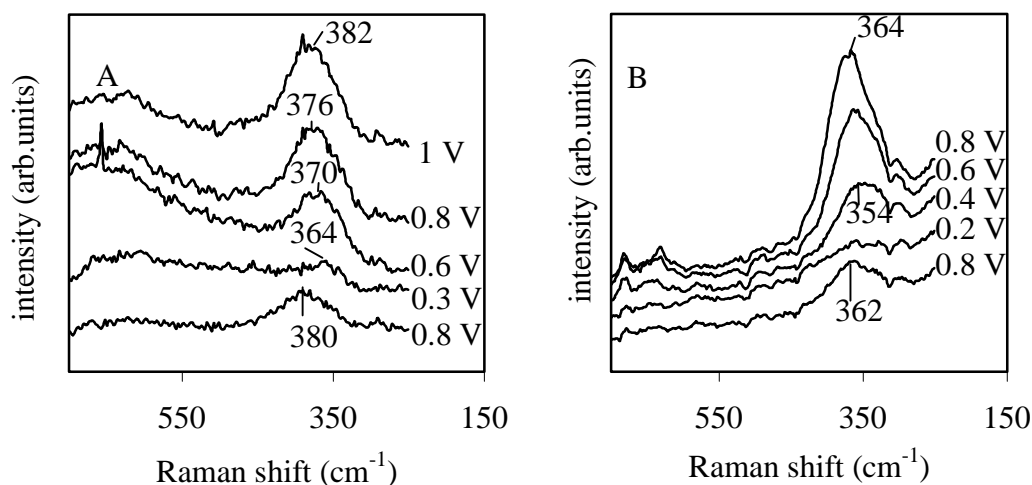


Figure 7.2: SER spectra obtained on gold at decreasing potentials indicated (vs. RHE) in $0.1 \text{ M NH}_3 + 0.1 \text{ M KOH}$ with (A) H_2O and (B) D_2O as solvent.

has been observed on a silver electrode [19]. Evidence that this band corresponds to hydrogenated (i.e., molecular) ammonia is obtained from the isotope redshift, ca. $15\text{--}20 \text{ cm}^{-1}$, observed by replacing D_2O for H_2O electrolyte; typical SERS data for the former are shown in figure 2B. (Note that such H/D exchange on ammonia will be very rapid in alkaline media.) As shown earlier for metal-OH vibrations [20,21], the isotope frequency shift for metal-adsorbate vibrations is roughly in accordance with the increased *overall* adsorbate mass, as anticipated in view of the much higher N-H vibrational frequency. While the computed ND_3/NH_3 isotopic redshift, 30 cm^{-1} ,

deduced on this basis, is significantly larger than observed, the presence of molecular ammonia is expected on electrochemical grounds, since the adsorption or desorption of ammonia is not associated with a faradaic current [6]. The anticipated detection of N-H/N-D stretching modes was thwarted by the low sensitivity of the Raman detector at such high frequencies. The $\nu_{\text{M-NH}_3}$ blueshifts seen towards high potentials are observed for other electron-rich chemisorbates, such as halogens [16]. The loss of the $\nu_{\text{M-NH}_3}$ feature at negative potentials is indicative of ammonia desorption, presumably due partly to the greater polarity of water molecules. Upon readjusting the potential to higher values, partial reappearance of the $\nu_{\text{M-NH}_3}$ band is observed, demonstrating reversible potential-dependent nature.

The $\nu_{\text{M-NH}_3}$ band disappears when the gold electrode is transferred to NH_3 -free electrolyte. This indicates that either the adsorbed ammonia does not survive the transfer, or all the ammonia desorbs after transfer into the clean solution, both implying a relatively weak ammonia-gold interaction. Significantly, we note that our SERS experiments provide no evidence for the formation of atomic nitrogen adsorbates at the gold-electrolyte interface, in harmony with the electrochemical evidence mentioned above.

Palladium

Figure 3 shows typical cyclic voltammograms on palladium (20 mV s^{-1}) in 0.1 M KOH in the presence (solid trace) and the absence (dotted trace) of 0.1 M NH_3 . The peak observed at 0.5 V during the positive-going scan is due to the oxidative dehydrogenation of ammonia, and is not accompanied by the formation of any N_2 as evidenced by our previous DEMS experiments [6]. The anodic current observed for potentials above 1.0 V is due to the formation of oxygenated nitrogen products such as N_2O . The cathodic peak at 0.3 V during the negative-going scan corresponds to the reduction of the existing nitrogen adsorbates back to ammonia. This reduction peak is also observed if the palladium electrode is transferred at 0.7 V to an ammonia-free solution containing either 0.1 M KOH or 1 M HClO_4 . This implies that at least some of the ammonia adsorbate formed at 0.7 V is irreversibly adsorbed on the palladium surface.

Figure 4A and B show potential-dependent SER spectra obtained in the ammonia-containing 0.1 M KOH electrolyte in H_2O and D_2O respectively.

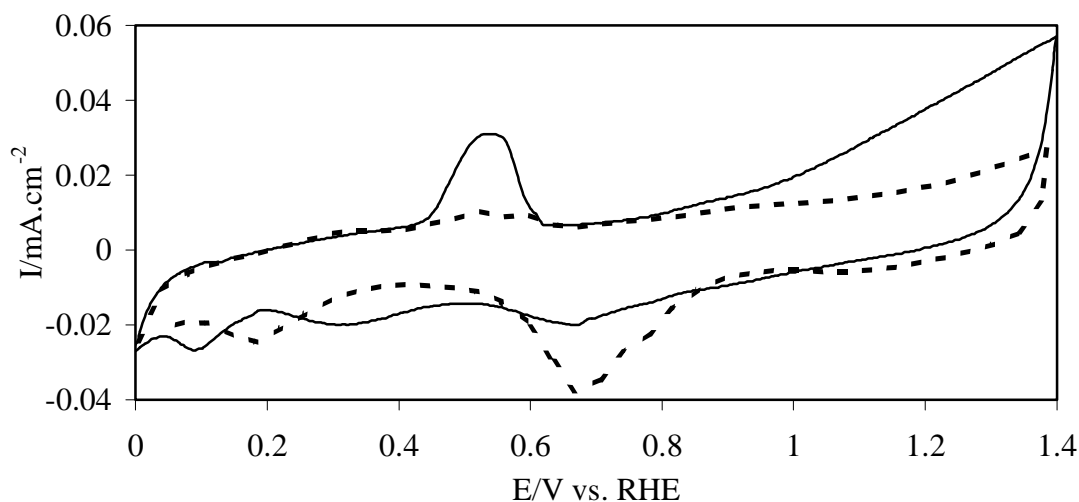


Figure 7.3: Anodic-cathodic cyclic voltammograms (20 mV s^{-1}) on palladium film electrode in 0.1 M KOH in the presence (solid trace) and absence (dotted trace) of 0.1 M NH_3 .

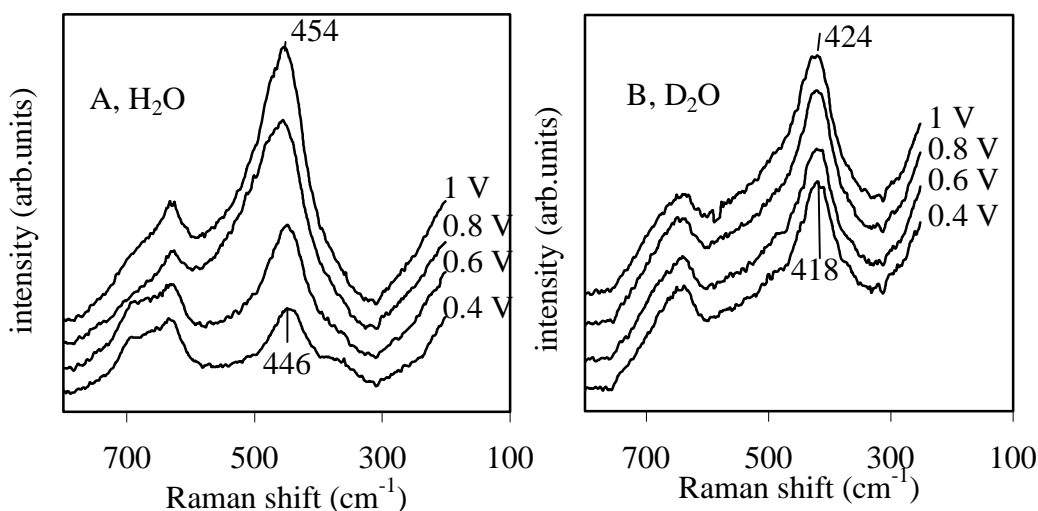


Figure 7.4: SER spectra obtained on palladium film electrode at decreasing potentials indicated (vs. RHE) in $0.1 \text{ M NH}_3 + 0.1 \text{ M KOH}$ with (A) H_2O and (B) D_2O as solvent.

The chief spectral feature is a band at $445\text{--}455 \text{ cm}^{-1}$ and $415\text{--}425 \text{ cm}^{-1}$ in the two solvents, which again blueshifts towards higher potentials. The D/H isotope redshift, ca. 30 cm^{-1} , is larger than observed for ammonia adsorption on gold. Note that the band frequencies are also significantly higher on palladium than on gold, implying (as expected) stronger ammonia binding on the former metal. From the foregoing discussion, the observed isotopic shift provides strong evidence for the presence of molecular adsorbed ammonia on palladium. While the reasons for the smaller D/H

shift obtained on gold are unclear, it is plausible that the disparity emanates from different extents of vibrational coupling with other low-frequency metal-adsorbate modes.

The most significant difference between the SER spectra on gold and palladium, however, is that, unlike the former metal, a metal-adsorbate vibration is also observed on palladium following transfer from the ammonia-containing electrolyte to 0.1 M KOH alone. A typical potential-dependent set corresponding to the latter conditions on palladium is shown in figure 5A. The top spectrum was observed at 0.9 V following transfer into 0.1 M KOH in D₂O, with those stacked below were obtained similarly at the potentials indicated (from 0.9 to 0.2 V) in 0.1 M KOH/H₂O. A band is observed at 455-465 cm⁻¹, again blueshifting towards increasing potential. Interestingly, however, the D/H isotope effect for this vibration is almost zero (< 5 cm⁻¹). This indicates that the band arises from a metal-nitrogen (ν_{M-N}) stretching mode, so that the adsorbate is dehydrogenated, i.e. is chemisorbed atomic nitrogen. Further evidence supporting this spectral assignment was obtained by the observation of a near-identical metal-adsorbate band upon transfer of the palladium electrode to ammonia-free acidic compared to alkaline electrolyte, since any remaining adsorbed ammonia will be protonated to yield NH₄⁺, which will desorb in acidic solution.

The spectral differences observed on palladium in the absence and presence of solution ammonia are clarified further in figure 5B. The upper spectral pair (a and b) were obtained at 0.9 V in 0.1 M KOH/D₂O in the presence (a) and after removal (b) of solution ammonia. The additional lower-frequency band component seen in the former spectrum, associated with reversibly adsorbed ammonia, is clearly apparent. The lower spectral pair (c and d) in figure 5B are corresponding data obtained in 0.1 M KOH/H₂O. The marked (ca. 25 cm⁻¹) D/H isotope redshift seen for the reversibly adsorbed component (a versus c), along with the absence of a shift for the irreversibly adsorbed species (b versus d), indicates further that they arise from fully hydrogenated and dehydrogenated nitrogen species, respectively.

Also evident in the spectra on palladium, especially in the presence of ammonia in the solution, is a weaker feature at ca. 630-650 cm⁻¹ (figures 4,5).

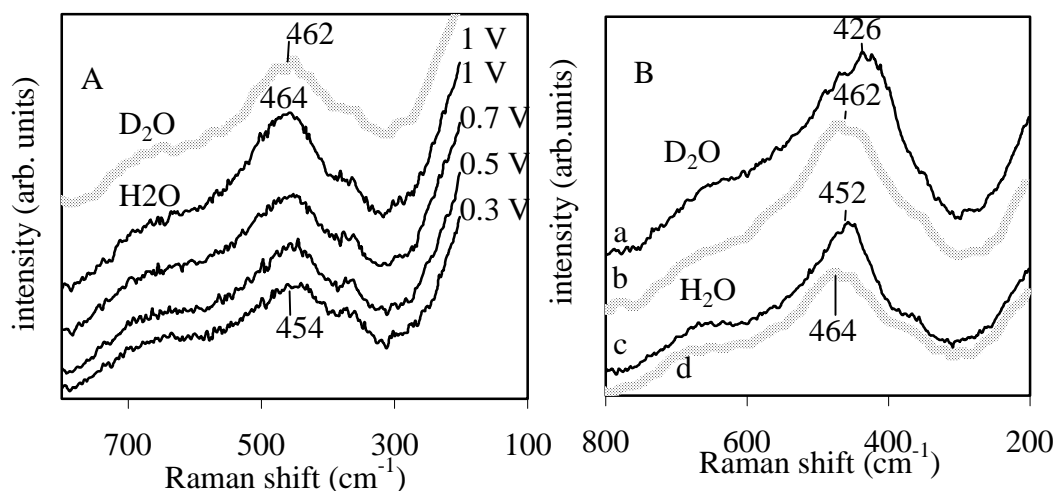


Figure 7.5: (A) Top: SER spectrum on palladium at 0.9 V after transfer from 0.1M $\text{NH}_3 + 0.1 \text{ M KOH}$ to 0.1 M KOH alone in D_2O ; Lower four spectra: obtained similarly at electrode potentials indicated in 0.1 M KOH with H_2O as solvent. (B) Upper spectral pair (a and b) obtained at 0.9 V in 0.1M KOH in D_2O before (a) and after (b) removal of ammonia solute. Lower spectral pair (c and d) obtained similarly, but with H_2O as solvent.

Although the assignment of this band is uncertain, it may arise from binding ammonia species to different adsorption sites, perhaps in atop rather than bridging geometries. Some supporting evidence is found from EELS measurements of adsorbed atomic nitrogen on Pd(110), which exhibit multiple vibrational bands in this frequency range [22].

Similar SERS experiments were also undertaken for platinum, rhodium, and iridium electrodes. Roughly comparable findings were obtained on the first metal as for the palladium-based data described here, although spectral interferences were obtained from surface oxide formation [21]. This complication was found to be more serious on the more easily oxidized rhodium and iridium electrodes, and essentially thwarted the identification of the adsorbed ammonia species on these metals.

4. Mechanistic implications

The SERS results presented in this chapter demonstrate convincingly the existence of a fully dehydrogenated ammonia adsorbate (i.e. N_{ads}) at the palladium electrode surface. Comparison with previous electrochemical and DEMS

measurements [6] shows that this surface species is not active in the formation of dinitrogen N_2 . This conclusion supports the Gerischer-Mauerer mechanism in which N_{ads} is an inactive surface poison rather than an active intermediate in the selective oxidation of ammonia to N_2 . The SERS data also show that gold is incapable of dehydrogenating ammonia at the electrochemical interface at room temperature, explaining its complete inactivity for N_2 formation. We hope that in the future we can extend these studies to platinum and iridium electrodes, at which partially dehydrogenated ammonia adsorbates are believed to be the active intermediates in the selective oxidation of ammonia to N_2 [6].

References:

- [1] H.G. Oswin, M. Salomon, *Can. J. Chem.* 41 (1963) 1686
- [2] R. Ukropec, B.F.M. Kuster, J.C. Schouten, R.A. van Santen, *Appl. Catal. B* 23 (1999) 45
- [3] H. Gerischer, A. Mauerer, *J. Electroanal. Chem.* 25 (1970) 421
- [4] S. Wasmus, E.J. Vasini, M. Krausa, H.T. Mishima, W. Vielstich, *Electrochim. Acta* 39 (1994) 23
- [5] J.F.E. Gootzen, A.H. Wonders, W. Visscher, R.A. van Santen, J.A.R. van Veen, *Electrochim. Acta* 43 (1998) 1851
- [6] A.C.A. de Vooy, M.T.M. Koper, R.A. van Santen, J.A.R. van Veen, *J. Electroanal. Chem.*, in press.
- [7] G. Papapolymerou, V. Bontozoglou, *J. Mol. Catal. A* 120 (1997) 165
- [8] J.M. Bradley, A. Hopkinson, D.A. King, *J. Phys. Chem.* 99 (1995) 17032
- [9] A.C.M. van den Broek, J. van Grondelle, R.A. van Santen, *J. Catal.* 185 (1999) 297
- [10] R.A. van Santen, J.M. Niemantsverdriet, *Chemical Kinetics and Catalysis*, Plenum Press, New York (1995) 251
- [11] M.J. Weaver, S. Zou, H.Y.H. Chan, *Anal. Chem.* 72 (2000) A38
- [12] S. Zou, M.J. Weaver, *Anal. Chem.* 70 (1998) 2387
- [13] S. Zou, C.T. Williams, E. K.-Y. Chen, M.J. Weaver, *J. Phys. Chem. B* 102 (1998) 9039
- [14] X. Gao, Y. Zhang, M.J. Weaver, *Langmuir* 8 (1992) 668
- [15] P. Gao, D. Gosztola, L.-W.H. Leung, M.J. Weaver, *J. Electroanal. Chem.* 207 (1986) 377
- [16] M. Mrozek, M.J. Weaver, *J. Am. Chem. Soc.* 122 (2000) 150
- [17] G.B. Fisher, G.E. Mitchell, *J. Electron Spect. Related Phenom.* 29 (1983) 253
- [18] J.E. Parmeter, Y. Wang, C.B. Mullins, W.H. Weinberg, *J. Chem. Phys.* 88 (1988) 5225
- [19] L.A. Sanchez, J.R. Lombardi, R.L. Birke, *Chem. Phys. Lett.* 108 (1984) 45
- [20] Y. Zhang, X. Gao, M.J. Weaver, *J. Phys. Chem.* 97 (1993) 8656
- [21] H.Y.H. Chan, S. Zou, M.J. Weaver, *J. Phys. Chem. B* 103 (1999) 11141
- [22] Y. Kuwahara, M. Fujisawa, M. Jo, M. Onchi, M. Nishijima, *Surf. Sci.* 188 (1987) 490

Summary

In this thesis the reduction and oxidation reactions of small inorganic nitrogen-containing molecules and ions is investigated. The main motivation of this research is to counteract environmental problems caused by especially nitrate (NO_3^-), nitric oxide (NO) and ammonia (NH_3). The desired product of these reactions is the environmentally benign N_2 . Since all other products are toxic, the selectivity of the reactions will be a main theme, next to the rate of the reactions. In industry, catalysts are often used to “steer” the reaction to the right products, and in this thesis we will also use catalysts. The catalysts will be noble metals (platinum (Pt), palladium (Pd), rhodium (Rh), iridium (Ir), ruthenium (Ru), gold (Au) and sometimes silver (Ag) and copper (Cu)), since these do not rust or dissolve in acidic and alkaline solutions. The objective of this thesis is to understand the reactions of NO_3^- , NO and NH_3 at a molecular level, the role of the catalyst, and to search for general features by which these reactions can be described.

Noble metals themselves are inactive in the reduction of NO_3^- , copper has to be added to get an active catalyst. The role of copper promotion and of palladium as the noble metal is investigated in chapter 2. In acidic electrolytes the activity increases linearly with copper coverage, showing that copper is active in the first step. The intermediate of this reaction is NO, so the first step of the reaction is the reduction of NO_3^- to NO. When the amount of palladium at the surface is increased, i.e. the coverage of copper decreased, the selectivity to N_2 increases. This is attributed to the high activity of palladium in the selective reduction of NO to N_2 , other metals produce different products. When sulfate (SO_4^{2-}) adsorbs at the surface there is less room for NO_3^- to adsorb, which lowers both the activity and the selectivity to N_2 . The trends in activity and selectivity are explained in terms of the amount of NO_3^- and NO near the surface.

Since the reduction of NO is a crucial step in the reduction of NO_3^- , and is an interesting reaction in its own right, a systematic study was performed to determine the mechanism of the NO reduction. Since platinum shows the best reproducibility, this metal was chosen to perform an in-dept study (chapter 3). Both the reduction of NO in the presence of NO in the solution and the reduction of adsorbed NO in a clean electrolyte were investigated.

The adsorbate reduction takes place through a combined proton/electron transfer in equilibrium followed by a rate determining chemical step. NH_3 is the only product in the absence of NO in solution. The reduction in the presence of NO in the solution at high potentials yields N_2O as the only product. The mechanism of this reaction is not of the Langmuir-Hinshelwood type, but rather involves the combination of a surface-bonded NO molecule with a NO molecule from the solution and a simultaneous electron transfer. A protonation takes place prior to this step. In alkaline solutions a chemical step appears to be partially rate determining. The continuous reduction of NO at low potentials yields mainly NH_3 . The mechanism of this reaction is the same as for the adsorbate reduction.

In chapter 4 it is shown that the behaviour of the other transition metals (Pd, Rh, Ru, Ir and Au) is very similar to that of platinum, suggesting that the reaction schemes are essentially the same. This is true for both for the reduction of adsorbed NO and for the continuous NO reduction. In the presence of NO all metals show a high selectivity to N_2O at high potentials and a high selectivity to NH_3 at low potentials, whereas N_2 is formed at intermediate potentials (although gold forms mainly N_2O , and little NH_3). Like platinum, the mechanism that leads to N_2O is believed to involve the formation of a NO-dimer intermediate. The reduction of adsorbed NO leads on all metals only to formation of NH_3 , no N_2O or N_2 are formed, and also in this case is the mechanism similar to that found for platinum. The formation of N_2 , produced at potentials between the formation of N_2O and NH_3 , most likely takes place by the reduction of previously formed N_2O . Palladium has the highest activity in the N_2O reduction and therefore also the highest selectivity in the reduction of NO to N_2 .

Chapter 5 deals with the oxidation of NO on Pt, Pd, Rh, Ir, Ru and Au. The oxidation in the presence of NO takes place in two steps. In the first step HNO_2 is formed, in a mechanism where the first electron transfer is rate determining. The rate of this reaction is independent of the metal, indicating that no strongly adsorbed species are involved in the rate-determining step. In the second step NO_3^- is formed, and, opposed to the formation of HNO_2 , this reaction is metal dependent. The oxidation of adsorbed NO is again metal-independent, suggesting a link between continuous oxidation and adsorbate oxidation. Both in the oxidation in the presence of NO and in the adsorbate oxidation surface oxides might play an important role, this

should be investigated using non-electrochemical techniques, like surface enhanced raman spectroscopy (SERS).

The relationship between the activity for ammonia oxidation and the intermediates formed during the reaction on Pt, Pd, Rh, Ir, Ru, Au, Ag and Cu is discussed in chapter 6. The activity in the selective oxidation to N_2 is directly related to the nature of the species at the surface: the electrode is active if NH_{ads} (or $NH_{2,ads}$) is present, and deactivates when N_{ads} is present. The potential at which NH_{ads} or N_{ads} are formed is metal dependent. The observed trend in the strength of adsorption of N_{ads} is $Ru > Rh > Pd > Ir > Pt >> Au, Ag, Cu$. This trend corresponds well with the trend observed in the calculated heat of adsorption of atomic nitrogen, with only iridium being an exception.

Platinum is the best catalyst for this reaction because N_{ads} is formed at high potential, compared to the other transition noble metals, but NH_{ads} seems to be stabilized rather well. Gold, silver and copper do not form NH_{ads} or N_{ads} , and show only an activity when the surface becomes oxidized. The metal electrodisolution is enhanced by ammonia under these conditions. Most metals produce oxygen containing products, like NO and N_2O , at potentials where the surface becomes oxidized.

Proof that N_{ads} is indeed the species at the surface of a deactivated electrode is given in chapter 7, by identifying the chemisorbates formed from ammonia-containing electrolyte on gold and palladium electrodes using SERS. On gold, a band at ca. $365-385\text{ cm}^{-1}$ is observed, which is identified as the Au- NH_3 vibration based of the frequency redshift observed upon deuteration (replacement of H_2O with D_2O). The Pd- NH_3 vibration is observed at $440-455\text{ cm}^{-1}$, which also shows the H/D redshift. On palladium, a transfer of the deactivated electrode to an ammonia-free electrolyte yielded a vibrational band at $455-465\text{ cm}^{-1}$. The near-zero H/D frequency shift identifies this vibration as the Pd-N vibration, without any hydrogen atoms attached to the nitrogen.

Samenvatting

Dit proefschrift gaat over de elektrochemische oxidatie en reductie van kleine anorganische stikstofhoudende moleculen. De reden voor dit onderzoek is de milieuproblemen veroorzaakt door, met name, nitraat (NO_3^-), stikstofmonoxide (NO) en ammoniak (NH_3). Deze stoffen moeten verwijderd worden uit afval- en drinkwater door ze om te zetten in ongevaarlijk stikstof (N_2). Het is heel belangrijk dat stikstof het enige product is, omdat andere producten soms giftiger zijn dan de uitgangsstof. De selectiviteit van de omzettingsreactie is daarom één van de hoofdthema's van dit proefschrift, samen met de activiteit (de snelheid van de reactie). In de industrie wordt vaak een katalysator gebruikt om de reactie te sturen naar de juiste producten, en ook in dit proefschrift worden katalysatoren gebruikt. De gebruikte katalysatoren zijn de edelmetalen platina (Pt), palladium (Pd), rhodium (Rh), iridium (Ir), ruthenium (Ru) en goud (Au), en in sommige gevallen is ook zilver (Ag) en koper (Cu) gebruikt. Deze metalen zijn gekozen omdat ze niet roesten of oplossen in water (wat de reden is dat de metalen edel genoemd worden). Het doel van dit proefschrift is te onderzoeken hoe op moleculair niveau de reacties van kleine stikstofhoudende moleculen en ionen verlopen, wat de intermediären zijn en wat de rol van de katalysator is.

Hoofdstuk twee gaat over de reductie van NO_3^- . Omdat de edelmetalen zelf niet actief zijn in deze reactie wordt een tweede metaal toegevoegd, in ons geval koper. De rol van het koper is de activering van de eerste stap, de reductie van NO_3^- naar nitriet (NO_2^-), toevoeging van koper aan het oppervlak leidt tot een lineaire toename in de activiteit. Het palladium is nodig om van NO_2^- N_2 te maken, andere metalen maken NO (goud) of NH_3 (platina). Als het NO_3^- het oppervlak niet bereikt, omdat de concentratie te laag is of omdat iets anders in de weg zit, zoals sulfaat (SO_4^{2-}) of chloride (Cl), zal zowel de snelheid van de reactie als de selectiviteit naar N_2 zakken. De activiteit en selectiviteit kunnen dus verklaard worden door de samenstelling van het oppervlak en de reactant concentraties aan het oppervlak.

De reductie van NO op platina wordt behandeld in hoofdstuk 3. Er zijn grofweg twee manieren om de reductie uit te voeren: de reductie wordt uitgevoerd terwijl NO aanwezig is in de oplossing, of NO wordt eerst geadsorbeerd aan het oppervlak, naar een schone oplossing gebracht en dan pas gereduceerd. De reductie in

de aanwezigheid van NO in de oplossing gaat naar N₂O bij hoge potentialen, en naar NH₃ bij lage potentialen. Het mechanisme dat tot N₂O leidt gaat via een NO-dimeer aan het oppervlak, dat gevormd wordt uit een NO uit de oplossing gecombineerd met een NO geadsorbeerd aan het oppervlak, een proton en een elektron. In alkalische oplossingen is het elektron niet betrokken in de snelheidsbepalende stap. Het mechanisme dat tot NH₃ leidt is hetzelfde als het mechanisme van de reductie van geadsorbeerd NO. In dit mechanisme is er eerst een elektron-transfer in evenwicht, en de volgende stap is snelheidsbepalend.

In hoofdstuk 4 wordt aangetoond dat het schema, gevonden voor platina, ook geldt voor Pd, Rh, Ir, Ru, en Au. In alle gevallen wordt bij hoge potentiaal N₂O gevormd, niet via de reductie van geadsorbeerd NO, maar via een NO-dimeer aan het oppervlak. Bij lage potentialen wordt NH₃ gevormd, bij dezelfde potentialen en volgens hetzelfde mechanisme als de reductie van geadsorbeerd NO. Goud vormt weinig NH₃, omdat NO niet sterk geadsorbeerd wordt op goud. Bij potentialen tussen de N₂O en de NH₃ vorming wordt N₂ gemaakt, dit wordt waarschijnlijk gevormd uit de reductie van eerder gevormd N₂O.

De oxidatie van NO wordt behandeld in hoofdstuk 5. Ook hier blijken de oxidatie van NO in de oplossing en de oxidatie van geadsorbeerd NO verschillend te zijn. De oxidatie van NO in de oplossing verloopt in twee stappen, eerst wordt salpeterigzuur (HNO₂, de geprotoneerde vorm van NO₂⁻) gevormd en bij hogere potentialen NO₃⁻. Bij de vorming van HNO₂ is de eerste electron transfer snelheidsbepalend. Omdat de reactie vrijwel niet afhankelijk is van de keuze van het metaal, kan geconcludeerd worden dat er geen sterk geadsorbeerde moleculen betrokken zijn in de snelheidsbepalende stap. De oxidatie van geadsorbeerd NO is ook onafhankelijk van het gekozen metaal, wat er op zou kunnen duiden dat er een relatie is tussen de oxidatie van NO in de oplossing en van geadsorbeerd NO. Zowel met als zonder NO in de oplossing zouden oppervlakte-oxides een grote invloed kunnen hebben op de reactie. Om dit te kunnen onderzoeken zijn non-electrochemische methoden, zoals surface enhanced raman spectroscopy (SERS), nodig.

De oxidatie van NH₃, en de rol van de adsorbaten aan het oppervlak, op Pt, Pd, Rh, Ir, Ru, Au, Ag en Cu is onderzocht in hoofdstuk 6. Of een electrode actief is in de selectieve oxidatie naar N₂ hangt af van het soort adsorbaat aan het oppervlak: als N_{ads} aanwezig is deactiveert de elektrode, als NH_{x,ads} intermediair aanwezig is blijft de

elektrode actief. Wanneer N_{ads} gevormd wordt hangt af van de adsorptiewarmte van N_{ads} , een hogere vormingswarmte leidt tot een deaktivering bij lagere potentialen. Goud, zilver en koper zijn niet actief omdat N_{ads} noch $\text{NH}_{x,\text{ads}}$ gevormd worden. Platina is de beste katalysator omdat het $\text{NH}_{x,\text{ads}}$ al bij relatief lage potentialen stabiliseert, terwijl N_{ads} pas bij hoge potentialen gevormd wordt. Alle metalen (behalve koper) vertonen niet-selectieve oxidatie van NH_3 naar N_2O , NO , NO_2^- en/of NO_3^- bij hoge potentiaal, hier zijn de oppervlakte-oxides bij betrokken. Onder deze omstandigheden lossen met name Au, Ag en Cu elektrochemisch op.

Het bewijs dat N_{ads} inderdaad aanwezig is op een gedeactiveerd oppervlak wordt gegeven in hoofdstuk 7. Het surface enhanced raman spectrum van een gedeactiveerde palladium elektrode in een pure 0.1 M KOH oplossing laat een Pd-N vibratie zien. Aangezien het spectrum niet verandert als H_2O vervangen wordt door D_2O , is er geen waterstof gebonden aan het stikstof, en het adsorbaat is dus N_{ads} . In de aanwezigheid van NH_3 is er zowel op palladium als op goud een H/D effect, wat aantoont dat NH_3 geadsorbeerd is.

Appendix 1: Stripping voltammetry, Rotating Disk Electrode (RDE) and Rotating Ring-Disk Electrode (RRDE)

Stripping voltammetry

Stripping voltammetry is a specific form of cyclic voltammetry, which is used to study adsorbates at electrodes by reducing or oxidizing them, without any reactants in the solution. In cyclic voltammetry the potential is changed linearly in time at a certain scan rate, which changes sign when one of the two boundary potentials is reached. In figure 1 the cyclic voltammogram of polycrystalline platinum is shown as a typical example.

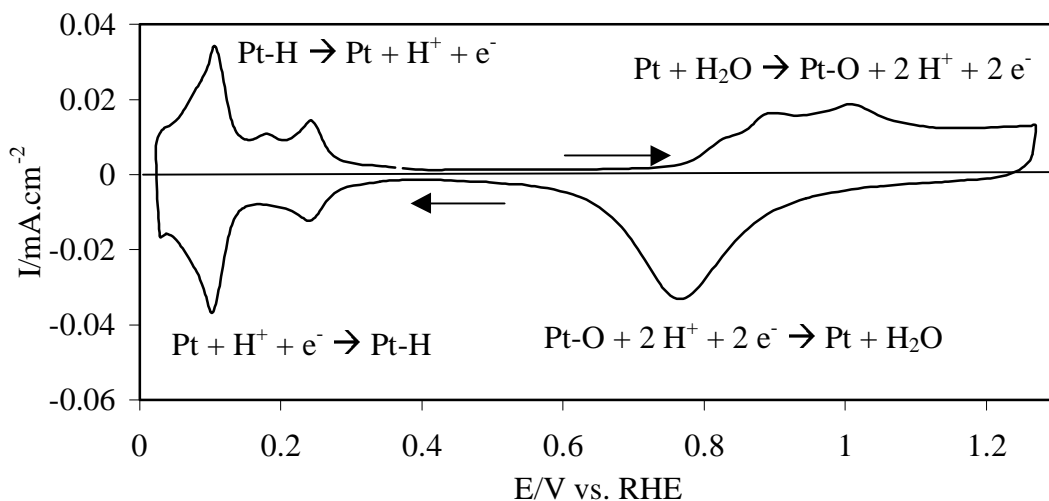


Figure 1: cyclic voltammogram of polycrystalline platinum in 0.1 M H₂SO₄, scan rate 20 mV.s⁻¹

In figure 1 can be seen that a number of processes take place, which lead to electric currents. The current in the potential window 0 - 0.4 V is due to the formation and oxidation of a monolayer of surface hydrides [1] (this reaction is commonly used to determine the real surface area of the electrode). In the charge is also included the possible adsorption/desorption of anions at the surface, in the case of figure 1 this is sulfate. The current in the potential window 0.6 – 1.4 V is due to the formation and reduction of surface oxides [1]. The profile of figure 1 is commonly used as a blank voltammogram, but the processes mentioned do not necessarily occur in the presence of adsorbed species, which may lead to problems as will be discussed later. Note that

the total charge (which equals the integral of the voltammogram) is zero, so there are no net changes if a full cycle is measured.

A typical stripping voltammogram shows a peak of the oxidation/reduction of the adsorbed species, which is not present in the blank voltammogram. An example is given in figure 2, for the oxidation of adsorbed CO on platinum. This peak contains two important parameters: the total charge (Q in Coulomb) and the peak position (E_{peak} in Volt, all potentials are referred to the Reversible Hydrogen Electrode). In figure 2 the oxidation of CO on platinum in the Differential Electrochemical Mass Spectroscopy (DEMS) setup is given. The overall reaction equation is given in equation 1:

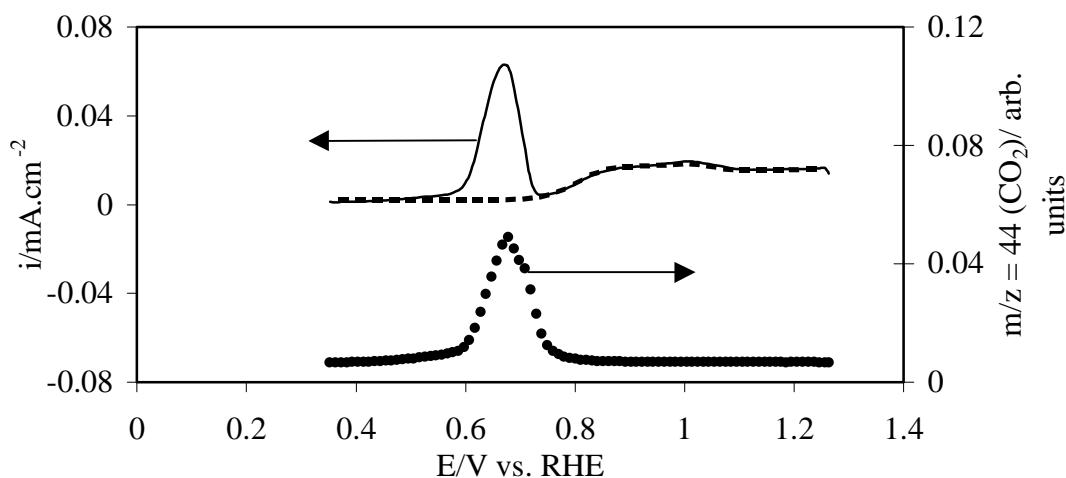
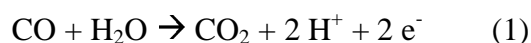


Figure 2: oxidation of adsorbed CO on platinum. Solid line current of CO oxidation, dotted line current of the blank, filled circles DEMS signal of mass 44 (CO_2). 20 mV/sec, 0.1 M H_2SO_4

From the surface area the coverage of the adsorbate can be determined, according to formula 1:

$$Q_{\text{net}} = Q - Q_{\text{blank}} = \theta_{\text{ads}} \cdot n \cdot A \quad (1)$$

with θ being the coverage (the number of adsorbate molecules divided by the number of surface atoms), n the number of electrons consumed/produced per adsorbate molecule and A the real surface area of the electrode. The surface area is usually determined by measuring Q_{net} in a process where the coverage and the number of electrons per adsorbate molecule are known, like the hydrogen Under Potential Deposition (UPD) process or the CO oxidation process. The number of electrons per adsorbate molecule is determined by the overall reaction equation, which requires knowledge of both the adsorbate and the product. Usually the adsorbate and the product are known, and the reaction equation can be written. If necessary, the nature of the adsorbate can be determined by techniques like Infra-Red Absorption Spectroscopy (IRAS) and Surface Enhanced Raman Spectroscopy (SERS). If the product is unknown, or if several products are formed, techniques like Differential Electrochemical Mass Spectroscopy (DEMS) and the Rotating Ring-Disk Electrode (RRDE) can be used to determine the nature and amount of product. The amount of CO_2 in figure 2 is an example of the way the products can be determined in the DEMS setup. Note that, although the scale of the DEMS signal is in arbitrary units, the DEMS can be calibrated to give quantitative information.

The term Q_{blank} covers all the processes that are not associated with the adsorbate being studied. Common examples are the formation of surface oxides (figure 2, chapter 5), the hydrogen UPD layer (chapters 3, 4 and 6) or anion adsorption (chapter 6, [2]). In most cases Q_{blank} can be determined by performing the same procedure as for the adsorbate oxidation/reduction, but in the absence of the adsorbate. In some cases this is incorrect, because processes take place during the blank procedure that do not take place during the adsorbate procedure. An example is encountered in chapter 6 during the oxidation of the ammonia adsorbate (figure 6.6). The charge obtained by integrating the profile of the blank between 0.57 and 0.77 V is higher than the charge of the adsorbate. Therefore, if the oxidation charge of the ammonia adsorbate would be corrected for the blank, then a negative value would be obtained, which has no physical meaning. Another example is encountered during the adsorption of CO at single crystal surfaces. On Pt (111) the charge of CO-oxidation should be corrected for the desorption of anions, like SO_4^{2-} , which are displaced from

the surface by the adsorption of CO [2]. In figure 2 the charge of anion displacement should also be taken into account.

It is assumed in formula 1 that all reactants are present at the surface at the start of the reaction. This means that no reactant may come from the electrolyte, i.e. the electrolyte, and all of its components, should be inert. In practice this is not always the case, and there are three compounds in the electrolyte that require special attention: the precursor for the adsorbate, oxygen from the surrounding air and contaminations. Oxygen can be removed by purging the electrolyte with argon, and keeping the cell under argon at all times. Care has to be taken to keep the setup clean (if an experiment failed in the course of our research, it was most of the time due to contaminations).

The removal of the precursor of the adsorbate can be done in three ways: by placing the electrode in an inert electrolyte, by purging the cell with inert electrolyte, or, in the case of a gaseous precursor, like CO, by purging the cell with argon. When the first approach is used the electrode will not be under potential control for a short time, and can therefore only be used if this would have a negligible effect on the adsorbates. The disadvantage of the second approach is that care has to be taken that all the reactant is removed from the cell, which usually requires four rinsing cycles or more.

An indication whether the stripping of the adsorbate is complete, or if the electrode is contaminated, can be obtained by taking a cyclic voltammogram immediately after the stripping voltammetry. If the product is electrochemically inert, i.e. will not be oxidized/reduced in the potential window of the cyclic voltammogram, then the blank cyclic voltammogram should be obtained. Performing a scan before and after a stripping voltammogram should be considered good laboratory practice.

The peak potential of the stripping voltammetry can be used to obtain mechanistic information on the process. To obtain this information a plot of the logarithm of the scan rate versus the peak potential is measured. The slope of this plot gives the same information as a Tafel slope, which is the change of the logarithm of the current of a continuous process with the potential. Proof is given in refs. [3,4], for a reaction that is first or second order in the coverage of the adsorbate, which is

usually the case. In some cases the Tafel slope can be derived from the mechanism [3], some typical cases are:

- The Tafel slope is infinite, i.e. the reaction is not potential dependent; the reaction is limited by a non-electrochemical step
- The Tafel slope is 120 mV/dec.; the reaction is limited by the first electron transfer
- The Tafel slope is 60 mV/dec.; prior to the rate-determining step an electron transfer is in equilibrium, the rate-determining step itself is non-electrochemical.
- The Tafel slope is 40 mV/dec.; prior to the rate-determining step an electron transfer is in equilibrium, the rate-determining step itself is the subsequent electron transfer.

Usually any observed value within 10 % of one of the cases mentioned is treated as an instance of that case.

Rotating Disk Electrode (RDE)

The RDE setup enables measurements of the kinetically limited current without the interference of diffusion of the reactants to the surface. It is therefore especially useful when the concentration of reactant is low, for instance when NO is dissolved in water. In an RDE setup the electrode is mounted in an inert encasing, so that only the disk surface is exposed to the electrolyte. The electrode can be rotated, which gives a controlled convection profile near the surface. Figure 3 gives an impression of an RDE electrode.

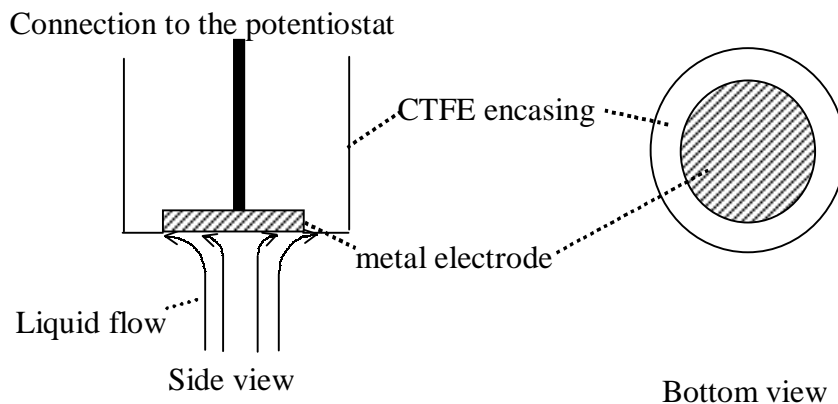


Figure 3: schematic representation of the rotating disk electrode

The convection of the reactant from the solution in the direction of the disk is controlled by the rotation of the electrode, as is the thickness of the diffusion layer. The transport of reactants to the surface can be calculated by solving the hydrodynamic equations [5], which results in the Levich equation:

$$\frac{1}{I_{diff}} = \frac{1}{I_{kin}} + \frac{1}{0.62nFAC * D^{2/3} \nu^{-1/6}} * \frac{1}{\omega^{1/2}} \quad (3)$$

I_{diff}	partially diffusion controlled electrical current
I_{kin}	kinetically limited electrical current
n	number of electrons per reacted molecule
A	surface area
C^*	the bulk concentration of the reactant
D	diffusion constant of the reactant
ν	kinematic viscosity
ω	rotation speed (in rad/s)

In a Levich plot $1/I_{diff}$ is plotted vs. $1/\omega^{1/2}$, a typical example is given in figure 4. The parameters derived from such a plot are I_{kin} and n .

Note that in figure 4 the actual currents change only little with potential, while the kinetically limited current, which is the intersection of the trendline with the y-axis, changes by a factor of 2. Also note that relatively small error bars in the determination of I_{diff} can result in large error bars in the determination of I_{kin} .

The number of electrons per reacted molecule, which can be derived from the slope of the Levich plot, is determined by the selectivity of the reaction. Therefore, the number of electrons per molecule changes with a change in selectivity. Examples of this behavior can be seen in chapters 3 and 4, where the selectivity of the NO reduction changes with potential. When this occurs, the kinetically limited current can not be determined from the Levich equation any more, because the Levich plot will not yield straight lines.

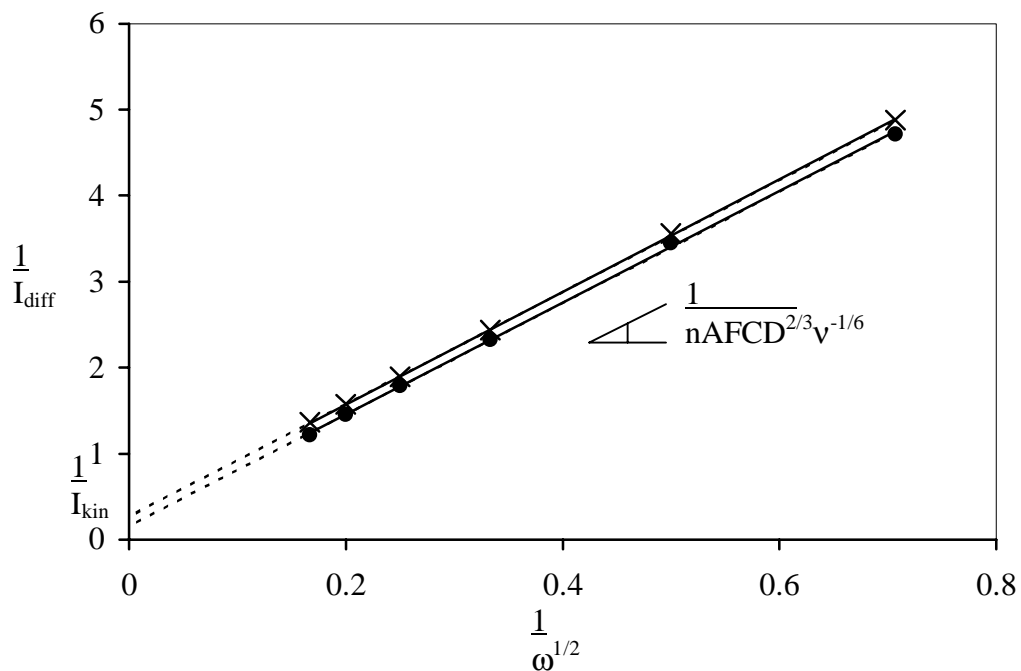


Figure 4: reduction of NO on platinum, 0.1 M H₂SO₄, saturated with NO, dots 0.3 V vs. RHE, crosses 0.4 V.

Rotating Ring-Disk Electrode (RRDE)

The RRDE setup is similar to the RDE setup, with an extra ring around the disk. Figure 5 gives an impression of the setup.

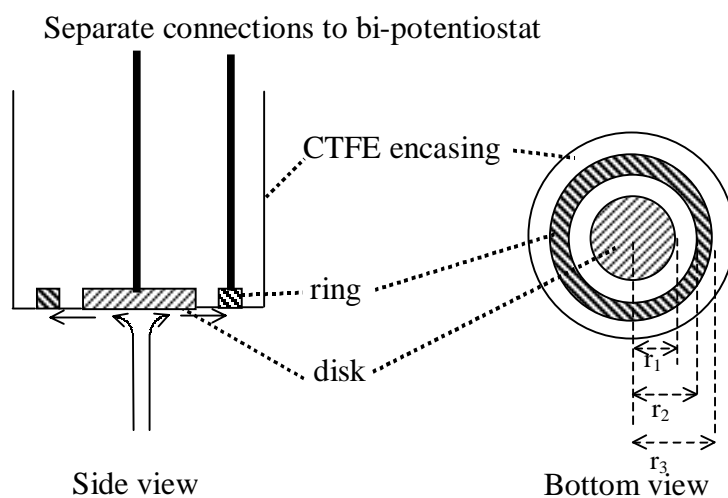


Figure 5: schematic representation of the Rotating Ring-Disk setup

The ring is a second electrode, which requires that the potentiostat is able to keep two working electrodes at a controlled potential versus the same reference electrode (a so-called bipotentiostat). While keeping all of the advantages of the RDE setup, the ring can be used to detect the products leaving the surface of the disk.

It can be shown, in a calculation similar to the derivation of the Levich equation [5], that the amount of product that comes in contact to the ring is only dependent on the dimensions of the disk and the ring (r_1 , r_2 and r_3), not of the rotation frequency. This means that the amount of products detected at the ring divided by the amount of product produced at the disk, the collection factor, is constant, and that the amount of product can be quantified. The electrodes used in our research had a collection factor of ca. 23 %.

There is no need for the ring potential to be constant, it is possible to use cyclic voltammetry to identify the product. There is also no need for the ring to be made of the same material as the disk. It is therefore possible to choose a material which is active in reducing/oxidizing the product and not in any other reactions. For example, in chapter 2 the disk (palladium/copper) is active in the reduction of NO_3^- , whereas the ring (platinum) is only active in the reduction of NO, not in the reduction of NO_3^- .

References:

- [1] H. Angerstein-Kozłowska, B.E. Conway and W.B.A. Sharp, *J. Electroanal. Chem.* 43 (1973) 9
- [2] R. Gomez, J.M. Feliu, A. Aldaz and M.J. Weaver, *Surf. Sci.* 410 (1998) 48
- [3] *Techniques and Mechanisms in Electrochemistry*, P.A. Christensen and A. Hamnett, Blackie Academic & Professional 1994
- [4] M.T.M. Koper, A.P.J. Jansen, R.A. van Santen, J.J. Lukkien and P.A.J. Hilbers *J. Chem. Phys.* 109 (1998) 6051
- [5] *Electrochemical Methods*, A.J. Bard and L.R. Faulkner, J. Wiley & Sons, New York 1980

List of publications

Chapter 2: A.C.A. de Vooy, R.A. van Santen and J.A.R. van Veen, *Journal of Molecular Catalysis A* 154 (2000) 203

Chapter 3: A.C.A. de Vooy, M.T.M. Koper, R.A. van Santen and J.A.R. van Veen, *Electrochimica Acta* 46 (2001) 923

Chapter 4: A.C.A. de Vooy, M.T.M. Koper, R.A. van Santen and J.A.R. van Veen, *Journal of Catalysis*, submitted

Chapter 6: A.C.A. de Vooy, M.T.M. Koper, R.A. van Santen and J.A.R. van Veen, *Journal of Electroanalytical Chemistry*, accepted

Chapter 7: A.C.A. de Vooy, M.F. Mrozek, M.T.M. Koper, R.A. van Santen, J.A.R. van Veen, and M.J. Weaver, *Electrochemical Communications*, accepted

Dankwoord:

Hoewel wetenschap een eenzame bezigheid is, zeker als je alleen bent, was dit proefschrift nooit tot stand gekomen zonder de hulp van een aantal mensen, die ik hierbij wil bedanken.

Marc, jouw hoge standaarden hebben dit proefschrift hopelijk een blijvende waarde gegeven. Ik heb niet alleen wetenschappelijk, maar ook op het persoonlijke vlak veel van je geleerd. Ik hoop dat ik als tegenprestatie jou heb kunnen interesseren in de stikstofchemie, en ik beloof je, mocht je er mee verder gaan: dit proefschrift is slechts het topje van de ijsberg.

Rob, jij vormde een sterk koppel met Marc, omdat jullie interesses en aanpak elkaar aanvulden. Daarnaast heb je ook gezorgd voor de ondersteuning, in tijd, apparatuur en geld. Nu ik er over na denk, merk ik dat ik niets tekort gekomen ben.

Dear Natalia, thank you for teaching how to do proper(e) electrochemistry. I always enjoyed your company and the discussions we had, and you made me realize how crazy the Dutch can be at times.

Ad, bedankt voor al die momenten dat je voor mij klaar stond en er voor gezorgd hebt dat ik mijn onderzoek kon doen. Pas toen je een tijdje weg was begon ik te beseffen wat een enorme hoop werk je deed.

Rutger, jouw interesse en energie heeft mij altijd gemotiveerd. Jouw steun was vitaal voor mijn onderzoek, en ik heb daar altijd op kunnen rekenen.

Mike and Melissa, thank you for your hospitality and your time invested in accomplishing a vital part of this thesis. I could not have done this without you, and I hope you appreciate our work as much as I do.

Ruben, Owen, en natuurlijk boven alles Bart; het feit dat de metingen die jullie voor mij gedaan hebben, vrijwel allemaal in het boekje terecht zijn gekomen zegt genoeg. Ik denk met genoegen aan de tijd dat jullie hier waren.

Albert, Anton en Wil, de oude garde (in mijn perspectief), bedankt voor de eerste lessen, en het gebruik van het straalkacheltje.

Verder wil ik iedereen bedanken die mij geholpen heeft, en door wie ik mijn tijd hier met een positief gevoel afsluit.

Curriculum Vitae:

Arnoud Cornelis Adriaan de Vooy is geboren op 25 augustus 1972 te Bunnik. In 1991 deed hij succesvol het VWO examen aan de Christelijke Scholengemeenschap Walcheren te Middelburg. In hetzelfde jaar begon hij aan de studie Scheikunde aan de Universiteit Utrecht, die hij afrondde in 1996 met het predikaat “met genoeg”. De afstudeeropdracht betrof een studie aan platinaclusters in L- en Y-zeoliet met behulp van CO adsorptie en ethaansplitsing, en werd uitgevoerd in de groep Anorganische chemie en Katalyse van prof. dr. J. Geus en prof. dr. D. Koningsberger.

In 1996 begon hij als Onderzoeker in Opleiding te werken in de groep van prof. dr. R. van Veen en prof. dr. R. van Santen aan de elektrochemische oxidatie en reductie van kleine anorganische stikstofhoudende componenten. De resultaten van dit onderzoek zijn beschreven in dit proefschrift.

Stellingen behorende bij het proefschrift:

Electrocatalytic Reactions of Inorganic Nitrogen-containing Compounds

door A.C.A. de Vooy:

1. Vergelijking van het mechanisme van een elektrochemische reactie en een reactie in UHV is alleen zinvol als er in de elektrochemische reactie geen water betrokken is ín, of vóór de snelheidsbepalende stap.
2. De meting waarin de bestudeerde reactie niet plaats vindt (de blanco) is net zo belangrijk als de meting waarin de reactie wel plaats vindt, omdat de informatie zit in het verschil tussen de metingen. De redacteurs van elektrochemische tijdschriften zouden daarom moeten eisen dat bij iedere meting ook de blanco gegeven wordt.
3. OH is één van de meest voorkomende en één van de katalytisch meest belangrijke ionen. Het is dan ook verbazingwekkend dat de adsorptie ervan zo weinig aandacht heeft gekregen in vergelijking met sommige andere ionen.
4. Het signaal van $m/z = 29$, gerapporteerd door Nart et al., gemeten tijdens de reductie van NO_3^- , komt niet van N_2H_2 , maar van de natuurlijke hoeveelheid N^{15} .
M. da Cunha, J. De Souza en F. Nart, Langmuir 16 (2000) 771
5. Tijdens de ammonia oxidatie op goud horen alleen goud, stikstof en zuurstof aan het oppervlak aanwezig te zijn. Als de bedekkingsgraad van koolstof dan 60 % blijkt te zijn, moeten vraagtekens gezet worden bij de experimentele procedure.
X. Zeng and S. Bruckenstein, J. Electroanal. Chem. 461 (1999) 131
6. Het bestaan van intermediären als NO^+ in sterk zure oplossingen ($> 1 \text{ M}$) verklaart de activiteit van platina en rhodium in de NO_3^- reductie in sterk zure oplossingen, en verklaart het gebrek aan activiteit in zwak zure oplossingen.
B.G. Snider en D.C. Johnson, Anal. Chim. Acta 105 (1979) 9; V.P. Razygraev, M.V. Lebedeva en S.A. Kabakchi, Elektrokhimiya 7 (1985) 567
7. Een elektrochemicus heeft een goede achtergrond in de “ouderwetse” anorganische chemie nodig.

8. Als een vergelijking gemaakt wordt tussen twee wetenschappelijke velden, zoals de elektrochemie en de surface science in hoofdstuk 4, is het belangrijk om de meest recente inzichten van beide velden te gebruiken.
9. De 50 Hz frequentie kan zowel in elektrochemie als in muziek een fatale storing zijn.
10. Moleculaire katalyse is soms net een puzzel leggen met te weinig stukjes.
11. Het is op het moment vrijwel onmogelijk voor A.I.O.'s in de chemie om voldoende experimenteel onderzoek binnen de gestelde termijn af te ronden en tegelijkertijd alle veiligheidsregels in acht te nemen.
12. Handel in financiële derivaten (zoals opties en futures) is slechts speculatie als de reden voor de handel niets te maken heeft met het onderliggende van het derivaat.